2017

Myo2 Motor Function in the Contractile Ring and the Regulation of Fission Yeast Cytokinesis

Luther Woodrow Pollard
University of Vermont

MYO2 MOTOR FUNCTION IN THE CONTRACTILE RING AND THE
REGULATION OF FISSION YEAST CYTOKINESIS

A Dissertation Presented

by

Luther Woodrow Pollard

to

The Faculty of the Graduate College

of

The University of Vermont

In Partial Fulfillment of the Requirements
For the Degree of Doctor of Philosophy
Specializing in Cellular, Molecular, and Biomedical Sciences

May, 2017

Defense Date: December 14, 2016
Dissertation Examination Committee:

Susan Lowey, Ph.D., Advisor
Jason Botten, Ph.D., Chairperson
Teresa Ruiz, Ph.D.
Jason Stumpff, Ph.D.
Cynthia J. Forehand, Ph.D., Dean of the Graduate College

ABSTRACT

Animals, fungi, and amoebas require an actomyosin contractile ring at the division site to perform cytokinesis. The contractile ring initiates and guides the invagination of the plasma membrane as it forms new barriers between the nuclei at the cell equator. Defects in the contractile ring can result in misdirected, delayed, or premature cytokinesis, which leads to abnormal chromosome numbers. Aneuploidies resulting from failed cytokinesis sometimes lead to aggressive forms of cancer. This dissertation was motivated by the goal of better understanding the properties of the contractile ring and how it drives cytokinesis.

Actomyosin is initially recruited to the cell equator through the coordination of scaffolding factors, actin-binding proteins, and signaling cascades. Subsequently, the sliding of actin filaments by myosin reshapes the resulting meshwork into a compact ring. Once fully assembled, the contractile ring establishes tension, which leads the plasma membrane inward. The primary motor proteins in the contractile ring of animal cells are class-II nonmuscle myosins, which typically function as bipolar filaments. Filament assembly is activated by phosphorylation and plays a central role in myosin function during cytokinesis. However, many underlying processes that regulate contractile ring function are poorly understood.

Current models of cytokinesis have been based on mechanistic insights provided by two decades of work in the fission yeast system *Schizosaccharomyces pombe*. In fission yeast, the class-II myosin Myo2 provides the major source of motor activity in the contractile ring. Myo2 is two-headed and has a rod-like tail, which is consistent with other class-II myosins. Yet, it was unknown whether Myo2 assembles into filaments, or how phosphorylation affects its activity. To investigate these features, recombinant Myo2 was purified from the baculovirus/*Sf*9 insect cell expression system. Hydrodynamic measurements were used to examine whether Myo2 forms filaments. These sedimentation velocity data gave no indication that Myo2 self-assembles under the typical physiological salt concentrations, which suggests that Myo2 is unlike any class-II myosin known to date. Myo2 was also treated *in vitro* with its native kinase Pak1. Phosphorylation of Myo2 molecules had no effect on self-assembly, however it reduced actin-binding in motility assays and increased steady-state ATPase rates by two fold. Our results imply that the function and regulation of fission yeast Myo2 during cytokinesis depends on a specific scaffolding scheme at the plasma membrane, which has not been observed in other eukaryotes.

Another interest of this dissertation was how the contractile ring is regulated during cytokinesis. We examined one cytokinesis protein, Cyk3, believed to mediate between the ring and extracellular processes. Genetics and live cell imaging analyses indicated that Cyk3 functions through a catalytically-inactive enzyme domain, which implicated Cyk3's involvement in one of the primary cytokinesis signaling pathways.

This dissertation sheds new light on core aspects of how fission yeast undergo cytokinesis, especially with respect to the mechanism of Myo2 activity in the contractile ring. Characterizing the physical and enzymatic properties of an essential myosin in a simple organism should provide insights into cytokinesis in higher organisms.

CITATIONS

Material from this dissertation has been published in the following form:

Pollard, L.W., Onishi, M., Pringle, J.R., Lord, M.. (2012). Fission yeast Cyk3p is a transglutaminase-like protein that participates in cytokinesis and cell morphogenesis. Molecular Biology of the Cell. 23(13): 2433-44.

Stark, B.C., James, M.L., Pollard, L.W., Sirotkin, V., Lord, M.. (2013). UCS protein Rng3 is essential for myosin-II motor activity during cytokinesis in fission yeast. PLoS One. 8(11): e79593.

Clayton, J.E., Pollard, L.W., Sckolnick, M., Bookwalter, C.S., Hodges, A.R., Trybus, K.M., Lord, M.. (2014). Fission yeast tropomyosin specifies directed transport of myosin-V along actin cables. Molecular Biology of the Cell. 25(1): 66-75.

Clayton, J.E., Pollard, L.W., Murray, G.G., Lord, M.. (2015). Myosin motor isoforms direct specification of actomyosin function by tropomyosins. Cytoskeleton. 72(3): 131-45.

ACKNOWLEDGEMENTS

I would like to thank Susan Lowey, Kathy Trybus, and Matt Lord for their kind mentorship and the opportunities to learn biochemistry (SL and KT) and cell biology (ML). I would also like to thank the Department of Molecular Physiology and Biophysics, the Cellular, Molecular, and Biomedical Sciences program, and my dissertation committee for providing a stimulating environment for intellectual pursuits. I thank my parents for their love and support. Finally, I need to thank Qing Tang, my soulmate and colleague, for her love and support, and for deep scientific and philosophical discussions.

TABLE OF CONTENTS

LIST OF TABLES

LIST OF FIGURES

Page

x

CHAPTER 1: INTRODUCTION

1.1. OVERVIEW OF CYTOKINESIS

The cell division cycle controls the ability of cells to self-replicate. This cycle represents the sequential progression through several phases: initial growth (G1), followed by genome duplication/DNA synthesis (S), a second growth phase (G2), and finally mitosis/meiosis (M), where the mother cell is divided into two daughter cells. With the exception of the M-phase, the phases of the cell cycle are collectively known as interphase. The phases of the cell division cycle are timed by the oscillating concentrations of different cyclins that each activate specific cyclin dependent kinases (CDK). The M-phase describes two major phenomena- the segregation of nuclear genetic material, karyokinesis, and the splitting of cytoplasm between daughter cells, cytokinesis. M-phase is further delineated into several phases. It begins with prophase, where the chromatin condenses and, in many eukaryotes, the nuclear envelope is broken down. Subsequently, chromosome alignment occurs during metaphase and is followed by anaphase, where spindle microtubules pull the sister chromatids towards opposite poles of the cell. Finally, during telophase, the nuclear envelopes reform around the decondensing chromatin. Here, the focus is on cytokinesis, which occurs during telophase by the formation of new plasma membranes between the new nuclei. Cytokinesis, like all aspects of the cell division cycle, is of fundamental importance to all life. Dysfunction of the cytokinetic process manifests diverse phenotypes in metazoans such as embryonic lethality, developmental defects, and cancers caused by aneuploidies (abnormal chromosome numbers) (Li, 2007; Sagona and Stenmark, 2010; Lacroix and Maddox, 2012).

1

Animals, fungi, and amoebas are closely related phylogenic kingdoms within the domain of eukaryotes that share similarity in how they perform cytokinesis. These kingdoms employ contractile rings that guide the invagination of the plasma membrane of the mother cell, forming a cleavage furrow. Consequently, the daughter cells separate by the plasma membrane pinching inward. The principal components of the contractile ring are actin filaments, which are polar, bi-helical polymers of 42 kDa globular protein subunits, and myosins, their associated motor proteins (discussed in depth later in this chapter). Myosins are a diverse family of proteins that have been categorized based on sequence homology into over 35 classes (Odronitz and Kollmar, 2007). Myosin motor activity is characterized by the ability to couple ATP hydrolysis to the translocation of actin filaments. Myosin enzymatic activity and actin-binding occurs in the globular head domains. The tails of myosin functionalize them for different roles in the cell. In addition to actomyosin, the contractile ring also incorporates an extensive ensemble of core regulators. Some of the common structural components of contractile rings include the actin co-polymer tropomyosin and scaffolding factors such as anillins, IQGAPs, and F-BAR-containing proteins (Cheffings et al., 2016). The myosin motor activity in the contractile ring serves to generate physical stress at the cell cortex, the region of the cytoplasm at the plasma membrane interface. The force provided by the ring delineates the division site and elicits the formation of the cleavage furrow.

Although the signaling that leads to actomyosin at the division site in animal cells is well characterized, little is known about the protein interactions and mechanisms that occur within the contractile ring itself (Pollard, 2014; Cheffings et al., 2016). The functions

of many contractile ring proteins are better characterized in the well-established fission yeast system; however, major gaps remain in the understanding of cytokinesis in this system as well. For instance, it is unclear how certain myosins are anchored and function specifically during cytokinesis. We examined the physical and enzymatic properties as well as some potential regulatory mechanisms of the myosin that is essential for cytokinesis in fission yeast in order to better understand how force is produced in the contractile ring.

Identifying new ways that the contractile ring communicates with other cellular processes that facilitate cytokinesis is another important aim because it broadens our knowledge of how the contractile ring functions as mechanically-coupled signaling platform to regulate cytokinesis. The contractile ring integrates many complex signaling pathways. One example is the pathway in yeast that regulates the cell wall-based septum which is synthesized at the extracellular interface of the cleavage furrow. To better understand how the contractile ring regulates cytokinesis, we investigated the role of another protein of the contractile ring, Cyk3, which was generally implicated in ring-based signaling (Mishra et al., 2004; Roberts-Galbraith et al., 2010).

1.2. THE FISSION YEAST CONTRACTILE RING

Actin Structure	Nucleation Factor	Actin Organization	Myosin Motor	Cellular Role
Patches:	Arp2/3 Complex	branched network	Myo1 (type-I)	Endocytosis
Ring:	formin Cdc12	unbranched anti-parallel bundles	Myo2, Myp2 (-II) Myo51 (-V)	Cytokinesis
Cables:	formin For3	unbranched parallel bundles	Myo52 (-V)	Polarized transport
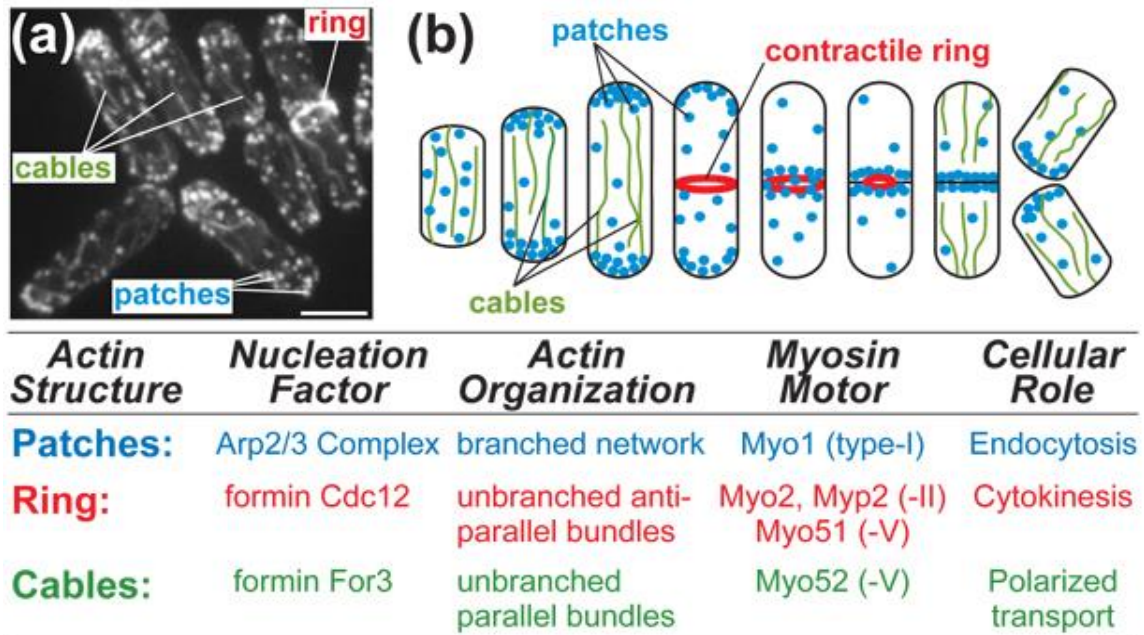
Figure 1-1: Actomyosin structures in fission yeast.
(a) A population live yeast cells expressing a marker for actin. (b) Cartoon of the three actomyosin structures throughout the cell cycle. Figure taken with permission from (Kovar et al., 2011).

Cytokinesis has been widely studied in the fission yeast *Schizosaccharomyces pombe* system because it is easy to maintain and offers greater genetic tractability compared to animal cells. Part of the fungal kingdom, fission yeast employ actomyosin contractile rings that share many of the same components as those of animal cells, and have a relatively simple genome, making it an ideal organism for studying the molecular biology of cytokinesis. Under normal growth conditions, actomyosin in the fission yeast system is organized rather simply into three distinct structures: the contractile ring, polar transport cables, and endocytic patches (**Figure 1-1**). Fission yeast expresses only five myosins in total, representing three classes, whereas the human genome contains around 40 myosin

genes. Class-I myosin, Myo1, mediates endocytosis throughout the cell cycle as a component of the Arp2/3-nucleated branched actin networks that form patches at the cell cortex, especially at the growing polar tips of the cell (Lee et al., 2000). The class-II myosins, Myo2 and Myp2, both function exclusively in contractile rings during M-phase (Bezanilla et al., 2000). The two class-V myosins have disparate roles in the cell. One class-V, Myo51, decorates rings and cables, while the other, Myo52, is a more typical class-V myosin since it transports cellular cargos along the cables to sites of growth at the cell poles (Win et al., 2001; Doyle et al., 2009; Clayton et al., 2014; Wang et al., 2014; Dudin et al., 2016). The relative simplicity of the yeast cytoskeleton is due to the fact that they grow and divide vegetatively. Yeast cells are encapsulated by a cell wall that prevents migration, i.e. they have neither cilia nor flagella and do not undergo amoeboid motility, and thus they lack the associated cytoskeletal elements. Growth and cytokinesis require cell wall remodeling, where parts of the wall are broken down and more wall is deposited. The three actin structures offer frameworks for different types of wall remodeling. Fission yeast are also particularly amenable for imaging in microscopy because their contractile rings are large compared to those of budding yeast. The many advantages of the fission yeast system have made it an excellent model for the study of cytokinesis over the past few decades.
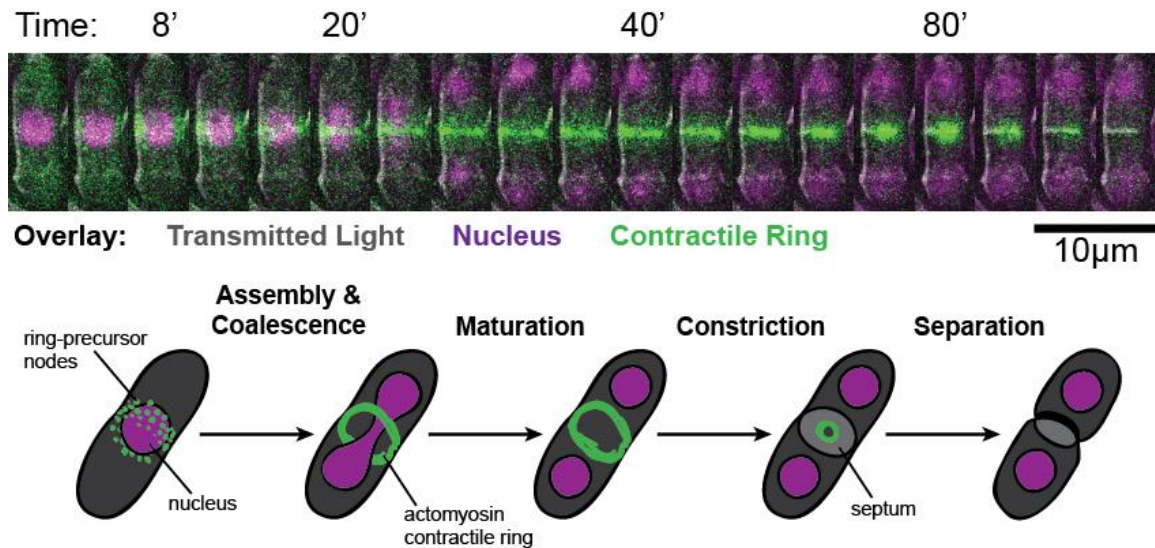
Figure 1-2: Stages of the contractile ring and cytokinesis in fission yeast.
(Above) A kymograph of a live yeast cell undergoing cytokinesis with fluorescently tagged proteins labelling the nucleus and the ring. (Below) A cartoon representation of the same process, where the cell is tilted to show the ring at an oblique angle.

The contractile ring in fission yeast has been widely observed to self-assemble from nodes (**Figure 1-2**), which are presumed to be modular units of the ring. The assembly of nodes occurs by the sequential recruitment of scaffolding proteins that ultimately localize actomyosin to the cell equator (Laporte et al., 2011). Node assembly is initiated by interconnected signaling pathways that coordinate the progression through mitosis and the growth of the cell (Willet et al., 2015b). As actin filaments are polymerized and extend from the nodes, these nodes coalesce into a compact ring (**Figures 1-2** and **1-3**). Subsequently, the ring matures and constricts while leading the plasma membrane and division septum. Because this chapter goes into fission yeast cytokinesis in depth, **Table 1-1** was included as a reference for the fission yeast gene names referred to throughout this dissertation.

Table 1-1: Fission yeast names and abbreviations.

Fission Yeast Name	Protein Family	Gene Deletion Viability
Cdc4	myosin essential light chain (ELC)	inviable
Cdc8	tropomyosin (Tpm)	inviable
Cdc12	formin	inviable
Cdc15	F-BAR protein	inviable
Cdr2	Ser/Thr kinase	viable
Clp1	Cdc14-related phosphatase	viable
Cyk3	transglutaminase-like protein	viable
Gef2	guanine exchange factor (GEF)	viable
Imp2	F-BAR protein	viable
Mid1	anillin	viable
Myo1	class-I myosin heavy chain	viable
Myo2	class-II myosin heavy chain	inviable
Myo51	class-V myosin heavy chain	viable
Myo52	class-V myosin heavy chain	viable
Myp2 (Myo3)	class-II myosin heavy chain	viable
Pak1 (Shk1/Orb2)	p21/Cdc42-activated kinase (PAK)	inviable
Plo1	polo kinase	inviable
Pom1	dual-specificity tyrosine-phosphorylation-regulated kinase (DYRK)-family kinase	viable
Pxl1	paxillin	viable
Rgf3	Rho GEF	inviable
Rho1	Rho-family GTPase	inviable
Rlc1	myosin regulatory light chain (RLC)	viable
Rng2	IQGAP	inviable
Rng3	Unc45/Cro1/She4 (UCS) family chaperone	inviable
Rng8	Myo51 tail partner	viable
Rng9	Myo51 tail partner	viable
Sid2	nuclear dbf2-related (NDR) kinase	inviable

Abbreviation	Full Name	Description
SIN	Septation Initiation Network	kinase signaling
SPB	Spindle Pole Bodies	microtubule organizers
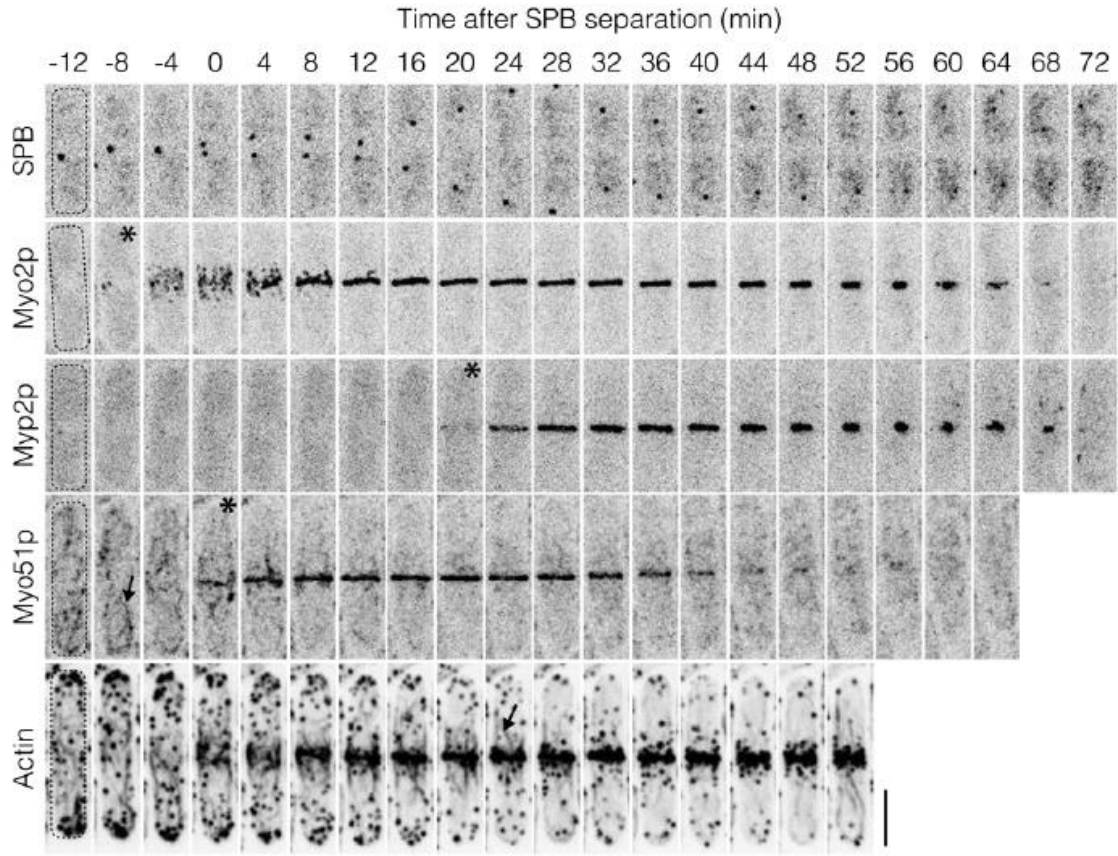
Figure 1-3: Timing the three myosins in the contractile ring.
Live cell fluorescence microscopy of fission yeast showing actin structures and the timing of the three myosins, Myo2, Myp2, and Myo51, relative to the mitotic spindle (spindle pole bodies are labeled; SPB; top panel). Scale bar: 5 μm. Adapted with permission from (Laplante et al., 2015).

The stages of cytokinesis in fission yeast are controlled by three myosins, Myo2 (class-II), Myp2 (-II), and Myo51 (-V), that differentially contribute to contractile ring dynamics. The myosins localize to the contractile ring with distinct timing (**Figure 1-3**). The first myosin, Myo2, is recruited to nodes and does not rely on actin filaments for localization to the division site (Takaine et al., 2014). Myo2 is the only essential myosin in fission yeast (Kitayama et al., 1997), whereas every other myosin gene in fission yeast can be deleted and the cells are still viable, despite various cellular defects (Bezanilla et al.,

8

1997; Lee et al., 2000; Win et al., 2001). When the gene coding for Myo2 is deleted, the cells are inviable because they form abnormally thick septa and consequently fail to separate and grow (Kitayama et al., 1997). Based on phenotypic analysis, Myo2 motor activity is necessary for contractile ring coalescence (Lord et al., 2005; Stark et al., 2010; Laporte et al., 2011; Laplante et al., 2015), which enables the ring to guide the formation of a thin septum. Myo2 also helps facilitate ring constriction (Mishra et al., 2013; Laplante et al., 2015). Myo51 is the second myosin to be recruited to the division site and appears to transition from the cables into the ring (**Figure 1-3**). Myo51 localizes between the nodes in a manner that requires actin filaments, yet, interestingly, the myosin head domain is not required for localization (Win et al., 2001; Wang et al., 2014; Laplante et al., 2015). The tail of Myo51 was recently found to form a complex with proteins Rng8 and Rng9 that contribute an additional, ATP-insensitive actin-binding site (Wang et al., 2014; Tang et al., 2016). Myo51 functions as a single-headed myosin with the Rng8/9 complex (Tang et al., 2016), which is a first since every other myosin-V studied to date functions to transport cargo by a "walking" mechanism with two heads (Trybus, 2008; Pollard and Lord, 2014). The only other example of a single-headed myosin-V is the budding yeast Myo4, but it functions as a two-headed complex with adapters and cargo (Krementsova et al., 2011; Sladewski et al., 2013). Despite being atypical for a myosin-V, purified Myo51 exhibits myosin motor activity (Clayton et al., 2010; Tang et al., 2016). Myo51 helps Myo2 to power contractile ring coalescence and weakly contributes to constriction (Wang et al., 2014; Laplante et al., 2015). Little is known about the last myosin, Myp2, which localizes after ring assembly is complete (**Figure 1-3**). Evidence indicates that Myp2's localization

depends on head-actin binding (Takaine et al., 2015). Work on recombinant Myp2 tails suggested that Myp2 could be single-headed (Bezanilla and Pollard, 2000), but the full length Myp2 has never been purified. Therefore, Myp2's structure remains to be seen. Class-II myosins, like class-V myosins, are conventionally two-headed, so it would be unique if Myp2 truly was single-headed. Cytokinesis can be supported by a Myp2-head-Myo2-tail fusion when native Myo2 function is lost (Bezanilla and Pollard, 2000; Lord et al., 2005), which suggests that the heads of Myp2 and Myo2 have similar motor properties. Myp2 contributes force mainly during constriction, and does not normally participate in coalescence because it arrives after the ring is fully compacted (Mishra et al., 2013; Laplante et al., 2015). Although myosins are critical for the function of the contractile ring, they cannot perform cytokinesis by themselves. Many factors regulate the contractile ring, some of which, e.g. IQGAP and F-BAR, like actomyosin, have critical roles in contractile ring assembly and constriction. **Chapter one** summarizes some of the current knowledge of the contractile ring in fission yeast with an emphasis on how actomyosin is assembled at the division site and on some of the ways the contractile ring regulates cytokinesis.

1.2.1. ANILLIN/MID1 ORIENTS CONTRACTILE RINGS
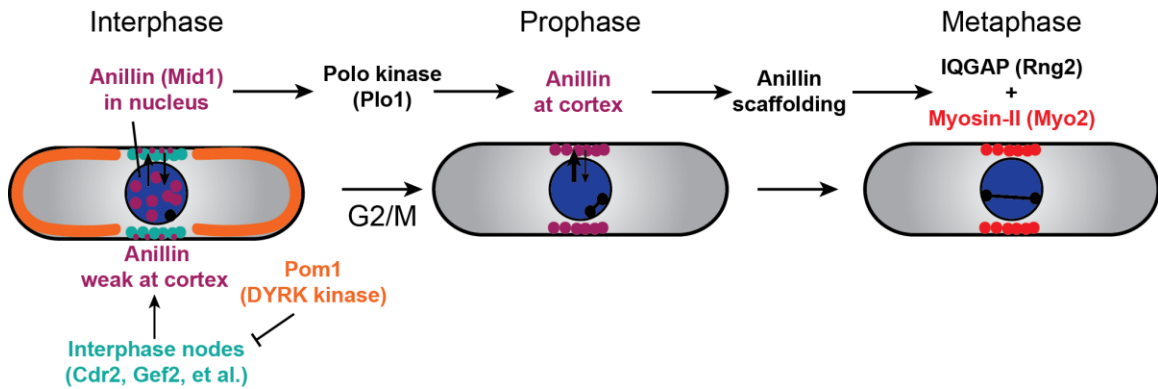
Figure 1-4: Anillin/Mid1 scaffolds the contractile ring mid-cell during M-phase.
During interphase, the Cdr2-Pom1 pathway retains small amounts of anillin^{Mid1} at the cell cortex (the pointed arrow means recruitment, whereas the blunt arrow indicates inhibition), while it shuttles between the nucleus and the cytosol. At the start of mitosis, anillin is phosphorylated and exported out of the nucleus. Once stably bound to the plasma membrane, anillin^{Mid1} can then recruit other proteins, leading to the assembly of the contractile ring. SPBs are shown as black dots; the spindle is shown in black.

Controlling the position of the contractile ring is essential for the proper allocation of cytoplasm during cell division. The membrane-associated scaffolding protein anillin is an early marker of the division site in many eukaryotes (Green et al., 2012). In fission yeast the 102 kDa anillin-like Mid1 (anillin^{Mid1}) is essential for the fidelity of the medial position of cytokinesis nodes that assemble into the contractile ring (Chang et al., 1996; Sohrmann et al., 1996; Bahler et al., 1998a; Hachet and Simanis, 2008). The pathways through which anillin^{Mid1} is spatiotemporally regulated are well studied (**Figure 1-4**). Anillin^{Mid1} dynamically exchanges between the nucleus and the medial cell cortex during interphase until it is phosphorylated by polo kinase Plo1 at the G2/M transition, which causes anillin^{Mid1} to become active and enriched at the cortex (Bahler et al., 1998a; Paoletti and

Chang, 2000; Almonacid et al., 2011). In order to identify the correct position for the division site, anillin[Mid1] must use cellular landmarks to identify the medial cell cortex. It is thought that anillin[Mid1] can position itself mid-cell using the nucleus by virtue of its nuclear-cytoplasmic shuttling (Paoletti and Chang, 2000; Almonacid et al., 2009). Additionally, lateral diffusion of anillin[Mid1] in the cortex away from the nucleus may be restricted by the cortical endoplasmic reticulum (ER) (Zhang et al., 2010). It is also important to consider how anillin[Mid1] localizes to the cortex. Evidence suggests that an amphipathic helix within the C2 domain near the carboxy (C)-terminus of anillin[Mid1] can bind to phosphatidylinositol-4,5-bisphosphate (PI(4,5)P2) at the plasma membrane (Sun et al., 2015). In parallel, anillin[Mid1] can be recruited to the cortex through interactions with interphase nodes mediated by the Rho guanine nucleotide exchange factor (GEF) Gef2 (Ye et al., 2012; Guzman-Vendrell et al., 2013; Sun et al., 2015). Interphase nodes are organized independently at the medial cortex by the kinase Cdr2, which is inhibited from binding the plasma membrane near the cell poles by the kinase Pom1 (Morrell et al., 2004; Martin and Berthelot-Grosjean, 2009; Moseley et al., 2009; Rincon et al., 2014). While the Cdr2-Pom1 pathway's primary role is to coordinate cell size with mitotic entry, it also serves to ensure timely ring assembly by recruiting anillin[Mid1] to the cortex during interphase (Bahler et al., 1998a; Almonacid et al., 2009; Moseley et al., 2009; Rincon et al., 2014; Ullal et al., 2015).

1.2.2. ASSEMBLY OF CYTOKINESIS NODES

The core components of the contractile ring are actin filaments and myosin, both of which rely on upstream factors for recruitment to the division site. As discussed in the previous section, anillin[Mid1] represents a recruitment factor that is critical for positioning the ring correctly. However, anillin[Mid1] is dispensable for contractile ring assembly to occur (Wu et al., 2003; Wu et al., 2006; Hachet and Simanis, 2008; Huang et al., 2008; Saha and Pollard, 2012a; Bohnert et al., 2013). Other than anillin[Mid1], additional scaffold-like proteins have been identified in the ring, which are thought to function in the recruitment of actomyosin at the division site.

Myo2 is one of the earliest proteins to localize to nodes (**Figure 1-3**), which occurs ~10 min. (at 25°C) before actin polymerization at the division site (Wu et al., 2003; Laporte et al., 2011). Several studies indicate how Myo2 may be recruited to nodes. Domain analyses from independent studies mapped the region responsible for Myo2 recruitment to a ~100-300 amino acid sequence at the C-terminus of the tail domain (Mulvihill et al., 2001; Motegi et al., 2004). Myo2 localization to nodes both coincides with, and requires the 172 kDa IQGAP Rng2 (IQGAP[Rng2]) (Wu et al., 2003; Laporte et al., 2011; Takaine et al., 2014). IQGAP[Rng2] was also reported to bind to anillin[Mid1] (Almonacid et al., 2011). Congruently, severing the bond between IQGAP[Rng2] and anillin[Mid1] through domain mutations or deletions uncouples the formation of the ring from anillin[Mid1] localization (Almonacid et al., 2011; Padmanabhan et al., 2011; Saha and Pollard, 2012b). The evidence for IQGAP[Rng2] arbitrating the link between anillin[Mid1] and the ring is bolstered by the finding that medial ring positioning in Mid1-deleted cells can be partially rescued by

artificially linking IQGAP^{Rng2} to Cdr2, which positions IQGAP^{Rng2} mid-cell independent of anillin^{Mid1} (Tao et al., 2014). Thus, IQGAP^{Rng2} evidently plays an integral role in contractile ring assembly. While the implicit role of IQGAP^{Rng2} is to recruit Myo2, evidence to support a direct interaction is lacking since the complex remains to be reconstituted *in vitro*.

Actin at the division site is polymerized by the cytokinesis-specific formin Cdc12 (208 kDa; formin^{Cdc12}) (Chang et al., 1996; Chang et al., 1997; Kovar et al., 2003). Evidence suggests that formin^{Cdc12} is recruited to nodes through interactions with both the IQGAP^{Rng2} pathway and the 102 kDa F-BAR domain protein Cdc15 (F-BAR^{Cdc15}) (Laporte et al., 2011). F-BAR^{Cdc15} acts as a protein scaffold at the contractile ring that binds to lipid membranes (Roberts-Galbraith et al., 2010; McDonald et al., 2015). The F-BAR domain of Cdc15 was reported to have a high affinity (K$_D$: 1.1nM) for a motif within the amino (N)-terminus of formin^{Cdc12} (Willet et al., 2015a), suggesting that F-BAR^{Cdc15} directly recruits formin^{Cdc12}. Otherwise, it is unclear how formin^{Cdc12} interacts with the IQGAP^{Rng2} module such that contractile rings can form independently of F-BAR^{Cdc15} (Laporte et al., 2011). It is conceivable that F-BAR^{Cdc15}-independent rings could arise through the capture of actin filaments by Myo2 and/or the c̲alponin h̲omology d̲omain (CHD) of IQGAP^{Rng2} (Takaine et al., 2009; Tebbs and Pollard, 2013). Despite retaining the ability to form contractile rings, F-BAR^{Cdc15}-defective cells are unable to perform cytokinesis (Fankhauser et al., 1995; Balasubramanian et al., 1998; Zhu et al., 2013). Therefore, F-BAR^{Cdc15} is generally considered an integral link between the contractile ring and the plasma membrane.

1.2.3. CONTRACTILE RING COALESCENCE AND MATURATION

Actin polymerization by formin[Cdc12] at the medial cortex immediately precedes the coalescence of the cytokinesis nodes into compact rings, which is thought to be an actomyosin-driven process. A popular way to describe how ring coalescence might occur at the molecular level is the "Search, Capture, Pull, and Release" (SCPR) model (Vavylonis et al., 2008; Lee et al., 2012). The SCPR model proposes that cytokinesis nodes are modular units of the contractile ring that contain both formin[Cdc12] and Myo2, and thus adjacent nodes can pull themselves together through Myo2 applying force on formin[Cdc12]-bound actin filaments. In order to establish an optimal distance between nodes, the model also assumes that connections between nodes must be released at some rate, which is thought to occur partially though actin filament severing by cofilin (Chen and Pollard, 2011). Additionally, the composition of actin filament crosslinkers, α-actinin, transgelin, and fimbrin, as well as the rates of constituent turnover in the contractile ring are thought to tailor its mechanical properties in a manner that prevents collapse or unraveling (Laporte et al., 2012; Stachowiak et al., 2014).

Anillin[Mid1] disperses from the division site after the compact ring is formed (Wu et al., 2003; Laporte et al., 2011; Saha and Pollard, 2012a). However, Myo2, formin[Cdc12], F-BAR[Cdc15], and IQGAP[Rng2] persist in the contractile ring over the entirety of its lifetime (Wu et al., 2003). It is unclear how Myo2 and IQGAP[Rng2] maintain their association with the cortex without anillin[Mid1]. An interaction between IQGAP[Rng2] and F-BAR[Cdc15] has been suggested (Roberts-Galbraith et al., 2010), which might allow persistent anchorage to the

plasma membrane. Potentially, anchorage could also be achieved by IQGAP^{Rng2} binding to one or more membrane-bound GTPases at the division site through its GTPase activating protein (GAP) domain, which was reported to be essential for localization and function (Tebbs and Pollard, 2013). As of now, one can only speculate as to the orientation of IQGAP^{Rng2} and Myo2 in the contractile ring.

As the ring coalesces, additional factors are recruited to reinforce and maintain the structure, some of which are myosins Myo51 and Myp2. As mentioned earlier, Myo51 aids Myo2 during late coalescence, whereas Myp2 functions with the other myosins during ring constriction (Laplante et al., 2015). The maturation of the contractile ring is controlled by the Septation Initiation Network (SIN), which is a kinase cascade that coordinates with the mitotic spindle and drives contractile ring assembly (Simanis, 2015). Sid2, the terminal kinase of the SIN, was reported to enhance formin^{Cdc12} function by phosphorylating it and inhibiting its oligomerization (Bohnert et al., 2013). Phosphorylation by Sid2 also activates the Cdc14-family phosphatase Clp1/Flp1 (Mishra et al., 2005b; Chen et al., 2008), whose conserved function is to antagonize the negative regulation of mitotic exit/cytokinesis by the cyclin dependent kinase CDK1 (Bembenek and Yu, 2003; Stegmeier and Amon, 2004; Chen et al., 2013). Notably, Clp1 dephosphorylates F-BAR^{Cdc15}, making it competent to scaffold a complement of contractile ring components (Clifford et al., 2008; Roberts-Galbraith et al., 2010). Cells lacking Clp1 function exhibit hypersensitivity to subtle defects in the contractile ring, which can be compensated for by increased SIN activity (Mishra et al., 2004; Mishra et al., 2005b). The implication is that Clp1 mediates a compensatory feedback mechanism that reinforces the SIN's ability to potentiate the integrity of the

contractile ring. Congruently, Clp1 was reported to dephosphorylate part of the SIN pathway and enhance its signaling (Chen et al., 2013). One speculation is that Clp1 may be able to sense the structural integrity of the ring by the concentration of substrates therein, which would govern the amount Clp1 available to target the SIN and stimulate reinforcement. In sum, the progression of the contractile ring requires the recruitment of auxiliary factors stimulated by increased SIN signaling, which is sensitive to the integrity of the ring in a Clp1-dependent manner.

1.2.4. CONSTRICTION AND SEPTATION

After the chromosomes are segregated, the contractile ring constricts. However, recent work indicates that the contractile ring itself does not provide enough mechanical stress to set the rate of constriction (Poirier et al., 2012; Proctor et al., 2012; Stachowiak et al., 2014; Thiyagarajan et al., 2015). For organisms that lack cell walls, modeling, coupled with experimental evidence, predicts that cleavage furrow ingression is driven mainly by the passive pressure stemming from heterogeneities in surface tension and membrane curvature (Poirier et al., 2012). Importantly, contractile ring constriction in fission yeast is coupled to the synthesis of cell wall on the extracellular surface of the plasma membrane. The new cell wall, or septum, is constructed in layers by α- and β- glucan synthases that catalyze the formation of branched and unbranched D-glucose polysaccharides (Garcia Cortes et al., 2016). The synthesis of the septum and the turgor pressure have been observed to have dominating effects on constriction speed (Proctor et al., 2012), suggesting that cytokinesis in walled cells is rate-limited by these factors. Rather than to mechanically

power furrow ingression, it is believed that the ring functions as a guide. Isometric tension from the contractile ring has been proposed to regulate the curvature of the plasma membrane (Poirier et al., 2012; Stachowiak et al., 2014). Mechanistically, this regulation is predicted to ensure that septum synthesis occurs symmetrically, consistent with observations that loss of actomyosin ring function correlates to thickened, irregular septa (Thiyagarajan et al., 2015; Zhou et al., 2015). As the ring constricts, it disassembles (Wu and Pollard, 2005). After the completion of the constriction phase, cytokinesis requires additional steps to separate the daughter cells. To close the final gap between daughter cells, the plasma membrane must undergo abscission, which is a conserved process that generally involves membrane deformation by <u>E</u>ndosomal <u>S</u>orting <u>C</u>omplex <u>R</u>equired for <u>T</u>ransport (ESCRT) proteins (Bhutta et al., 2014). In fission yeast, once the septum is completed, the new cell wall is partially degraded by the specific targeting of glucanases (Garcia Cortes et al., 2016), which leads to the final separation of the daughter cells.

How does contractile ring tension regulate cell wall remodeling? One major pathway is mediated by the small, membrane-bound GTPase Rho that is critically involved in cytokinesis and other actin-organizing processes across eukaryotes. In fungi, Rho1 helps to couple the actin cytoskeleton to the regulation of the glucan synthases that build the cell wall and septum (Arellano et al., 1996; Nakano et al., 1997; Onishi et al., 2013). The Rho1 homolog in animal cells, RhoA, can be regulated by certain transglutaminases, which are enzymes that covalently link lysine and glutamine residues (Horiguchi et al., 1997; Schmidt et al., 1998; Singh et al., 2001). The study in **Chapter two** of this dissertation identified a transglutaminase-like regulator of cell wall remodeling, Cyk3. The function of

Cyk3 was investigated to expand our understanding of the various pathways with which the contractile ring regulates cytokinesis. Importantly, this study laid the groundwork for more recent evidence indicating that Cyk3 regulates Rho1 (Onishi et al., 2013), which is discussed in detail in **Chapter four**. Overall, **Chapter two** contributes to the understanding how the ring communicates with the cell wall machinery.

1.3. MYO2 MOTILITY DURING CYTOKINESIS

In order to build upon models of cytokinesis, it is necessary to understand how myosins apply force in the contractile ring. A major motivation of this dissertation was to characterize the physical and enzymatic properties of fission yeast Myo2 because of its importance to understanding the forces of the contractile ring in a simple organism. It is known that Myo2 is a two-headed myosin that pulls on actin filaments in the contractile ring (Bezanilla and Pollard, 2000; Lord and Pollard, 2004; Lord et al., 2008; Stark et al., 2010), and is part of the class-II myosin family, which includes the muscle and nonmuscle isoforms in animals. The class-II family is the largest and most well-studied. Nearly a century of knowledge accumulated on striated muscle myosins built the foundation for understanding the mechanochemistry of all myosins. Myo2's essential role during contractile ring coalescence makes it an ideal candidate for study. However, it is not clear whether Myo2 functions similarly to animal nonmuscle class-II myosins or by a node-dependent clustering (explained further in **Section 1.3.4**). Therefore, we compared the mechanism of Myo2 function with other well-characterized class-II myosins and investigated other ways by which Myo2 could be regulated. The following sections

19

elaborate upon what is known about the structure, function, and regulation of class-II myosins in order to provide the context leading up to the mechanistic *in vitro* studies of Myo2 described in **Chapter three**.

1.3.1. CLASS-II MYOSIN STRUCTURE AND FUNCTION
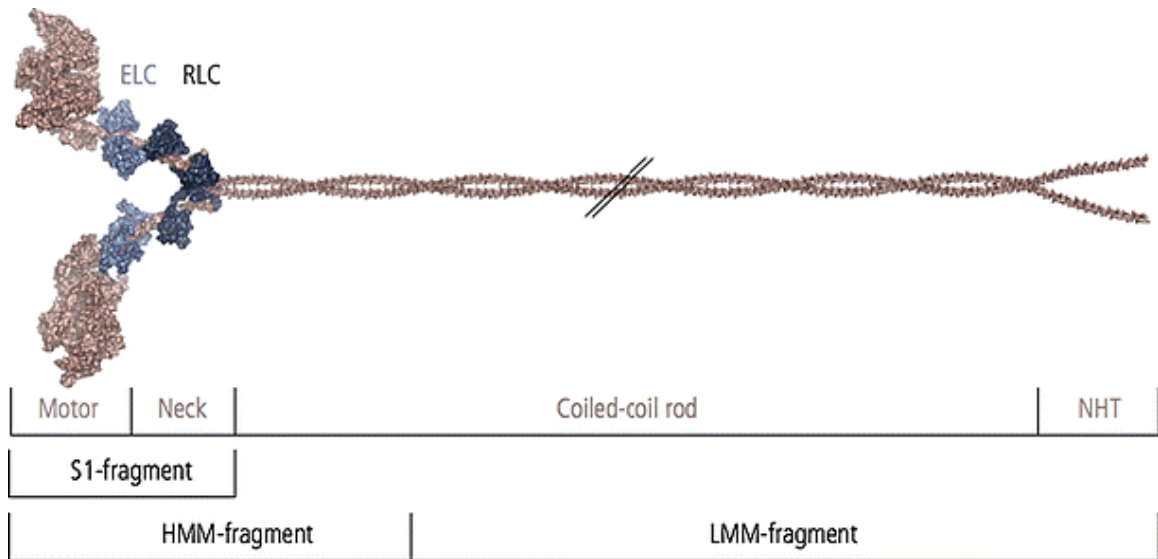
Figure 1-5: Domain structure of the typical class-II myosin.
A representative space-filling model of nonmuscle myosin-II. The coiled coil rod is shortened for the illustration (diagonal lines). Certain myosin-II tails, including that of nonmuscle, smooth muscle, and *Acanthamoeba*, terminate in nonhelical tailpieces (NHT). Limited proteolysis results in heavy meromyosin (HMM) and light meromyosin (LMM) fragments as well as the S1 and S2 subfragments of the HMM. Figure taken with permission from (Heissler and Manstein, 2013).

At the N-terminus, the typical class-II myosin molecule has two globular heads. Each head contains a motor domain, which is the site of actin-binding and ATP hydrolysis, and a neck domain (**Figure 1-5**). The neck domain is an 85 Å-long α-helix that binds the essential (ELC) and regulatory (RLC) light chains (Rayment et al., 1993). The neck is also called the lever arm because this domain extends the swinging action of the motor domain,

and thus adds leverage to the head (Warshaw et al., 2000). The swing, or the powerstroke, by the head produces force by translocating actin. The neck connects the motor to the C-terminal tail, which is an α-helical coiled-coil rod (**Figure 1-5**). The rod domain conventionally self-associates to assemble the myosin into bipolar filaments (discussed in depth later). The whole molecule, containing two heavy chains (HC) and four light chains, is around 400-500 kDa. By convention, one two-headed myosin with its light chains is considered a monomer (not to be confused with a single HC).
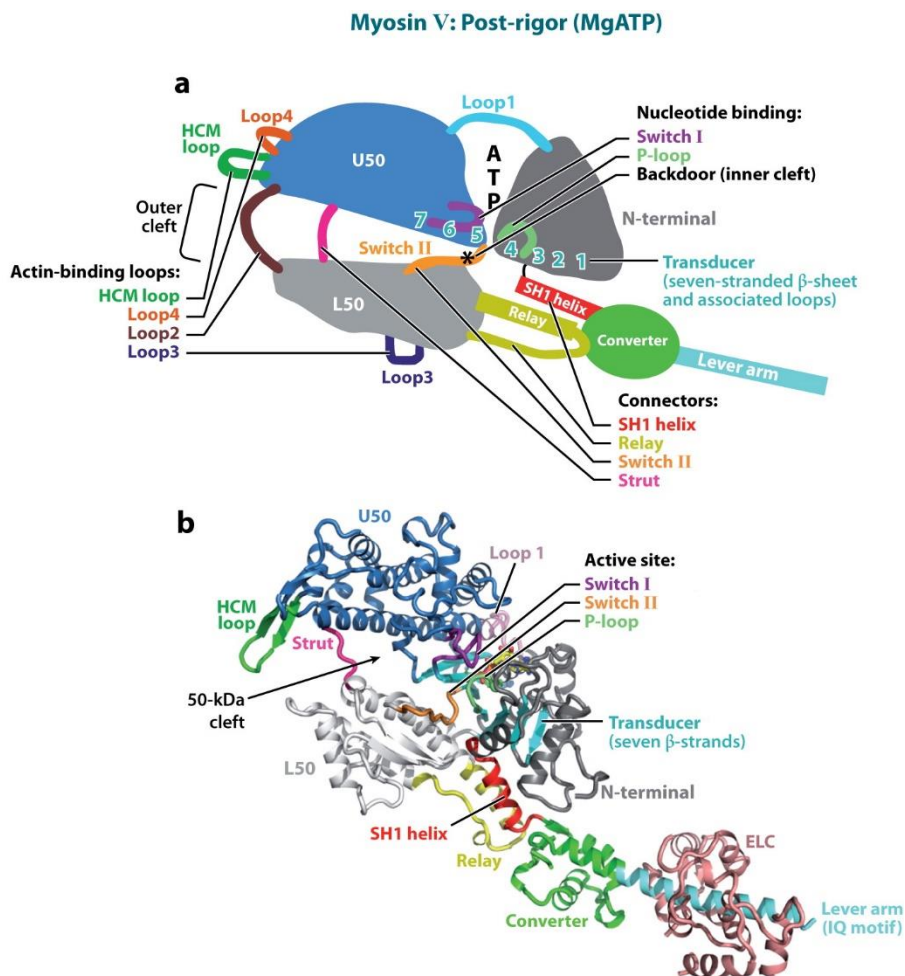
Figure 1-6: Essential elements of the myosin motor domain

(a) Cartoon and (b) ribbon diagrams of the myosin head structure. Conserved structural features are color-coded and labeled. Figure taken with permission from (Sweeney and Houdusse, 2010).

The structure of the motor domain consists of four interconnected subdomains, the N-terminal, upper-50, lower-50, and the converter, whose juxtaposition establishes the dependency between the nucleotide state, affinity for actin filaments, and position of the lever arm (**Figure 1-6**) (Sweeney and Houdusse, 2010). Overall, the motor domain is ~90 kDa and has the dimensions of roughly 100 Å long and 40 Å wide (Rayment et al., 1993). A prominent feature of the motor is the outer cleft that divides the central 50 kDa mid-portion into the upper and lower subdomains. The actin-binding site extends over both the upper- and the lower-50, which contribute several loops and a helix-loop-helix motif to this interface (**Figure 1-6**). Nucleotide binds to an active site within the inner cleft between the ~25 kDa N-terminal domain and the upper-50. The active site consists of the Switch I, Switch II, and P-loop structural elements that bind and hydrolyze ATP with a coordinated Mg^{2+} cofactor (**Figure 1-6**) (Yang et al., 2008). The core structure surrounding the active site, which includes a central β-sheet and six α-helices, is conserved in the microtubule-based motor kinesin (Kull et al., 1996), indicating that they evolved from a common ancestral motor. The structural conservation of this region underscores its importance to the mechanochemistry of myosin. In fact, the seven-stranded β-sheet of myosin's transducer region mediates the communication between the clefts and the lever arm (Coureux et al., 2004). The movements of the first three subdomains are amplified by two flexible joints, the relay and the SH1 helix, that cause a large, ~65° rotation of the fourth domain, the ~15 kDa converter, that connects the lever arm to the rest of the motor

(Mesentean et al., 2007). This swing, when propagated by the ~85 Å lever produces a displacement of ~10 nm, which has been measured in optical trapping experiments (Finer et al., 1994). Together, the dynamics of the four subdomains dictate myosin's function as a mechanoenzyme.
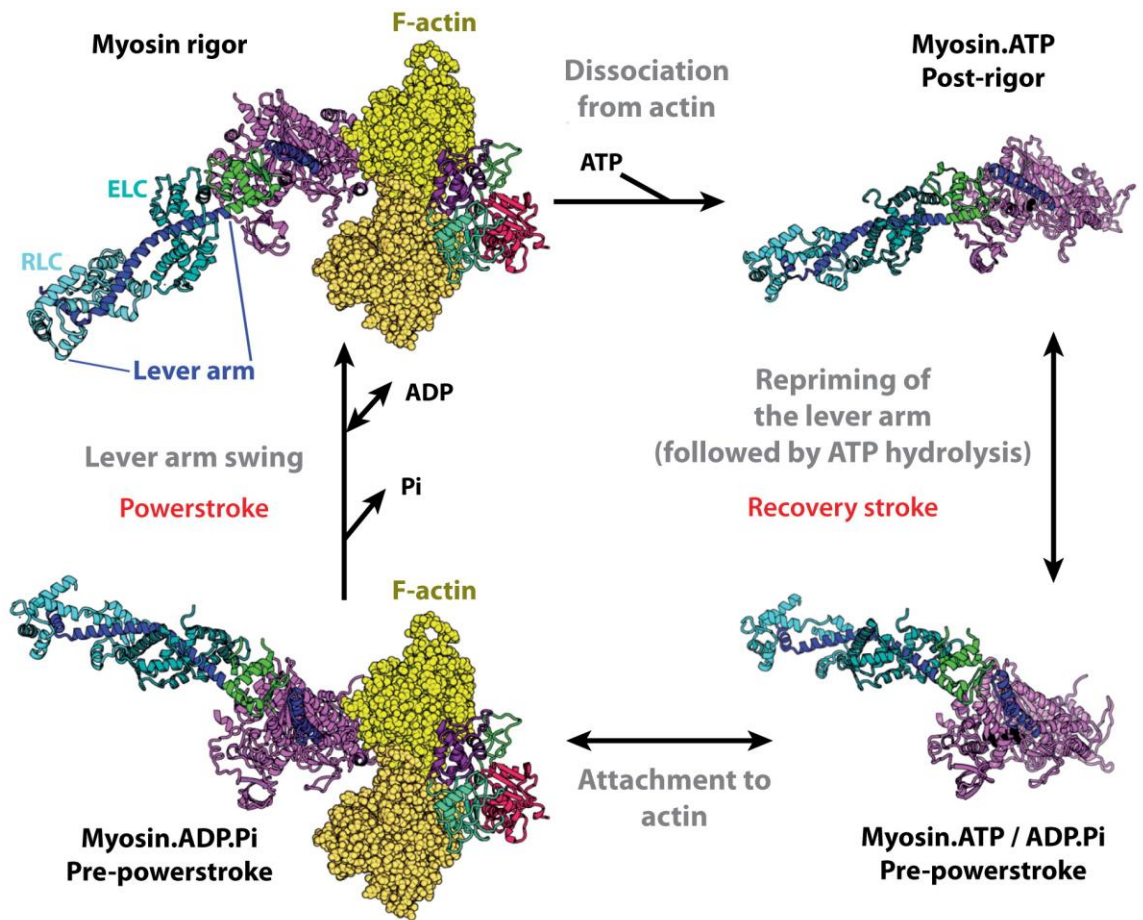
Figure 1-7: Myosin structural states in the force-generating cycle.
Taken from (Sweeney and Houdusse, 2010).

Motor activity occurs through the sequential progression through a cycle of nucleotide- and actin- binding steps (**Figure 1-7**). Below describes this cycle from a structural point of view, beginning with the MgATP-bound myosin. The opening of the inner cleft by ATP also expands the outer cleft, and thus the actin-binding loops of the

23

upper- and lower-50 become separated. In this state, myosin has a weak affinity for actin. Meanwhile, the lever arm swings into pre-powerstroke conformation. This swing is coupled to isomerization of the motor into a hydrolysis-competent state (Trivedi et al., 2015). ATP hydrolysis into ADP and inorganic phosphate (P_i) occurs rapidly, on the order of milliseconds, and re-primes the lever arm by locking it into the pre-powerstroke state. The release of P_i is very slow unless catalyzed by actin-binding, which evidence suggests causes a shift of Switch I that creates a back door for P_i to escape (Kintses et al., 2007). The initial weak binding of actin in the ADP-P_i state induces the release of P_i and initiates cleft closure (Sun et al., 2008). This closure restores the high-affinity actin-binding interface of the upper- and lower-50 subdomains (Klein et al., 2008). Myosin can then strongly bind to actin, at which point the myosin undergoes the powerstroke to displace actin (Trivedi et al., 2015). Post-powerstroke, ADP can exchange into and out of the active site. The relative affinity for ADP varies for different myosins and helps to determine the length of time they spend in the strong acting-binding state (De La Cruz et al., 1999). In order to progress through the cycle, ADP must dissociate so that ATP can bind into the active site. The apo, nucleotide free, state of myosin is otherwise known as the rigor state, where myosin remains strongly bound to actin. ATP binding to the rigor myosin re-opens the outer cleft, lowers actomyosin affinity, and allows the myosin to dissociate. Thus, a new cycle begins.

The ratio of time spent in strong actin-binding states over the total ATPase cycle is called the duty ratio. The duty ratio is an important characteristic to note since it directly impacts how long a particular motor complex can remain attached to an actin filament. For

example, the two-headed myosin-Va has a high duty ratio (> 50%), and thus is able to maintain one or both heads bound over multiple ATPase cycles (Mehta et al., 1999). Therefore, myosin-Va is considered a processive motor, i.e. able to walk along actin filaments over some distance before both heads dissociate and the molecule diffuses away. Myosins with low duty ratios must anchor in a way that clusters a proportionally large number of motors to maintain their association with actin. As exhibited by class-I myosins, membrane-binding is one way of clustering enough myosins to overcome their low duty ratios (De La Cruz and Ostap, 2004). Most class-II myosins have low duty ratios as well. Smooth and skeletal muscle myosins are classical examples that exhibit a duty ratio of around 4% (Harris and Warshaw, 1993). The mammalian nonmuscle myosin-II B isoform is an exception, with duty ratio measurements ranging between ~20% and ~80% (Rosenfeld et al., 2003; Wang et al., 2003). The low duty ratio of most class-II myosins means that they must anchor multiple molecules together to have productive associations with actin filaments. The rod-like tails achieve this by assembling myosins into filaments.

1.3.2. FOLDING THE MYOSIN MOTOR DOMAIN

The complex myosin motor domain requires specialized chaperone activity for folding. The general chaperones Heat Shock Proteins (HSP) -70 and -90 recruit additional co-chaperones to adapt their activity to fold various client proteins (Rohl et al., 2013). The Unc45/Cro1/She4-related (UCS) family of proteins serve as co-chaperones to help HSP90 to fold myosin motors (Barral et al., 2002; Liu et al., 2008; Srikakulam et al., 2008; Lee et al., 2014). UCS proteins have also been observed to buffer against the unfolding of myosin

(Melkani et al., 2010; Kaiser et al., 2012). The UCS protein in animal cells, Unc45, has three domains. At the N-terminus there is a tetratricopeptide repeat (TPR) domain that binds HSP90. Following the TPR domain, the central domain appears to play a structural role and perhaps oligomerizes the protein or contributes to myosin-binding (Gazda et al., 2013; Bujalowski et al., 2014). The conserved myosin binding site is at the C-terminus and is called the UCS domain (Barral et al., 2002; Lee et al., 2014). Vertebrates have two isoforms of Unc45, Unc45A is expressed in all cells and Unc45B is specialized in certain tissues, especially in striated muscle (Price et al., 2002; Hansen et al., 2014). Invertebrates such as *Caenorhabditis elegans* (worms) and *Drosophila melanogaster* (flies) have one isoform that is ubiquitously expressed (Barral et al., 1998; Venolia et al., 1999; Lee et al., 2011b). Fungi have UCS-domain containing proteins as well, which lack the TPR domain found in animals. Budding yeast (*Saccharomyces cerevisiae*) expresses She4, and fission yeast expresses Rng3 (Wong et al., 2000; Wesche et al., 2003). Despite lacking a TPR domain, two-hybrid and co-immunoprecipitation assays suggest that Rng3 could physically interact with HSP90 (Mishra et al., 2005a). UCS chaperone-defective yeast mutants exhibit phenotypes associated with loss of myosin function (Wong et al., 2000; Wesche et al., 2003), which suggests that the role of myosin chaperoning is conserved across eukaryotes. Additional functions for UCS proteins in yeast have been proposed. Rng3 was hypothesized to function as a cofactor for Myo2 and modify its motor activity (Lord and Pollard, 2004). The putative role of Rng3 as a cofactor for Myo2 in fission yeast is explored in **Chapter three**. UCS proteins range in size from ~80 to ~100 kDa. All UCS-family proteins consist of <u>arm</u>adillo repeat (ARM) domains derived from a series of helix-

turn-helix motifs (Shi and Blobel, 2010; Lee et al., 2011a; Gazda et al., 2013). Evidence suggests that the ARMs of UCS proteins may expose hydrophobic patches to unfolded myosin clients in order to prevent aggregation (Bujalowski et al., 2015). Importantly, the heterologous expression of certain myosins for *in vitro* characterization studies can require the co-expression of species or tissue-specific UCS chaperones (Bird et al., 2014; Bookwalter et al., 2014). To date, no striated muscle myosin has been expressed in the baculovirus/*Sf*9 insect cell system. Thus, there are clearly other factors, in addition to the UCS chaperone, involved in myosin folding yet to be discovered.

1.3.3. REGULATION OF MYOSIN BY TROPOMYOSIN

Tropomyosin (Tpm), which is an α-helical coiled-coil protein, binds cooperatively along the length of actin filaments in unbranched networks such as in muscle, stress fibers, and the contractile ring (Gunning et al., 2015). Myosin regulation by Tpm is well understood in striated muscle, where Tpm functions with troponin to gate myosin binding in a calcium-sensitive manner (Gordon et al., 2000). However, the mechanism that occurs in striated muscle does not occur in smooth muscle and nonmuscle cells, which do not express troponin. In most cells, this regulation is not as well understood. Mammalian cells can express around 40 Tpm isoforms by alternative splicing, which are widely thought to sort myosins and other actin binding proteins in the cell (Gunning et al., 2015). For example, the efficiency of myosin-Va cargo transport depends on which Tpm isoform decorates actin in single-molecule motility assays (Sckolnick et al., 2016). In contrast to the many Tpm isoforms in mammals, fission yeast expresses a single Tpm, Cdc8

(Tpm^{Cdc8}), that is alternatively regulated by N-terminal acetylation (Skoumpla et al., 2007). N-terminal acetylation is also important for Tpm function in animal cells (Urbancikova and Hitchcock-DeGregori, 1994; Gunning et al., 2015). Studies suggest the contractile ring is decorated by acetylated Tpm^{Cdc8}, while the unacetylated isoform decorates the polar transport cables (Skoumpla et al., 2007; Coulton et al., 2010; Johnson et al., 2014). Tpm^{Cdc8} is essential for fission yeast cytokinesis (Balasubramanian et al., 1992). It both facilitates the recruitment of the Myo51 tail complex to the actin (Tang et al., 2016) and enhances the actomyosin affinity of Myo2, which is thought to occur by enhancement of the duty ratio (Stark et al., 2010; Clayton et al., 2015). Duty ratio enhancement may also explain how Tpm enables the processive movement of Myo52 along actin cables (Clayton et al., 2014; Pollard and Lord, 2014). Depending on the myosin and Tpm isoforms involved, Tpm can enhance, inhibit, or have no effect on myosin activity (Clayton et al., 2010; Barua et al., 2014). Tpm's effects on actomyosin affinity may be due to periodic repeats of conserved charged residues that occur along the length of Tpm that have been implicated in ionic interactions with myosin (Barua et al., 2012). The differences between isoforms of Tpm and myosins that lead to variable regulation are still an open area of investigation.

1.3.4. MYOSIN FILAMENT ASSEMBLY AND RLC PHOSPHORYLATION
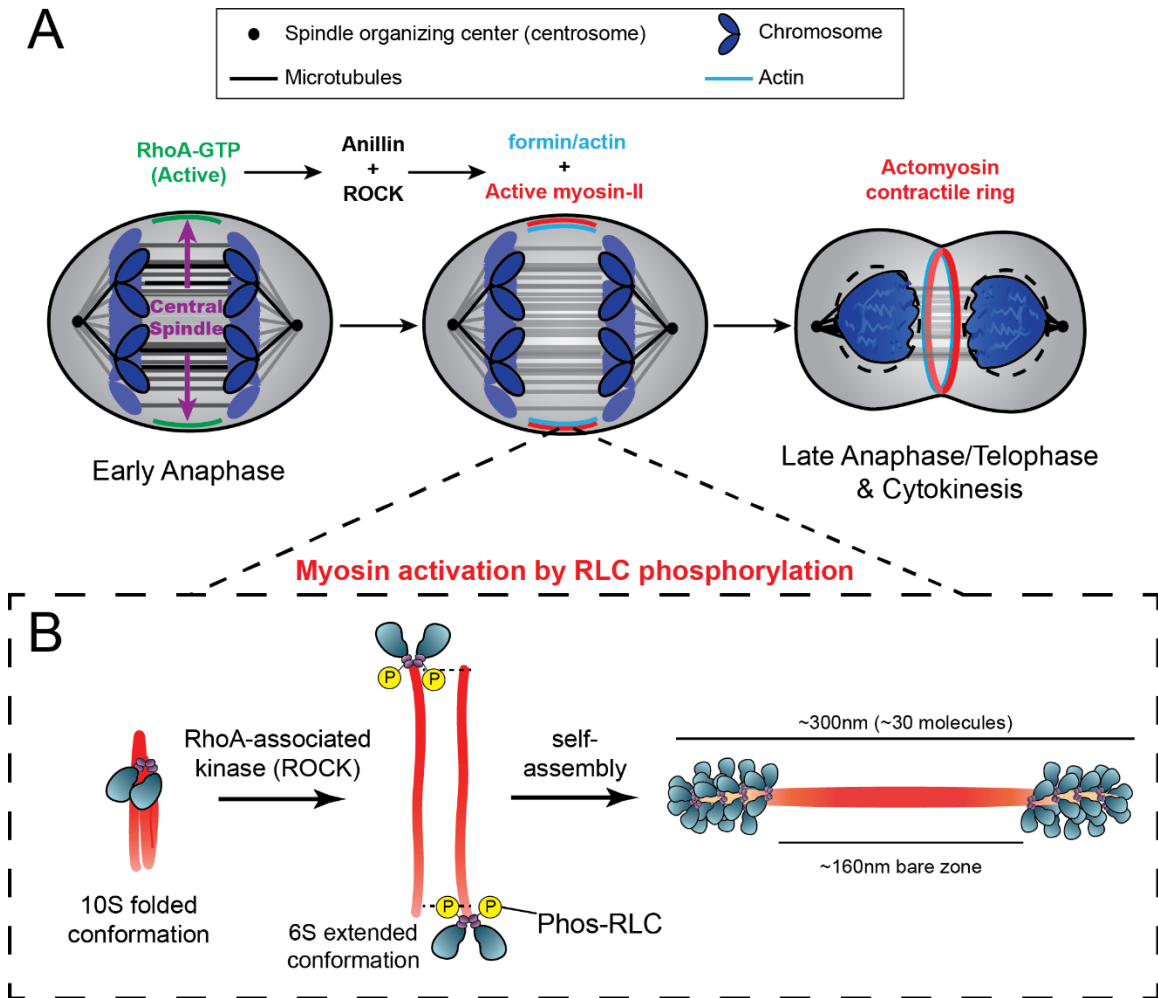
Figure 1-8: RhoA estabishes the contractile ring in animal cells.
(A) During anaphase, when chromosomes are segregated, the central spindle microtubules localize GEF activity mid-cell, which leads to GTP exchange-activation of RhoA (Green et al., 2012). RhoA in turn recruits anillin and RhoA-associated kinases (ROCK). Shortly thereafter, actomyosin is enriched at the presumptive division site and initiates cytokinesis, while the chromosomes de-condense and the nuclear envelope reforms (telophase). (B) RhoA-ROCK phosphorylates nonmuscle class-II myosins, which then become active bipolar minifilaments in the contractile ring.

To date, all well-characterized class-II myosins have been shown to form filaments

in vitro. The self-association of the rods occurs through specific ionic interactions at

physiological salt concentrations (~150 mM KCl or below), and dissociates in high salt (~0.5 M KCl). Filament assembly has been widely studied in the vertebrate class-II myosins, whose ~160 nm tails contain periodic charge distributions that are predicted to facilitate packing the molecules together with regular spacing between the heads (McLachlan and Karn, 1982). In humans, there are eight striated muscle (skeletal and cardiac) myosin genes, three nonmuscle myosins (NM-II A, B, and C), and a smooth muscle myosin that is closely related to the nonmuscle (Heissler and Manstein, 2013). As their name implies, the muscle isoforms contract the striated and smooth muscle tissues. However, the nonmuscle isoforms help to power many different cellular processes, including cell migration and adhesion, as well as cytokinesis. Vertebrate class-II myosins assemble into different types of filaments. Nonmuscle myosins form ~300 nm bipolar minifilaments that are composed of ~30 molecules (60 heads) (Billington et al., 2013), unlike striated muscle myosins that form much larger (1.6 μm) thick filaments. Smooth muscle myosins form unique, side-polar filaments that appear slanted and extend up to several microns (Craig and Megerman, 1977; Trybus and Lowey, 1987). The assembly of smooth and nonmuscle myosins into minifilaments is regulated by phosphorylation of the RLC. When unphosphorylated, these myosins are 10S folded monomers that have no motor activity because the two heads interact (Wendt et al., 1999; Wendt et al., 2001). Phosphorylation of the RLC disrupts the head-head interactions, allowing the molecules to extend into active 6S monomers, which self-assemble into bipolar filaments (Trybus et al., 1982; Craig et al., 1983; Trybus and Lowey, 1984). During cytokinesis in animal cells, the active, GTP-bound form of RhoA recruits anillin and activates the RhoA-associated

30

kinases (ROCK) that phosphorylate the RLC of nonmuscle myosin-II, which then assemble filaments (**Figure 1-8**; Sun et al., 2015; Roy et al., 2016). This chain of events is thought to be required for contractile ring assembly in animal cells. In contrast, the striated muscle myosins form thick filaments independent of RLC phosphorylation, which, instead of regulating assembly, has been observed to increase the force of the motors by about 25% (Karabina et al., 2015).

The relationship between the variations in tail sequences and different types of filament assembly is not fully understood. Residue insertions within the heptad repeats of the coiled-coil, or skip residues that occur along the length of the tail, cause disruptions of the coiled-coil, which may play a role in differentiating filament assembly (Taylor et al., 2015). Generally speaking, the particular discontinuities of the coiled-coil as well as the patterned distribution of charges in the rod are predicted to dictate the filament assembly properties of each class-II myosin. Large differences in filament assembly mechanisms are readily apparent in unicellular eukaryotes, where myosin-II rods associate according to disparate schemes. Notable examples are from the amoebozoans *Acanthamoeba castellanii* and *Dictyostelium discoideum*. The ~100 nm long tails of *Acanthamoeba* myosin-II dimerize through the formation of an antiparallel overlap of ~15 nm at the C-termini, and then form an antiparallel octamer through the staggered association of dimers (Turbedsky and Pollard, 2005). Phosphorylation of the nonhelical tail piece (**Figure 1-5**) of the *Acanthamoeba* myosin decreases the stagger with which the dimers associate (Liu et al., 2013). Conversely, the tails of *Dictyostelium* myosin-II are about twice as long (~200 nm) and form parallel dimers (four heads on one side) through an interaction spanning ~100 nm

in the middle of the rod, which is inhibited by phosphorylation in this region (Pasternak et al., 1989). *Dictyostelium* myosin dimers further interact to form tetramers that are predominantly antiparallel through 14-24 nm C-terminal overlaps, although, interestingly, tetramers have also been observed on rare occurrence to form parallel "bouquets" (Pasternak et al., 1989). The physiological relevance of this bouquet arrangement is undetermined, but it would be intriguing if they were reminiscent of some ancestral form of assembly. *Dictyostelium* myosin-II further assembles into bipolar filaments around 450 nm in length from the addition of the parallel dimers onto the antiparallel tetramers (Mahajan and Pardee, 1996). Although fungi are more closely related to animals than amoebas, it is unknown whether the class-II myosins of any fungi assemble into filaments. Understanding the process of filament assembly is particularly important when considering how different class-II myosins function in the cell because the way myosin is anchored determines how and where force is applied. Furthermore, the number of heads per filament is proportional to their capacity to produce force. A major gap in understanding the forces driving cytokinesis in fission yeast is how the essential myosin, Myo2, is anchored in the contractile ring. Two plausible models of how Myo2 is anchored could explain is function during contractile ring assembly: (1) Myo2 assembles minifilaments and thus self-anchors by crosslinking antiparallel actin filaments (like nonmuscle myosins), or (2) Myo2 tails are persistently anchored to the node by interaction(s) with other node proteins. The second model is based on Myo2's actin-independent localization to the node (Takaine et al., 2014). To probe the validity of the first model, **Chapter three** of this dissertation examines filament formation and RLC phosphorylation of Myo2.

1.4. REFERENCES

Almonacid, M., S. Celton-Morizur, J.L. Jakubowski, F. Dingli, D. Loew, A. Mayeux, J.S. Chen, K.L. Gould, D.M. Clifford, and A. Paoletti. 2011. Temporal control of contractile ring assembly by Plo1 regulation of myosin II recruitment by Mid1/anillin. *Current biology : CB*. 21:473-479.

Almonacid, M., J.B. Moseley, J. Janvore, A. Mayeux, V. Fraisier, P. Nurse, and A. Paoletti. 2009. Spatial control of cytokinesis by Cdr2 kinase and Mid1/anillin nuclear export. *Current biology : CB*. 19:961-966.

Arellano, M., A. Duran, and P. Perez. 1996. Rho 1 GTPase activates the (1-3)beta-D-glucan synthase and is involved in Schizosaccharomyces pombe morphogenesis. *The EMBO journal*. 15:4584-4591.

Bahler, J., A.B. Steever, S. Wheatley, Y. Wang, J.R. Pringle, K.L. Gould, and D. McCollum. 1998. Role of polo kinase and Mid1p in determining the site of cell division in fission yeast. *The Journal of cell biology*. 143:1603-1616.

Balasubramanian, M.K., D.M. Helfman, and S.M. Hemmingsen. 1992. A new tropomyosin essential for cytokinesis in the fission yeast S. pombe. *Nature*. 360:84-87.

Balasubramanian, M.K., D. McCollum, L. Chang, K.C. Wong, N.I. Naqvi, X. He, S. Sazer, and K.L. Gould. 1998. Isolation and characterization of new fission yeast cytokinesis mutants. *Genetics*. 149:1265-1275.

Barral, J.M., C.C. Bauer, I. Ortiz, and H.F. Epstein. 1998. Unc-45 mutations in Caenorhabditis elegans implicate a CRO1/She4p-like domain in myosin assembly. *The Journal of cell biology*. 143:1215-1225.

Barral, J.M., A.H. Hutagalung, A. Brinker, F.U. Hartl, and H.F. Epstein. 2002. Role of the myosin assembly protein UNC-45 as a molecular chaperone for myosin. *Science (New York, N.Y.)*. 295:669-671.

Barua, B., A. Nagy, J.R. Sellers, and S.E. Hitchcock-DeGregori. 2014. Regulation of Nonmuscle Myosin II by Tropomyosin. *Biochemistry*. 53:4015-4024.

Barua, B., D.A. Winkelmann, H.D. White, and S.E. Hitchcock-DeGregori. 2012. Regulation of actin-myosin interaction by conserved periodic sites of tropomyosin. *Proceedings of the National Academy of Sciences of the United States of America*. 109:18425-18430.

Bembenek, J., and H. Yu. 2003. Regulation of CDC14: pathways and checkpoints of mitotic exit. *Frontiers in bioscience : a journal and virtual library*. 8:d1275-1287.

Bezanilla, M., S.L. Forsburg, and T.D. Pollard. 1997. Identification of a second myosin-II in Schizosaccharomyces pombe: Myp2p is conditionally required for cytokinesis. *Molecular biology of the cell*. 8:2693-2705.

Bezanilla, M., and T.D. Pollard. 2000. Myosin-II tails confer unique functions in Schizosaccharomyces pombe: characterization of a novel myosin-II tail. *Molecular biology of the cell*. 11:79-91.

Bezanilla, M., J.M. Wilson, and T.D. Pollard. 2000. Fission yeast myosin-II isoforms assemble into contractile rings at distinct times during mitosis. *Current biology : CB*. 10:397-400.

Bhutta, M.S., C.J. McInerny, and G.W. Gould. 2014. ESCRT function in cytokinesis: location, dynamics and regulation by mitotic kinases. *International journal of molecular sciences*. 15:21723-21739.

Billington, N., A. Wang, J. Mao, R.S. Adelstein, and J.R. Sellers. 2013. Characterization of three full-length human nonmuscle myosin II paralogs. *The Journal of biological chemistry*. 288:33398-33410.

Bird, J.E., Y. Takagi, N. Billington, M.P. Strub, J.R. Sellers, and T.B. Friedman. 2014. Chaperone-enhanced purification of unconventional myosin 15, a molecular motor specialized for stereocilia protein trafficking. *Proceedings of the National Academy of Sciences of the United States of America*. 111:12390-12395.

Bohnert, K.A., A.P. Grzegorzewska, A.H. Willet, C.W. Vander Kooi, D.R. Kovar, and K.L. Gould. 2013. SIN-dependent phosphoinhibition of formin multimerization controls fission yeast cytokinesis. *Genes & development*. 27:2164-2177.

Bookwalter, C.S., A. Kelsen, J.M. Leung, G.E. Ward, and K.M. Trybus. 2014. A Toxoplasma gondii class XIV myosin, expressed in Sf9 cells with a parasite co-chaperone, requires two light chains for fast motility. *The Journal of biological chemistry*. 289:30832-30841.

Bujalowski, P.J., P. Nicholls, J.M. Barral, and A.F. Oberhauser. 2015. Thermally-induced structural changes in an armadillo repeat protein suggest a novel thermosensor mechanism in a molecular chaperone. *FEBS letters*. 589:123-130.

Bujalowski, P.J., P. Nicholls, and A.F. Oberhauser. 2014. UNC-45B chaperone: the role of its domains in the interaction with the myosin motor domain. *Biophysical journal*. 107:654-661.

Chang, F., D. Drubin, and P. Nurse. 1997. cdc12p, a protein required for cytokinesis in fission yeast, is a component of the cell division ring and interacts with profilin. *The Journal of cell biology*. 137:169-182.

Chang, F., A. Woollard, and P. Nurse. 1996. Isolation and characterization of fission yeast mutants defective in the assembly and placement of the contractile actin ring. *Journal of cell science*. 109 (Pt 1):131-142.

Cheffings, T.H., N.J. Burroughs, and M.K. Balasubramanian. 2016. Actomyosin Ring Formation and Tension Generation in Eukaryotic Cytokinesis. *Current biology : CB*. 26:R719-737.

Chen, C.T., A. Feoktistova, J.S. Chen, Y.S. Shim, D.M. Clifford, K.L. Gould, and D. McCollum. 2008. The SIN kinase Sid2 regulates cytoplasmic retention of the S. pombe Cdc14-like phosphatase Clp1. *Current biology : CB*. 18:1594-1599.

Chen, J.S., M.R. Broadus, J.R. McLean, A. Feoktistova, L. Ren, and K.L. Gould. 2013. Comprehensive proteomics analysis reveals new substrates and regulators of the fission yeast clp1/cdc14 phosphatase. *Molecular & cellular proteomics : MCP*. 12:1074-1086.

Chen, Q., and T.D. Pollard. 2011. Actin filament severing by cofilin is more important for assembly than constriction of the cytokinetic contractile ring. *The Journal of cell biology*. 195:485-498.

Clayton, J.E., L.W. Pollard, G.G. Murray, and M. Lord. 2015. Myosin motor isoforms direct specification of actomyosin function by tropomyosins. *Cytoskeleton (Hoboken, N.J.)*. 72:131-145.

Clayton, J.E., L.W. Pollard, M. Sckolnick, C.S. Bookwalter, A.R. Hodges, K.M. Trybus, and M. Lord. 2014. Fission yeast tropomyosin specifies directed transport of myosin-V along actin cables. *Molecular biology of the cell*. 25:66-75.

Clayton, J.E., M.R. Sammons, B.C. Stark, A.R. Hodges, and M. Lord. 2010. Differential regulation of unconventional fission yeast myosins via the actin track. *Current biology : CB*. 20:1423-1431.

Clifford, D.M., B.A. Wolfe, R.H. Roberts-Galbraith, W.H. McDonald, J.R. Yates, 3rd, and K.L. Gould. 2008. The Clp1/Cdc14 phosphatase contributes to the robustness of cytokinesis by association with anillin-related Mid1. *The Journal of cell biology*. 181:79-88.

Coulton, A.T., D.A. East, A. Galinska-Rakoczy, W. Lehman, and D.P. Mulvihill. 2010. The recruitment of acetylated and unacetylated tropomyosin to distinct actin

polymers permits the discrete regulation of specific myosins in fission yeast. *Journal of cell science*. 123:3235-3243.

Coureux, P.D., H.L. Sweeney, and A. Houdusse. 2004. Three myosin V structures delineate essential features of chemo-mechanical transduction. *The EMBO journal*. 23:4527-4537.

Craig, R., and J. Megerman. 1977. Assembly of smooth muscle myosin into side-polar filaments. *The Journal of cell biology*. 75:990-996.

Craig, R., R. Smith, and J. Kendrick-Jones. 1983. Light-chain phosphorylation controls the conformation of vertebrate non-muscle and smooth muscle myosin molecules. *Nature*. 302:436-439.

De La Cruz, E.M., and E.M. Ostap. 2004. Relating biochemistry and function in the myosin superfamily. *Current opinion in cell biology*. 16:61-67.

De La Cruz, E.M., A.L. Wells, S.S. Rosenfeld, E.M. Ostap, and H.L. Sweeney. 1999. The kinetic mechanism of myosin V. *Proceedings of the National Academy of Sciences of the United States of America*. 96:13726-13731.

Doyle, A., R. Martin-Garcia, A.T. Coulton, S. Bagley, and D.P. Mulvihill. 2009. Fission yeast Myo51 is a meiotic spindle pole body component with discrete roles during cell fusion and spore formation. *Journal of cell science*. 122:4330-4340.

Dudin, O., L. Merlini, and S.G. Martin. 2016. Spatial focalization of pheromone/MAPK signaling triggers commitment to cell-cell fusion. *Genes & development*. 30:2226-2239.

Fankhauser, C., A. Reymond, L. Cerutti, S. Utzig, K. Hofmann, and V. Simanis. 1995. The S. pombe cdc15 gene is a key element in the reorganization of F-actin at mitosis. *Cell*. 82:435-444.

Finer, J.T., R.M. Simmons, and J.A. Spudich. 1994. Single myosin molecule mechanics: piconewton forces and nanometre steps. *Nature*. 368:113-119.

Garcia Cortes, J.C., M. Ramos, M. Osumi, P. Perez, and J.C. Ribas. 2016. The Cell Biology of Fission Yeast Septation. *Microbiology and molecular biology reviews : MMBR*. 80:779-791.

Gazda, L., W. Pokrzywa, D. Hellerschmied, T. Lowe, I. Forne, F. Mueller-Planitz, T. Hoppe, and T. Clausen. 2013. The myosin chaperone UNC-45 is organized in tandem modules to support myofilament formation in C. elegans. *Cell*. 152:183-195.

Gordon, A.M., E. Homsher, and M. Regnier. 2000. Regulation of contraction in striated muscle. *Physiol Rev*. 80:853-924.

Green, R.A., E. Paluch, and K. Oegema. 2012. Cytokinesis in animal cells. *Annual review of cell and developmental biology*. 28:29-58.

Gunning, P.W., E.C. Hardeman, P. Lappalainen, and D.P. Mulvihill. 2015. Tropomyosin - master regulator of actin filament function in the cytoskeleton. *Journal of cell science*. 128:2965-2974.

Guzman-Vendrell, M., S. Baldissard, M. Almonacid, A. Mayeux, A. Paoletti, and J.B. Moseley. 2013. Blt1 and Mid1 provide overlapping membrane anchors to position the division plane in fission yeast. *Molecular and cellular biology*. 33:418-428.

Hachet, O., and V. Simanis. 2008. Mid1p/anillin and the septation initiation network orchestrate contractile ring assembly for cytokinesis. *Genes & development*. 22:3205-3216.

Hansen, L., S. Comyn, Y. Mang, A. Lind-Thomsen, L. Myhre, F. Jean, H. Eiberg, N. Tommerup, T. Rosenberg, and D. Pilgrim. 2014. The myosin chaperone UNC45B is involved in lens development and autosomal dominant juvenile cataract. *European journal of human genetics : EJHG*. 22:1290-1297.

Harris, D.E., and D.M. Warshaw. 1993. Smooth and skeletal muscle myosin both exhibit low duty cycles at zero load in vitro. *The Journal of biological chemistry*. 268:14764-14768.

Heissler, S.M., and D.J. Manstein. 2013. Nonmuscle myosin-2: mix and match. *Cellular and molecular life sciences : CMLS*. 70:1-21.

Horiguchi, Y., N. Inoue, M. Masuda, T. Kashimoto, J. Katahira, N. Sugimoto, and M. Matsuda. 1997. Bordetella bronchiseptica dermonecrotizing toxin induces reorganization of actin stress fibers through deamidation of Gln-63 of the GTP-binding protein Rho. *Proceedings of the National Academy of Sciences of the United States of America*. 94:11623-11626.

Huang, Y., H. Yan, and M.K. Balasubramanian. 2008. Assembly of normal actomyosin rings in the absence of Mid1p and cortical nodes in fission yeast. *The Journal of cell biology*. 183:979-988.

Johnson, M., D.A. East, and D.P. Mulvihill. 2014. Formins determine the functional properties of actin filaments in yeast. *Current biology : CB*. 24:1525-1530.

Kaiser, C.M., P.J. Bujalowski, L. Ma, J. Anderson, H.F. Epstein, and A.F. Oberhauser. 2012. Tracking UNC-45 chaperone-myosin interaction with a titin mechanical reporter. *Biophysical journal*. 102:2212-2219.

Karabina, A., K. Kazmierczak, D. Szczesna-Cordary, and J.R. Moore. 2015. Myosin regulatory light chain phosphorylation enhances cardiac beta-myosin in vitro motility under load. *Archives of biochemistry and biophysics*. 580:14-21.

Kintses, B., M. Gyimesi, D.S. Pearson, M.A. Geeves, W. Zeng, C.R. Bagshaw, and A. Malnasi-Csizmadia. 2007. Reversible movement of switch 1 loop of myosin determines actin interaction. *The EMBO journal*. 26:265-274.

Kitayama, C., A. Sugimoto, and M. Yamamoto. 1997. Type II myosin heavy chain encoded by the myo2 gene composes the contractile ring during cytokinesis in Schizosaccharomyces pombe. *The Journal of cell biology*. 137:1309-1319.

Klein, J.C., A.R. Burr, B. Svensson, D.J. Kennedy, J. Allingham, M.A. Titus, I. Rayment, and D.D. Thomas. 2008. Actin-binding cleft closure in myosin II probed by site-directed spin labeling and pulsed EPR. *Proceedings of the National Academy of Sciences of the United States of America*. 105:12867-12872.

Kovar, D.R., J.R. Kuhn, A.L. Tichy, and T.D. Pollard. 2003. The fission yeast cytokinesis formin Cdc12p is a barbed end actin filament capping protein gated by profilin. *The Journal of cell biology*. 161:875-887.

Kovar, D.R., V. Sirotkin, and M. Lord. 2011. Three's company: the fission yeast actin cytoskeleton. *Trends in cell biology*. 21:177-187.

Krementsova, E.B., A.R. Hodges, C.S. Bookwalter, T.E. Sladewski, M. Travaglia, H.L. Sweeney, and K.M. Trybus. 2011. Two single-headed myosin V motors bound to a tetrameric adapter protein form a processive complex. *The Journal of cell biology*. 195:631-641.

Kull, F.J., E.P. Sablin, R. Lau, R.J. Fletterick, and R.D. Vale. 1996. Crystal structure of the kinesin motor domain reveals a structural similarity to myosin. *Nature*. 380:550-555.

Lacroix, B., and A.S. Maddox. 2012. Cytokinesis, ploidy and aneuploidy. *The Journal of pathology*. 226:338-351.

Laplante, C., J. Berro, E. Karatekin, A. Hernandez-Leyva, R. Lee, and T.D. Pollard. 2015. Three myosins contribute uniquely to the assembly and constriction of the fission yeast cytokinetic contractile ring. *Current biology : CB*. 25:1955-1965.

Laporte, D., V.C. Coffman, I.J. Lee, and J.Q. Wu. 2011. Assembly and architecture of precursor nodes during fission yeast cytokinesis. *The Journal of cell biology*. 192:1005-1021.

Laporte, D., N. Ojkic, D. Vavylonis, and J.Q. Wu. 2012. alpha-Actinin and fimbrin cooperate with myosin II to organize actomyosin bundles during contractile-ring assembly. *Molecular biology of the cell*. 23:3094-3110.

Lee, C.F., A.V. Hauenstein, J.K. Fleming, W.C. Gasper, V. Engelke, B. Sankaran, S.I. Bernstein, and T. Huxford. 2011a. X-ray crystal structure of the UCS domain-containing UNC-45 myosin chaperone from Drosophila melanogaster. *Structure (London, England : 1993)*. 19:397-408.

Lee, C.F., G.C. Melkani, and S.I. Bernstein. 2014. The UNC-45 myosin chaperone: from worms to flies to vertebrates. *International review of cell and molecular biology*. 313:103-144.

Lee, C.F., G.C. Melkani, Q. Yu, J.A. Suggs, W.A. Kronert, Y. Suzuki, L. Hipolito, M.G. Price, H.F. Epstein, and S.I. Bernstein. 2011b. Drosophila UNC-45 accumulates in embryonic blastoderm and in muscles, and is essential for muscle myosin stability. *Journal of cell science*. 124:699-705.

Lee, I.J., V.C. Coffman, and J.Q. Wu. 2012. Contractile-ring assembly in fission yeast cytokinesis: Recent advances and new perspectives. *Cytoskeleton (Hoboken, N.J.)*. 69:751-763.

Lee, W.L., M. Bezanilla, and T.D. Pollard. 2000. Fission yeast myosin-I, Myo1p, stimulates actin assembly by Arp2/3 complex and shares functions with WASp. *The Journal of cell biology*. 151:789-800.

Li, R. 2007. Cytokinesis in development and disease: variations on a common theme. *Cellular and molecular life sciences : CMLS*. 64:3044-3058.

Liu, L., R. Srikakulam, and D.A. Winkelmann. 2008. Unc45 activates Hsp90-dependent folding of the myosin motor domain. *The Journal of biological chemistry*. 283:13185-13193.

Liu, X., M.S. Hong, S. Shu, S. Yu, and E.D. Korn. 2013. Regulation of the filament structure and assembly of Acanthamoeba myosin II by phosphorylation of serines in the heavy-chain nonhelical tailpiece. *Proceedings of the National Academy of Sciences of the United States of America*. 110:E33-40.

Lord, M., E. Laves, and T.D. Pollard. 2005. Cytokinesis depends on the motor domains of myosin-II in fission yeast but not in budding yeast. *Molecular biology of the cell*. 16:5346-5355.

Lord, M., and T.D. Pollard. 2004. UCS protein Rng3p activates actin filament gliding by fission yeast myosin-II. *The Journal of cell biology*. 167:315-325.

Lord, M., T.E. Sladewski, and T.D. Pollard. 2008. Yeast UCS proteins promote actomyosin interactions and limit myosin turnover in cells. *Proceedings of the National Academy of Sciences of the United States of America*. 105:8014-8019.

Mahajan, R.K., and J.D. Pardee. 1996. Assembly mechanism of Dictyostelium myosin II: regulation by K+, Mg2+, and actin filaments. *Biochemistry*. 35:15504-15514.

Martin, S.G., and M. Berthelot-Grosjean. 2009. Polar gradients of the DYRK-family kinase Pom1 couple cell length with the cell cycle. *Nature*. 459:852-856.

McDonald, N.A., C.W. Vander Kooi, M.D. Ohi, and K.L. Gould. 2015. Oligomerization but Not Membrane Bending Underlies the Function of Certain F-BAR Proteins in Cell Motility and Cytokinesis. *Developmental cell*. 35:725-736.

McLachlan, A.D., and J. Karn. 1982. Periodic charge distributions in the myosin rod amino acid sequence match cross-bridge spacings in muscle. *Nature*. 299:226-231.

Mehta, A.D., R.S. Rock, M. Rief, J.A. Spudich, M.S. Mooseker, and R.E. Cheney. 1999. Myosin-V is a processive actin-based motor. *Nature*. 400:590-593.

Melkani, G.C., C.F. Lee, A. Cammarato, and S.I. Bernstein. 2010. Drosophila UNC-45 prevents heat-induced aggregation of skeletal muscle myosin and facilitates refolding of citrate synthase. *Biochemical and biophysical research communications*. 396:317-322.

Mesentean, S., S. Koppole, J.C. Smith, and S. Fischer. 2007. The principal motions involved in the coupling mechanism of the recovery stroke of the myosin motor. *J Mol Biol*. 367:591-602.

Mishra, M., M. D'Souza V, K.C. Chang, Y. Huang, and M.K. Balasubramanian. 2005a. Hsp90 protein in fission yeast Swo1p and UCS protein Rng3p facilitate myosin II assembly and function. *Eukaryotic cell*. 4:567-576.

Mishra, M., J. Karagiannis, M. Sevugan, P. Singh, and M.K. Balasubramanian. 2005b. The 14-3-3 protein rad24p modulates function of the cdc14p family phosphatase clp1p/flp1p in fission yeast. *Current biology : CB*. 15:1376-1383.

Mishra, M., J. Karagiannis, S. Trautmann, H. Wang, D. McCollum, and M.K. Balasubramanian. 2004. The Clp1p/Flp1p phosphatase ensures completion of cytokinesis in response to minor perturbation of the cell division machinery in Schizosaccharomyces pombe. *Journal of cell science*. 117:3897-3910.

Mishra, M., J. Kashiwazaki, T. Takagi, R. Srinivasan, Y. Huang, M.K. Balasubramanian, and I. Mabuchi. 2013. In vitro contraction of cytokinetic ring depends on myosin II but not on actin dynamics. *Nature cell biology*. 15:853-859.

Morrell, J.L., C.B. Nichols, and K.L. Gould. 2004. The GIN4 family kinase, Cdr2p, acts independently of septins in fission yeast. *Journal of cell science*. 117:5293-5302.

Moseley, J.B., A. Mayeux, A. Paoletti, and P. Nurse. 2009. A spatial gradient coordinates cell size and mitotic entry in fission yeast. *Nature*. 459:857-860.

Motegi, F., M. Mishra, M.K. Balasubramanian, and I. Mabuchi. 2004. Myosin-II reorganization during mitosis is controlled temporally by its dephosphorylation and spatially by Mid1 in fission yeast. *The Journal of cell biology*. 165:685-695.

Mulvihill, D.P., C. Barretto, and J.S. Hyams. 2001. Localization of fission yeast type II myosin, Myo2, to the cytokinetic actin ring is regulated by phosphorylation of a C-terminal coiled-coil domain and requires a functional septation initiation network. *Molecular biology of the cell*. 12:4044-4053.

Nakano, K., R. Arai, and I. Mabuchi. 1997. The small GTP-binding protein Rho1 is a multifunctional protein that regulates actin localization, cell polarity, and septum formation in the fission yeast Schizosaccharomyces pombe. *Genes to cells : devoted to molecular & cellular mechanisms*. 2:679-694.

Odronitz, F., and M. Kollmar. 2007. Drawing the tree of eukaryotic life based on the analysis of 2,269 manually annotated myosins from 328 species. *Genome biology*. 8:R196.

Onishi, M., N. Ko, R. Nishihama, and J.R. Pringle. 2013. Distinct roles of Rho1, Cdc42, and Cyk3 in septum formation and abscission during yeast cytokinesis. *The Journal of cell biology*. 202:311-329.

Padmanabhan, A., K. Bakka, M. Sevugan, N.I. Naqvi, V. D'Souza, X. Tang, M. Mishra, and M.K. Balasubramanian. 2011. IQGAP-related Rng2p organizes cortical nodes and ensures position of cell division in fission yeast. *Current biology : CB*. 21:467-472.

Paoletti, A., and F. Chang. 2000. Analysis of mid1p, a protein required for placement of the cell division site, reveals a link between the nucleus and the cell surface in fission yeast. *Molecular biology of the cell*. 11:2757-2773.

Pasternak, C., P.F. Flicker, S. Ravid, and J.A. Spudich. 1989. Intermolecular versus intramolecular interactions of Dictyostelium myosin: possible regulation by heavy chain phosphorylation. *The Journal of cell biology*. 109:203-210.

Poirier, C.C., W.P. Ng, D.N. Robinson, and P.A. Iglesias. 2012. Deconvolution of the cellular force-generating subsystems that govern cytokinesis furrow ingression. *PLoS computational biology*. 8:e1002467.

Pollard, L.W., and M. Lord. 2014. Getting myosin-V on the right track: Tropomyosin sorts transport in yeast. *Bioarchitecture*. 4:35-38.

Pollard, T.D. 2014. The value of mechanistic biophysical information for systems-level understanding of complex biological processes such as cytokinesis. *Biophysical journal*. 107:2499-2507.

Price, M.G., M.L. Landsverk, J.M. Barral, and H.F. Epstein. 2002. Two mammalian UNC-45 isoforms are related to distinct cytoskeletal and muscle-specific functions. *Journal of cell science*. 115:4013-4023.

Proctor, S.A., N. Minc, A. Boudaoud, and F. Chang. 2012. Contributions of turgor pressure, the contractile ring, and septum assembly to forces in cytokinesis in fission yeast. *Current biology : CB*. 22:1601-1608.

Rayment, I., W.R. Rypniewski, K. Schmidt-Base, R. Smith, D.R. Tomchick, M.M. Benning, D.A. Winkelmann, G. Wesenberg, and H.M. Holden. 1993. Three-dimensional structure of myosin subfragment-1: a molecular motor. *Science (New York, N.Y.)*. 261:50-58.

Rincon, S.A., P. Bhatia, C. Bicho, M. Guzman-Vendrell, V. Fraisier, W.E. Borek, L. Alves Fde, F. Dingli, D. Loew, J. Rappsilber, K.E. Sawin, S.G. Martin, and A. Paoletti. 2014. Pom1 regulates the assembly of Cdr2-Mid1 cortical nodes for robust spatial control of cytokinesis. *The Journal of cell biology*. 206:61-77.

Roberts-Galbraith, R.H., M.D. Ohi, B.A. Ballif, J.S. Chen, I. McLeod, W.H. McDonald, S.P. Gygi, J.R. Yates, 3rd, and K.L. Gould. 2010. Dephosphorylation of F-BAR protein Cdc15 modulates its conformation and stimulates its scaffolding activity at the cell division site. *Molecular cell*. 39:86-99.

Rohl, A., J. Rohrberg, and J. Buchner. 2013. The chaperone Hsp90: changing partners for demanding clients. *Trends in biochemical sciences*. 38:253-262.

Rosenfeld, S.S., J. Xing, L.Q. Chen, and H.L. Sweeney. 2003. Myosin IIb is unconventionally conventional. *The Journal of biological chemistry*. 278:27449-27455.

Roy, A., L. Lordier, S. Mazzi, Y. Chang, V. Lapierre, J. Larghero, N. Debili, H. Raslova, and W. Vainchenker. 2016. Differential activity of nonmuscle myosin II isoforms determines their localization at the cleavage furrow of megakaryocytes. *Blood. in press.*

Sagona, A.P., and H. Stenmark. 2010. Cytokinesis and cancer. *FEBS letters*. 584:2652-2661.

Saha, S., and T.D. Pollard. 2012a. Anillin-related protein Mid1p coordinates the assembly of the cytokinetic contractile ring in fission yeast. *Molecular biology of the cell*. 23:3982-3992.

Saha, S., and T.D. Pollard. 2012b. Characterization of structural and functional domains of the anillin-related protein Mid1p that contribute to cytokinesis in fission yeast. *Molecular biology of the cell*. 23:3993-4007.

Schmidt, G., J. Selzer, M. Lerm, and K. Aktories. 1998. The Rho-deamidating cytotoxic necrotizing factor 1 from Escherichia coli possesses transglutaminase activity. Cysteine 866 and histidine 881 are essential for enzyme activity. *The Journal of biological chemistry*. 273:13669-13674.

Sckolnick, M., E.B. Krementsova, D.M. Warshaw, and K.M. Trybus. 2016. Tropomyosin isoforms bias actin track selection by vertebrate myosin Va. *Molecular biology of the cell*. 27:2889-2897.

Shi, H., and G. Blobel. 2010. UNC-45/CRO1/She4p (UCS) protein forms elongated dimer and joins two myosin heads near their actin binding region. *Proceedings of the National Academy of Sciences of the United States of America*. 107:21382-21387.

Simanis, V. 2015. Pombe's thirteen - control of fission yeast cell division by the septation initiation network. *Journal of cell science*. 128:1465-1474.

Singh, U.S., M.T. Kunar, Y.L. Kao, and K.M. Baker. 2001. Role of transglutaminase II in retinoic acid-induced activation of RhoA-associated kinase-2. *The EMBO journal*. 20:2413-2423.

Skoumpla, K., A.T. Coulton, W. Lehman, M.A. Geeves, and D.P. Mulvihill. 2007. Acetylation regulates tropomyosin function in the fission yeast Schizosaccharomyces pombe. *Journal of cell science*. 120:1635-1645.

Sladewski, T.E., C.S. Bookwalter, M.S. Hong, and K.M. Trybus. 2013. Single-molecule reconstitution of mRNA transport by a class V myosin. *Nature structural & molecular biology*. 20:952-957.

Sohrmann, M., C. Fankhauser, C. Brodbeck, and V. Simanis. 1996. The dmf1/mid1 gene is essential for correct positioning of the division septum in fission yeast. *Genes & development*. 10:2707-2719.

Srikakulam, R., L. Liu, and D.A. Winkelmann. 2008. Unc45b forms a cytosolic complex with Hsp90 and targets the unfolded myosin motor domain. *PloS one*. 3:e2137.

Stachowiak, M.R., C. Laplante, H.F. Chin, B. Guirao, E. Karatekin, T.D. Pollard, and B. O'Shaughnessy. 2014. Mechanism of cytokinetic contractile ring constriction in fission yeast. *Developmental cell*. 29:547-561.

Stark, B.C., T.E. Sladewski, L.W. Pollard, and M. Lord. 2010. Tropomyosin and myosin-II cellular levels promote actomyosin ring assembly in fission yeast. *Molecular biology of the cell*. 21:989-1000.

Stegmeier, F., and A. Amon. 2004. Closing mitosis: the functions of the Cdc14 phosphatase and its regulation. *Annual review of genetics*. 38:203-232.

Sun, L., R. Guan, I.J. Lee, Y. Liu, M. Chen, J. Wang, J.Q. Wu, and Z. Chen. 2015. Mechanistic insights into the anchorage of the contractile ring by anillin and Mid1. *Developmental cell*. 33:413-426.

Sun, M., M.B. Rose, S.K. Ananthanarayanan, D.J. Jacobs, and C.M. Yengo. 2008. Characterization of the pre-force-generation state in the actomyosin cross-bridge cycle. *Proceedings of the National Academy of Sciences of the United States of America*. 105:8631-8636.

Sweeney, H.L., and A. Houdusse. 2010. Structural and functional insights into the Myosin motor mechanism. *Annual review of biophysics*. 39:539-557.

Takaine, M., O. Numata, and K. Nakano. 2009. Fission yeast IQGAP arranges actin filaments into the cytokinetic contractile ring. *The EMBO journal*. 28:3117-3131.

Takaine, M., O. Numata, and K. Nakano. 2014. Fission yeast IQGAP maintains F-actin-independent localization of myosin-II in the contractile ring. *Genes to cells : devoted to molecular & cellular mechanisms*. 19:161-176.

Takaine, M., O. Numata, and K. Nakano. 2015. An actin-myosin-II interaction is involved in maintaining the contractile ring in fission yeast. *Journal of cell science*. 128:2903-2918.

Tang, Q., N. Billington, E.B. Krementsova, C.S. Bookwalter, M. Lord, and K.M. Trybus. 2016. A single-headed fission yeast myosin V transports actin in a tropomyosin-dependent manner. *The Journal of cell biology*. 214:167-179.

Taylor, K.C., M. Buvoli, E.N. Korkmaz, A. Buvoli, Y. Zheng, N.T. Heinze, Q. Cui, L.A. Leinwand, and I. Rayment. 2015. Skip residues modulate the structural properties of the myosin rod and guide thick filament assembly. *Proceedings of the National Academy of Sciences of the United States of America*. 112:E3806-3815.

Tebbs, I.R., and T.D. Pollard. 2013. Separate roles of IQGAP Rng2p in forming and constricting the Schizosaccharomyces pombe cytokinetic contractile ring. *Molecular biology of the cell*. 24:1904-1917.

Thiyagarajan, S., E.L. Munteanu, R. Arasada, T.D. Pollard, and B. O'Shaughnessy. 2015. The fission yeast cytokinetic contractile ring regulates septum shape and closure. *Journal of cell science*. 128:3672-3681.

Trivedi, D.V., J.M. Muretta, A.M. Swenson, J.P. Davis, D.D. Thomas, and C.M. Yengo. 2015. Direct measurements of the coordination of lever arm swing and the catalytic cycle in myosin V. *Proceedings of the National Academy of Sciences of the United States of America*. 112:14593-14598.

Trybus, K.M. 2008. Myosin V from head to tail. *Cellular and molecular life sciences : CMLS*. 65:1378-1389.

Trybus, K.M., T.W. Huiatt, and S. Lowey. 1982. A bent monomeric conformation of myosin from smooth muscle. *Proceedings of the National Academy of Sciences of the United States of America*. 79:6151-6155.

Trybus, K.M., and S. Lowey. 1984. Conformational states of smooth muscle myosin. Effects of light chain phosphorylation and ionic strength. *The Journal of biological chemistry*. 259:8564-8571.

Trybus, K.M., and S. Lowey. 1987. Assembly of smooth muscle myosin minifilaments: effects of phosphorylation and nucleotide binding. *The Journal of cell biology*. 105:3007-3019.

Turbedsky, K., and T.D. Pollard. 2005. Assembly of Acanthamoeba myosin-II minifilaments. Definition of C-terminal residues required to form coiled-coils, dimers, and octamers. *J Mol Biol*. 345:351-361.

Ullal, P., N.A. McDonald, J.S. Chen, L. Lo Presti, R.H. Roberts-Galbraith, K.L. Gould, and S.G. Martin. 2015. The DYRK-family kinase Pom1 phosphorylates the F-

BAR protein Cdc15 to prevent division at cell poles. *The Journal of cell biology*. 211:653-668.

Urbancikova, M., and S.E. Hitchcock-DeGregori. 1994. Requirement of amino-terminal modification for striated muscle alpha-tropomyosin function. *The Journal of biological chemistry*. 269:24310-24315.

Vavylonis, D., J.Q. Wu, S. Hao, B. O'Shaughnessy, and T.D. Pollard. 2008. Assembly mechanism of the contractile ring for cytokinesis by fission yeast. *Science (New York, N.Y.)*. 319:97-100.

Venolia, L., W. Ao, S. Kim, C. Kim, and D. Pilgrim. 1999. unc-45 gene of Caenorhabditis elegans encodes a muscle-specific tetratricopeptide repeat-containing protein. *Cell motility and the cytoskeleton*. 42:163-177.

Wang, F., M. Kovacs, A. Hu, J. Limouze, E.V. Harvey, and J.R. Sellers. 2003. Kinetic mechanism of non-muscle myosin IIB: functional adaptations for tension generation and maintenance. *The Journal of biological chemistry*. 278:27439-27448.

Wang, N., L. Lo Presti, Y.H. Zhu, M. Kang, Z. Wu, S.G. Martin, and J.Q. Wu. 2014. The novel proteins Rng8 and Rng9 regulate the myosin-V Myo51 during fission yeast cytokinesis. *The Journal of cell biology*. 205:357-375.

Warshaw, D.M., W.H. Guilford, Y. Freyzon, E. Krementsova, K.A. Palmiter, M.J. Tyska, J.E. Baker, and K.M. Trybus. 2000. The light chain binding domain of expressed smooth muscle heavy meromyosin acts as a mechanical lever. *The Journal of biological chemistry*. 275:37167-37172.

Wendt, T., D. Taylor, T. Messier, K.M. Trybus, and K.A. Taylor. 1999. Visualization of head-head interactions in the inhibited state of smooth muscle myosin. *The Journal of cell biology*. 147:1385-1390.

Wendt, T., D. Taylor, K.M. Trybus, and K. Taylor. 2001. Three-dimensional image reconstruction of dephosphorylated smooth muscle heavy meromyosin reveals asymmetry in the interaction between myosin heads and placement of subfragment 2. *Proceedings of the National Academy of Sciences of the United States of America*. 98:4361-4366.

Wesche, S., M. Arnold, and R.P. Jansen. 2003. The UCS domain protein She4p binds to myosin motor domains and is essential for class I and class V myosin function. *Current biology : CB*. 13:715-724.

Willet, A.H., N.A. McDonald, K.A. Bohnert, M.A. Baird, J.R. Allen, M.W. Davidson, and K.L. Gould. 2015a. The F-BAR Cdc15 promotes contractile ring formation through the direct recruitment of the formin Cdc12. *The Journal of cell biology*. 208:391-399.

Willet, A.H., N.A. McDonald, and K.L. Gould. 2015b. Regulation of contractile ring formation and septation in Schizosaccharomyces pombe. *Current opinion in microbiology*. 28:46-52.

Win, T.Z., Y. Gachet, D.P. Mulvihill, K.M. May, and J.S. Hyams. 2001. Two type V myosins with non-overlapping functions in the fission yeast Schizosaccharomyces pombe: Myo52 is concerned with growth polarity and cytokinesis, Myo51 is a component of the cytokinetic actin ring. *Journal of cell science*. 114:69-79.

Wong, K.C., N.I. Naqvi, Y. Iino, M. Yamamoto, and M.K. Balasubramanian. 2000. Fission yeast Rng3p: an UCS-domain protein that mediates myosin II assembly during cytokinesis. *Journal of cell science*. 113 (Pt 13):2421-2432.

Wu, J.Q., J.R. Kuhn, D.R. Kovar, and T.D. Pollard. 2003. Spatial and temporal pathway for assembly and constriction of the contractile ring in fission yeast cytokinesis. *Developmental cell*. 5:723-734.

Wu, J.Q., and T.D. Pollard. 2005. Counting cytokinesis proteins globally and locally in fission yeast. *Science (New York, N.Y.)*. 310:310-314.

Wu, J.Q., V. Sirotkin, D.R. Kovar, M. Lord, C.C. Beltzner, J.R. Kuhn, and T.D. Pollard. 2006. Assembly of the cytokinetic contractile ring from a broad band of nodes in fission yeast. *The Journal of cell biology*. 174:391-402.

Yang, Y., H. Yu, and Q. Cui. 2008. Extensive conformational transitions are required to turn on ATP hydrolysis in myosin. *J Mol Biol*. 381:1407-1420.

Ye, Y., I.J. Lee, K.W. Runge, and J.Q. Wu. 2012. Roles of putative Rho-GEF Gef2 in division-site positioning and contractile-ring function in fission yeast cytokinesis. *Molecular biology of the cell*. 23:1181-1195.

Zhang, D., A. Vjestica, and S. Oliferenko. 2010. The cortical ER network limits the permissive zone for actomyosin ring assembly. *Current biology : CB*. 20:1029-1034.

Zhou, Z., E.L. Munteanu, J. He, T. Ursell, M. Bathe, K.C. Huang, and F. Chang. 2015. The contractile ring coordinates curvature-dependent septum assembly during fission yeast cytokinesis. *Molecular biology of the cell*. 26:78-90.

Zhu, Y.H., Y. Ye, Z. Wu, and J.Q. Wu. 2013. Cooperation between Rho-GEF Gef2 and its binding partner Nod1 in the regulation of fission yeast cytokinesis. *Molecular biology of the cell*. 24:3187-3204.

CHAPTER 2: FISSION YEAST CYK3P IS A TRANSGLUTAMINASE-LIKE PROTEIN THAT PARTICIPATES IN CYTOKINESIS AND CELL MORPHOGENESIS

Luther W. Pollard[1], Masayuki Onishi[2], John R. Pringle[2], & Matthew Lord[1]

[1]Department of Molecular Physiology and Biophysics, University of Vermont, Burlington, Vermont, USA. [2]Department of Genetics, Stanford University School of Medicine, Stanford, California, USA.

Running Head: Roles of an inactive transglutaminase

Abbreviations:
EMM, Edinburgh minimal media; FRAP, fluorescence recovery after photo-bleaching; ROI, region of interest; SPB, spindle pole body; TGase, transglutaminase; YE5S, yeast extract plus supplements.

2.1. ABSTRACT

Cell morphogenesis is a complex process that relies on a diverse array of proteins and pathways. We have identified a transglutaminase-like protein (Cyk3p) that functions in fission yeast morphogenesis. The phenotype of a *cyk3* knockout strain indicates a primary role for Cyk3p in cytokinesis. Correspondingly, Cyk3p localizes both to the actomyosin contractile ring and the division septum, promoting ring constriction, septation, and subsequent cell separation following ring disassembly. In addition, Cyk3p localizes to polarized growth sites and plays a role in cell shape determination, and it also appears to contribute to cell integrity during stationary phase, given its accumulation as dynamic puncta at the cortex of such cells. Our results and the conservation of Cyk3p across fungi point to a role in cell wall synthesis and remodeling. Cyk3p possesses a transglutaminase domain that is essential for function, even though it lacks the catalytic active site. In a wider sense, our work illustrates the physiological importance of inactive members of the transglutaminase family, which are found throughout eukaryotes. We suggest that the proposed evolution of animal transglutaminase cross-linking activity from ancestral bacterial thiol proteases was accompanied by the emergence of a subclass whose function does not depend on enzymatic activity.

2.2. INTRODUCTION

Transglutaminases (TGases) are a family of enzymes that catalyze intramolecular or intermolecular protein cross-linking through isopeptide bond formation between lysine (or polyamines) and glutamine residues. The activity of the enzymes plays an important role in various intracellular and extracellular processes. For example, keratinocyte TGase functions in the terminal differentiation of keratinocytes and formation of the cornified cell envelope (Rice and Green, 1978; Thacher and Rice, 1985); tissue TGase (TG2) is found in many cell types and is involved in inflammation, apoptosis, cell adhesion, and cancer and other human diseases (Fesus and Szondy, 2005; Mangala and Mehta, 2005; Facchiano et al., 2006; Zemskov et al., 2006; Mehta et al., 2010). Factor XIII probably represents the best-studied TGase; it participates in blood clotting, tissue repair, and wound healing (Pisano et al., 1968; Schwartz et al., 1973; Mosher and Schad, 1979; Sakata and Aoki, 1980; Knox et al., 1986). A hallmark of these enzymes is a catalytic triad made up of conserved cysteine, histidine, and aspartate residues, each of which is essential for activity and defines the catalytic core (**Figure 2-1A** (Hettasch and Greenberg, 1994; Micanovic et al., 1994; Pedersen et al., 1994; Yee et al., 1994).

51
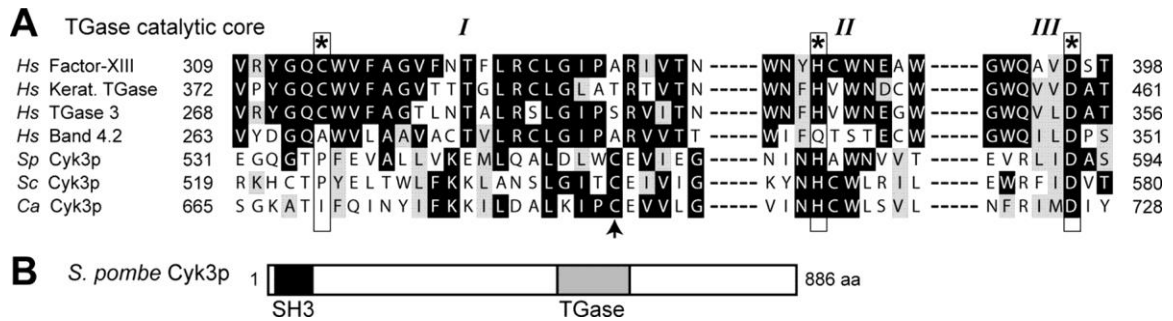
Figure 2-1: Conserved protein domains of Cyk3p.
Conserved protein domains of Cyk3p. (A) A sequence alignment comparing identities (black) and similarities (gray) among amino acids from four human transglutaminases and three Cyk3p homologues (*Sp*: fission yeast *S. pombe*; *Sc*, *Ca*: budding yeasts *S. cerevisiae* and *C. albicans*). The alignment centers on the active-site cysteine (motif I), histidine (II), and aspartate (III) residues (asterisks) forming the conserved catalytic triad in the transglutaminase core. The variable regions (dashed lines) between motifs I and II span 32 residues for the human transglutaminases (except TGase 3: 31 residues) and 14 residues for the Cyk3p proteins (except *Sc*: 12 residues); the variable regions between motifs II and III span 11 residues for human transglutaminases and 3 residues for the Cyk3p proteins. The arrowhead marks a cysteine residue (Cys-554 in *S. pombe*) conserved among the Cyk3p proteins. (B) Position of the SH3 (amino acids 10-65) and transglutaminase-like (amino acids 485-595) domains in the 886-residue fission yeast Cyk3p sequence. The domains were identified using the Blastp program.

The increasing abundance of protein sequence information has revealed a new inactive class of TGases that possesses a conserved catalytic domain lacking the catalytic triad (Makarova et al., 1999). For example, a red blood cell protein (band 4.2) possesses a TGase domain that lacks the catalytic cysteine and histidine residues (**Figure 2-1A**) and consequently lacks enzyme activity (Korsgren et al., 1990; Cohen et al., 1993). Naturally occurring mutations in the human band 4.2 gene cause congenital spherocytic anemia characterized by sphere-shaped (rather than biconcave disk–shaped) cells that are more prone to hemolysis (Yawata, 1994; Bruce et al., 2002; Dahl et al., 2004). This phenotype highlights the physiological relevance of proteins with inactive TGase domains, and may

reflect a structural role at the cell membrane in the case of band 4.2 (Satchwell et al., 2009). However, nothing is known regarding the cellular role (if any) of the inactive TGase domains themselves. In this study, we examined the role of an inactive TGase (Cyk3p) from the fission yeast *Schizosaccharomyces pombe.*

Cyk3p was originally identified in the budding yeast *Saccharomyces cerevisiae* (Korinek et al., 2000), and (based on available sequence data) represents a highly conserved fungal protein. Cyk3p participates in cytokinesis in *S. cerevisiae* (Korinek et al., 2000), and was recently found to be essential for cytokinesis and growth in the pathogenic budding yeast *Candida albicans* (Reijnst et al., 2010). Several studies in *S. cerevisiae* recently shed light on the molecular mechanisms governing Cyk3p function. Localization of Cyk3p at the division site depends on its N-terminal SH3 domain (Jendretzki et al., 2009), which mediates an interaction with a proline-rich region at the C-terminus of the C2 domain protein (Inn1p), a critical cytokinetic factor (Sanchez-Diaz et al., 2008; Jendretzki et al., 2009; Nishihama et al., 2009). Cell cycle–specific phosphorylation may regulate such complexes, because the division site localization of Cyk3p and Inn1p relies on the mitotic exit network (MEN; Meitinger et al., 2010), a conserved signaling pathway essential for the coordination of mitotic progression and cytokinesis (McCollum and Gould, 2001). Relatively little is known about fission yeast Cyk3p, although preliminary studies have pointed to a role in cytokinesis. Similar to several other fission yeast cytokinetic mutants, a *cyk3Δ* mutant was found to be sensitive to loss of the cytokinetic checkpoint mediated by the Cdc14 family phosphatase (Mishra et al., 2004). In addition, fission yeast Cyk3p was recently found to coprecipitate from cell extracts with F-BAR

protein Cdc15p (Roberts-Galbraith et al., 2010), an essential component of the contractile ring (Fankhauser et al., 1995).

In this study, we define roles for Cyk3p in fission yeast cytokinesis and morphogenesis and identify an inactive C-terminal TGase motif as the critical functional element. Overall, our study provides new insights into the mechanisms of Cyk3p function, cytokinesis, and cell morphogenesis in fungi, and more broadly identifies an important cellular role for the inactive subclass of the TGase family.

Table 2-1: Influence of Cyk3p on contractile ring dynamics.

| Strains | Rlc1p-GFP ring property (± SD)[a] | | | |
	assembly *(min)*	*dwell* *(min)*	*constriction* *(μm/min)*	*lifetime*[b] *(min)*
25°C				
cyk3[+]	17.9 ± 3.1	15.0 ± 3.1	0.40 ± 0.05	42.5
cyk3Δ	18.6 ± 3.9	20.7 ± 5.7	0.35 ± 0.10	52.1
36°C				
cyk3[+]	12.0 ± 1.7	12.6 ± 2.2	0.48 ± 0.05	35.5
cyk3Δ	18.5 ± 4.8	27.2 ± 14.0[c]	0.37 ± 0.10	56.9

2.3. MATERIALS AND METHODS

Table 2-2: Fission yeast strains.

Strain	Genotype	Source
MLP 3	h^+ leu1-32 ura4-D18 his7-366 ade6-M210 cyk3Δ::kan^R	This study
MLP 18	h^- leu1-32 ura4-D18 his7-366 ade6-M216 cyk3Δ::kan^R	This study
MLP 11	h^+ leu1-32 ura4-D18 his7-366 ade6-M210	This study
TP 6	h^+ leu1-32 his7-366 ade6-M216 cdc4-8	M. Balasubramanian
MLP 178	h^- leu1-32 ura4-D18 his7-366 ade6-M210 cdc4-8 cyk3Δ::kan^R	This study
TP 73	h^- leu1-32 ura4-D18 his7-366 ade6-M216 myo2-E1	M. Balasubramanian
MLP 17	h^- leu1-32 ura4-D18 his7-366 ade6-M210 myo2-E1 cyk3Δ::kan^R	This study
MLP 34	h^+ leu1-32 ura4-D18 his7-366 ade6-M210 myp2Δ::his7$^+$	T. Pollard
MLP 35	h^- leu1-32 ura4-D18 his7-366 ade6-M210 myp2Δ::his7$^+$ cyk3Δ::kan^R	This study
LP 112	h^- leu1-32 ura4-D18 his3-D1 ade6 chs2Δ::ura4$^+$ cyk3Δ::kan^R	This study
MLP 319	h^- leu1-32 ura4-D18 his7-366 ade6-M216 myo2-E1 rlc1-^{m}GFP:kan^R	This study
LP 109	h^+ leu1-32 ura4-D18 his7-366 ade6-M216 myo2-E1 cyk3Δ::kan^R rlc1-^{m}GFP:kan^R	This study
MLP 15	h^+ leu1-32 ura4-D18 his7-366 ade6-M210 cyk3-^{m}GFP::kan^R	This study
LP 37	h^+ leu1-32 ura4-D18 his3-D1 ade6 cyk3-3xGFP::kan^R	This study
MLY 757	h^- leu1-32 ura4-D18 his3-D1 ade6 cyk3-3xGFP::kan^R rlc1-^{m}Cherry::nat^R	This study
LP 116	h^+ leu1-32 ura4-D18 his3-D1 ade6 cdc25-22 cyk3-3xGFP::kan^R rlc1-^{m}Cherry::nat^R	This study
MLP 198	h^+ leu1-32 ura4-D18 his7-366 ade6-M210 rlc1-^{m}GFP:kan^R	This study
MLY 655	h^- leu1-32 ura4-D18 his7-366 ade6 cyk3Δ::kan^R rlc1-^{m}GFP:kan^R	This study
MLY 572	h^- leu1-32 ura4-D18 ade6 his3-D1 rlc1-^{m}GFP:kan^R sad1-^{m}GFP:kan^R	This study
MLY 657	h^- leu1-32 ura4-D18 ade6 his3-D1 cyk3Δ::kan^R rlc1-^{m}GFP:kan^R sad1-^{m}GFP:kan^R	This study
LP 33	h^- leu1-32 ura4-D18 his3-D1 ade6 cyk3-3xGFP::kan^R fim1-^{m}Cherry::nat^R	This study

Table 2-2: (continued).

Strain	Genotype	Source
TP 19	h^- *leu1-32 ura4-D18 his7-366 ade6-M216 cdc12-112*	M. Balasubramanian
MLP 323	h^- *leu1-32 ura4-D18 his7-366 ade6 cdc12-112 cyk3Δ::kan^R*	This study
TP 30	h^+ *leu1-32 ura4-D18 his7-366 ade6-M210 cdc15-127*	M. Balasubramanian
MLP 326	h^- *leu1-32 ura4-D18 his7-366 ade6 cdc15-127 cyk3Δ::kan^R*	This study
LP 69	h^- *leu1-32 ura4-D18 his3-D1 ade6 sid2-250 cyk3-3xGFP::kan^R rlc1-^{m}Cherry::nat^R*	This study

2.3.1. FISSION YEAST STRAINS, PLASMIDS, AND GENETIC METHODS

Strains were grown in EMM (Edinburgh minimal media) or YE5S (yeast extract plus supplements) medium, and standard genetic and cell biology protocols were used (Moreno et al., 1991). Table 2 lists the strains used in this study. Gene deletion mutants and strains expressing fusion proteins tagged with GFP, 3GFP, or Cherry were constructed using genomic integrations with the relevant *kan^R* or *nat^R* cassettes (Bahler et al., 1998b). Cyk3p-GFP and Cyk3p-3GFP fusions were functional based on their ability to fully support Cyk3p function in a *cdc4-8* background. Plasmids used in this study are listed in Table 3. The *cyk3* open reading frame (ORF) was amplified from a genomic library using the primers: 5′ *Xho*I-*cyk3 CTCGAG*ATGTCCATTCCTAAACAACTACCATGC; 3′ *Not*I-*cyk3 GCGGCCGC*CAACCGCCTGCCAGGTTGCATAGC. The ORF was ligated into *Xho*I/*Not*I-linearized pDS572a (overexpression vector with the *nmt1* high-strength promoter) and pDS572-81 (*nmt1-81* weak-strength promoter vector for plasmid-based complementation). A Cyk3p N-terminal truncation construct lacking amino acids 3–65

(spanning the entire SH3 domain and seven upstream residues) was made using the 5′ primer: *Xho*I-*cyk3-SH3Δ*: *CTCGAG*ATGAGTGATATTCCCACGGTACGACCTGGC. A Cyk3p Asp-592-Ala point mutant was constructed using overlap extension (Ho et al., 1989) to amplify a mutated 3′ 800–base pair fragment of the *cyk3* ORF. Overlapping subfragments were generated using the following primers: 1) 5′ *Ssp*I-*cyk3*: CTGTAGGTACT*AATATT*CATAACATG and 3′ Asp-592-Ala: GGCAAAACTAGCAGCAATTAGACG; and 2) 5′ Asp-592-Ala: CGTCTAATTG-CTGCTAGTTTTGCC and 3′ *Hpa*I-*cyk3*: GTTTCCCAGAAAGCCTGT*GTTAAC*GTG. The mutant fragment was amplified from the overlapping fragments (using the 5′ *Ssp*I and 3′ *Hpa*I primers) and subcloned into a Topo-*cyk3* clone via the unique *Ssp*I and *Hpa*I sites (which reside in the 3′ region of the *cyk3* ORF). The mutated *cyk3* ORFs were inserted into the pDS572a and pDS572-81 vectors. The same strategy was used to generate Cyk3p-Cys-554-Ala and -His-577-Ala mutants with the following primers (and their 3′ complements): 5′ Cys-554-Ala: GCACTAGATTTATGGGCTGAGGTTATCG and 5′ His-577-Ala: CCAGAGATATTAATATAAATGCTGCTTGGAATG. The fidelity of *cyk3* sequences was confirmed by DNA sequencing.

Table 2-3: Plasmids.

Plasmid	Comment	Source
pFA6a-kanMX6	template for gene replacement with a *kan^R*	(Bahler et al., 1998)
pFA6a-kanMX6/nat^R--3xGFP/-^{m}Cherry	casette templates for integration of C- the genome	J.-Q. Wu; W.-L. Lee; V. Sirotkin.
nmt1^{prom}	pDS572a (*nmt1* promoter, C-terminal GFP, *ura4$^+$*)	S. Forsburg
nmt1^{prom}-cyk3	pDS572a harboring wild-type *cyk3*	This study
nmt1^{prom}-cyk3-D592A	pDS572a harboring *cyk3-D592A*	This study
nmt1^{prom}-cyk3-H577A	pDS572a harboring *cyk3-H577A*	This study
nmt1^{prom}-cyk3-C554A	pDS572a harboring *cyk3-C554A*	This study
nmt1^{prom}-cyk3-SH3Δ	pDS572a harboring *cyk3-SH3Δ*	This study
pGFP	pDS572-81 (*nmt1-81x* promoter, C-terminal GFP, *ura4$^+$*)	S. Forsburg
cyk3-GFP	pDS572-81 harboring wild-type *cyk3*	This study
cyk3-D592A-GFP	pDS572-81 harboring *cyk3-D592A*	This study
cyk3-H577A-GFP	pDS572-81 harboring *cyk3-H577A*	This study
cyk3-C554A-GFP	pDS572-81 harboring *cyk3-C554A*	This study
cyk3-SH3Δ-GFP	pDS572-81 harboring *cyk3-SH3Δ*	This study

2.3.2. MICROSCOPY

Differential interference contrast (DIC) and epifluorescence cell images were captured using a Nikon (Melville, NY) TE2000-E2 inverted microscope with motorized fluorescence filter turret and a Plan Apo 60×/1.45 numerical aperture (NA) objective. For fluorescence, an EXFO X-CITE 120 illuminator was utilized. NIS Elements software was used to control the microscope, two Uniblitz shutters, a Photometrics CoolSNAP HQ2 14-bit camera, and auto-focusing. Time-lapse movies of cells monitored Cyk3p and/or Rlc1p

contractile ring dynamics (every 2–3 min for 2–3 h) and Cyk3p and/or Fim1p cortical patch lifetimes (by capturing images every 5–10 s for 5–10 min) using appropriate filters. For ring movies, autofocusing was performed on the DIC channel before each image capture. Cell suspensions (3 μl) were mounted on flat 30-μl media pads (solidified by 1% agarose) prepared on the slide surface. VALAP (1:1:1 vasoline:lanolin:paraffin) was used to seal slides and coverslips. For simultaneous tracking of SPBs (Sad1p-GFP) and rings (Rlc1p-GFP), a Z-stack of six images (taken every 0.75 μm spanning the depth of the cell) was collected every 2–3 min for 90–120 min. Images were captured using Nikon (Melville, NY) ND software, and analysis of ring and patch dynamics was performed using Image J, Microsoft Excel, and KaleidaGraph software. Ring dynamics were quantified by assessing individual phases: *assembly* was time taken for Rlc1p-GFP to compact into a mature ring following its appearance as a broad band of nodes; *dwell* was time from completion of ring compaction until initiation of constriction; *constriction* was change in ring circumference over time. Dwell times and constriction initiation were discerned by plotting ring diameter over time for each ring, and constriction rates were derived from the slopes of these plots.

FRAP experiments used confocal laser-scanning microscopy with a Zeiss LSM 510 META system equipped with an argon laser, META detector, and a Plan-Apo 100×/1.4 NA objective. Cells were mounted on 1% agarose pads (as described above) prior to microscopy at room temperature. A region of interest (ROI) was selected on Cyk3p-GFP rings for directed bleaching. Photobleaching iterations were performed briefly at high laser power, resulting in ∼90–100% signal loss. Signal recovery was monitored by time-lapse analysis at low laser power, with images collected every 5 s postbleach until the recovery

59

signal plateaued (~2 min). The criterion for determining whether Cyk3p rings were constricting or not lay in their diameters: if rings were clearly narrower than the cell diameter, we scored them as constricting; if they were the same diameter as the cell width, we viewed them as nonconstricting. The LSM 510 software (version 4.2) was used to collect images and perform data analysis (see Figure 4B legend). Recovery curves of Cyk3p-GFP signal versus time were plotted and fit using KaleidaGraph software. Data sets for each trace were corrected for any additional bleaching encountered during time-lapse imaging by a control ROI (derived from an unbleached ring in the same field of cells). To facilitate curve fitting, zero signal intensity was set for each trace by subtracting any residual Cyk3p-GFP signal (detected at the first time point postbleach, 0 s) from all trace values. The $t_{1/2}$ values ($\pm$ SD) represent the mean generated from the fits of each individual FRAP experiment. EM was performed as previously described (Nishihama *et al.*, 2009), with minor modifications. Cells were cultured overnight in YE5S medium at 25°C to mid-log phase, diluted to an OD_{600} of 0.1, and then regrown at 27.5°C to an OD_{600} of 0.5 (or at 37°C for 4 h). The cells were harvested, fixed with glutaraldehyde and potassium permanganate, stained with uranyl acetate, and embedded in LR White resin (Fluka, St. Louis, MO). Thin-section samples were poststained with uranyl acetate and lead citrate and were observed using a JEM1230/JEOL microscope (Tokyo, Japan) equipped with an ORIUS SC1000A cooled-CCD camera (Gatan, Pleasanton, CA).

2.3.3. WESTERN BLOTTING

Cyk3Δ cells harboring *pGFP* (vector alone), *cyk3-GFP*, *cyk3-Asp-592-Ala-GFP*, *cyk3-His-577-Ala-GFP*, *cyk3-Cys-554-Ala-GFP*, or *cyk3-SH3Δ-GFP* plasmids were grown to an OD_{595} of 1 in 200 ml of EMM Ura^- medium. Cells were then harvested and washed once in water and once in ice-cold lysis buffer (750 mM KCl, 25 mM Tris-HCl, pH 7.4, 4 mM $MgCl_2$, 20 mM $Na_4P_2O_7$, 2 mM ethylene glycol tetraacetic acid, and 0.1% Triton X-100). Pellets were resuspended in an equal volume of ice-cold lysis buffer with additives consisting of 1 mM dithiothreitol, 4 mM ATP, 2 mM phenylmethylsulfonyl fluoride, and complete EDTA-free protease inhibitors (Roche, Indianapolis, IN). From this point forward, all work was performed at 4°C and samples were stored on ice. Cells were lysed by glass bead beating with a Fastprep (MP Biochemicals, Solon, OH). Lysates were normalized for total protein using a Bradford mix (Bio-Rad, Hercules, CA), mixed 1:1 with 2X SDS–PAGE loading buffer, and boiled for 10 min. Samples were run on a 10% SDS–PAGE gel, transferred to nitrocellulose, and immunoblotted (Sambrook et al., 1989) using anti-GFP (Clontech, Mountain View, CA) and anti-actin (Chemicon, Temecula, CA) antibodies diluted 1:1000 in PBS containing 0.1% Tween-20. Horse radish peroxidase-conjugated secondary antibodies were used (diluted 1:3000).

2.4. RESULTS

2.4.1. FISSION YEAST CYK3P FUNCTIONS IN CYTOKINESIS AND

MORPHOGENESIS
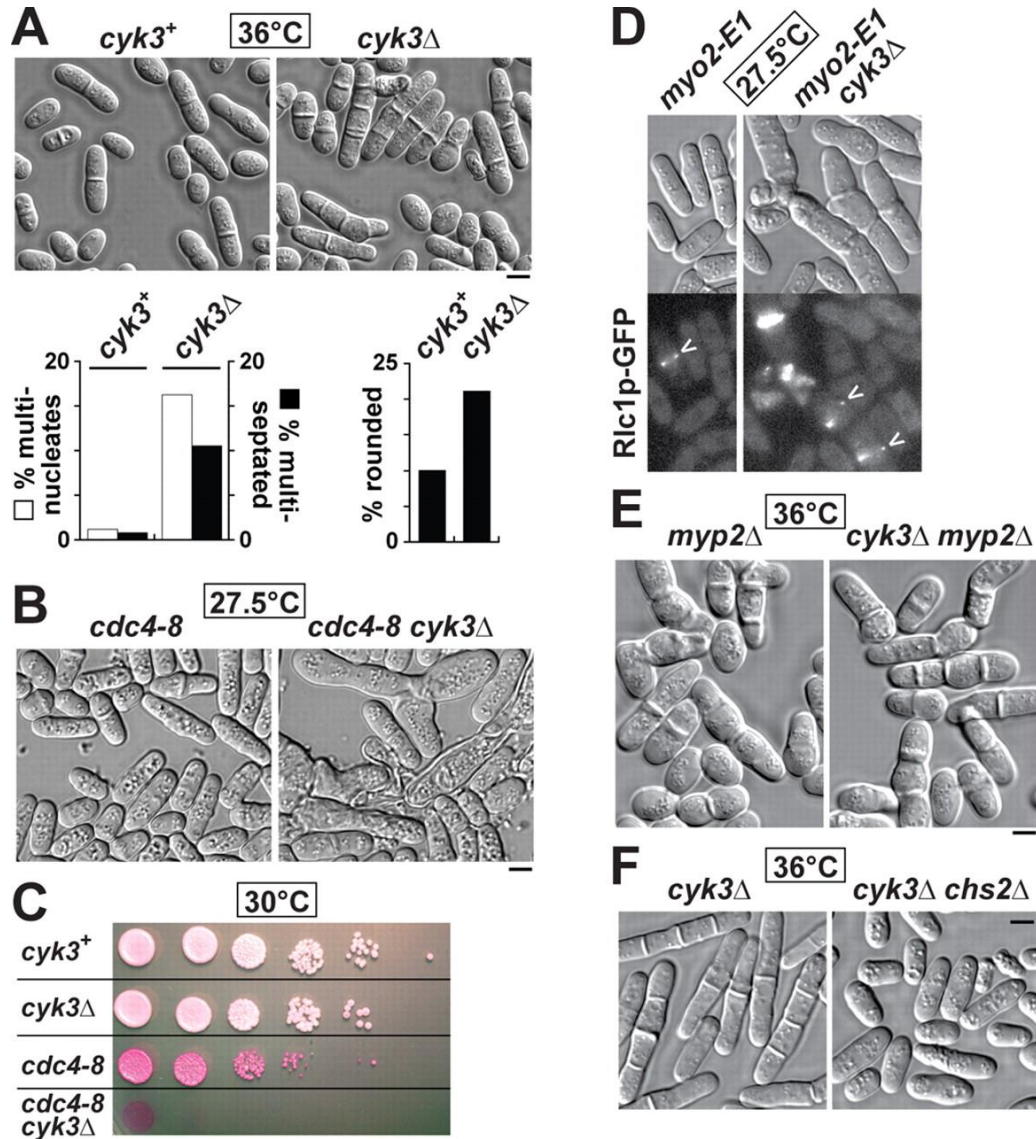
Figure 2-2: Cyk3p functions in cytokinesis and polarized growth.
Cyk3p functions in cytokinesis and polarized growth. (A) Representative DIC images of wild-type (MLP 11) and *cyk3Δ* (MLP 3) cells following growth at 36°C in YE5S medium. Plots below provide quantification of morphological defects observed under these conditions. Left, percentages of multinucleate cells (following treatment with 4′,6-diamidino-2-phenylindole stain: 3+ nuclei/cell, □; n = 750) and of cells possessing >1

division septa, ■ (which account for the majority of multinucleate cells). Right, percentages of cells with a rounded/swollen shape (n = 750). (B) Representative *cdc4-8* (TP 6) and *cdc4-8 cyk3Δ* (MLP 178) cells following growth at 27.5°C on YE5S medium. (C) Growth of wild-type, *cyk3Δ*, *cdc4-8*, and *cdc4-8 cyk3Δ* strains at 30°C. Five-microliter cell suspensions of identical optical density were spotted along with five 10-fold serial dilutions onto a YE5S plates. The plate contained 5 µg/ml phloxin B, a pink dye that accumulates inside dead cells (note the pink color of the *cdc4-8* and *cdc4-8 cyk3Δ* colonies). (D) Representative *myo2-E1* (TP 73) and *myo2-E1 cyk3Δ* (MLP 17) cells following growth at 27.5°C on YE5S medium. Top panels, DIC images; bottom panels, Rlc1p-GFP localization at rings (as denoted by arrowheads). (E) Representative *myp2Δ* (MLP 34) and *myp2Δ cyk3Δ* (MLP 35) cells following growth at 36°C on YE5S medium. (F) Representative *cyk3Δ* and *cyk3Δ chs2Δ* (LP 112) cells following growth at 36°C on YE5S medium. Counts of the percentages of multinucleate cells for the strains shown in (B), (D), (E), and (F) are provided in **Figure 2-S1**.

Like other known fungal members of this protein family (Korinek et al., 2000; Reijnst et al., 2010), fission yeast Cyk3p possesses an N-terminal SH3 domain (**Figure 2-1B**). In addition, we identified a TGase-like domain in the C-terminal half of the protein (**Figure 2-1B**), a domain preserved in Cyk3p sequences from other fungi. This 111–amino acid domain showed homology to TGase domains in *S. cerevisiae* Cyk3p (30% identical/51% similar) and animal TGases (e.g., 17%/41% vs. human factor XIII). The catalytic core of the TGase domain can be separated into three motifs centered on the conserved cysteine, histidine, and aspartic acid active-site residues that form the catalytic triad. Interestingly, the catalytic triads of the fungal Cyk3p proteins are all incomplete, containing the conserved histidine and aspartic acid residues in motifs II and III but lacking the active site cysteine in motif I (**Figure 2-1A**). Deletion of *cyk3* had no obvious effect on morphology or growth at 25–32°C. However, *cyk3Δ* cells exhibited temperature-sensitive defects in cell separation at 36°C, as reflected by the appearance of elongated cells with multiple septa and multiple nuclei (**Figure 2-2A**). In addition, *cyk3Δ* cells showed a greater

tendency to adopt a rounded/swollen morphology, as opposed to the typical cigar shape of fission yeast (**Figure 2-2A**). Consistent with a significant role for Cyk3p in cytokinesis, the *cyk3Δ* mutation showed synthetic defects when combined with mutations in genes encoding known contractile ring components, such as Myo2p (myosin II), Cdc4p (essential light chain), Cdc12p (formin), and Cdc15p (F-BAR protein) (**Figure 2-2**, **B** and **C**, and Supplemental **Figure 2-S1**). Although the contractile rings typically assembled in such double mutants, they showed obvious defects in cytokinesis (**Figure 2-2D**), suggesting a role for Cyk3p in ring constriction.

Surprisingly, unlike *myo2-E1* and many other cytokinetic mutations (Bezanilla et al., 1997; Motegi et al., 1997), *cyk3Δ* did not exhibit synergistic cytokinetic defects when combined with a *myp2* null (Figures 2E and S1). Myp2p is a nonessential myosin II required for normal cytokinesis (Bezanilla et al., 1997; Motegi et al., 1997), and the lack of an additive phenotype suggests that Cyk3p and Myp2p may share a specific function in cytokinesis. Myp2p is known to associate with chitin synthase (Chs2p), an inactive form of the enzyme that localizes to the contractile ring and contributes to septum formation in fission yeast (Martin-Garcia et al., 2003; Martin-Garcia and Valdivieso, 2006). We therefore also examined a *cyk3Δ chs2Δ* double mutant. Interestingly, loss of Chs2p completely suppressed the cytokinetic defects associated with loss of Cyk3p (**Figures 2-2F** and **2-S1**), suggesting a functional relationship between these two proteins at the septum.

64

2.4.2. CYK3P LOCALIZES TO THE CONTRACTILE RING, DIVISION

SEPTUM, AND SITES OF POLARIZED GROWTH
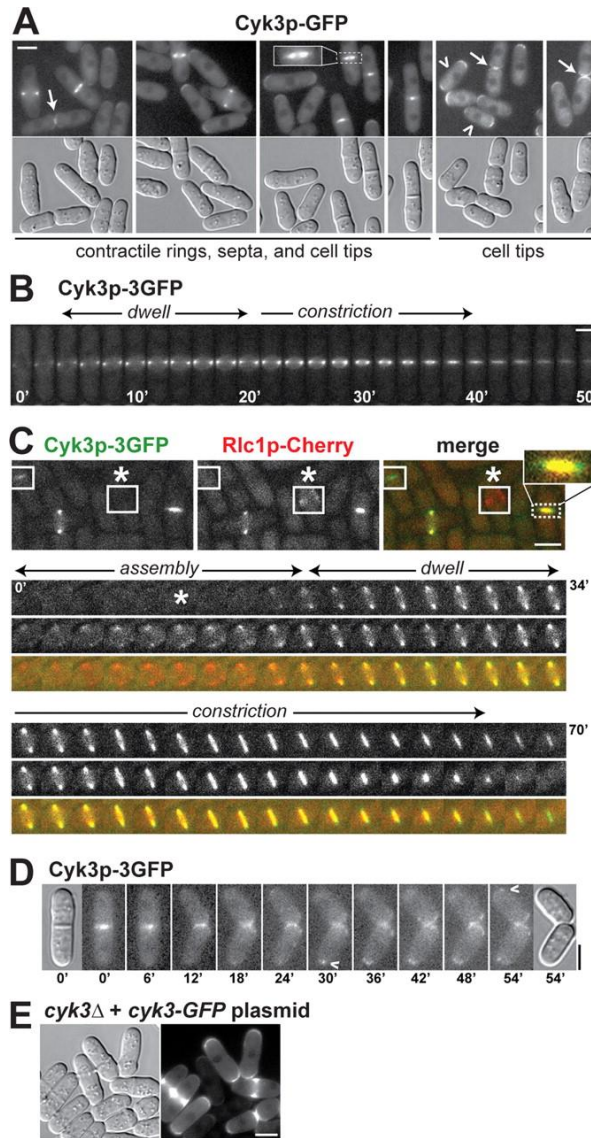
Figure 2-3: Cyk3p localization dynamics during cell division and growth.
Cyk3p localization dynamics during cell division and growth. (A) Localization of Cyk3p-GFP to contractile rings, septa, and cell tips (in strain MLP 15). Box, magnification of the division site of a cell undergoing ring constriction and septation; arrows, Cyk3p appearing at newly formed cell tips during cell separation; arrowheads, Cyk3p visible at both cell poles in separated cells. (B) Time-lapse observations of Cyk3p-3GFP (LP 37) at the division site from completion of ring assembly to shortly after ring disassembly. (C to D) Colocalization of Cyk3p and the myosin II RLC. (C) Representative cells (MLY 757) illustrating the distinct localization profiles of Cyk3p-3GFP (left and green in merge) and

Rlc1p-Cherry (center and red in the merge). Left box, a cell showing the continuing presence of Cyk3p at the division site following disappearance of the contractile ring; center box, absence of Cyk3p during ring assembly; right box in merge, overlapping Cyk3p and Rlc1p signals in the contractile ring (yellow) and the relatively faint Cyk3p signal in the septum surrounding the ring (green). (A time-lapse movie of this field of cells is provided in Movie S1.) Bottom panels, time-lapse observations showing the localization patterns of Cyk3p and Rlc1p. The 10-min image (asterisk) corresponds to the assembling-ring stage, as marked with an asterisk in (C). (D) Time-lapse observations of Cyk3p-3GFP localization from 12 min after completion of ring constriction and septation, which is also 12 min before cell separation. (E) Cyk3p-GFP localization following expression from a multi-copy plasmid with *cyk3-GFP* under control of the weak-strength *81nmt1*-inducible promoter. *cyk3Δ* cells were transformed and grown in EMM lacking uracil at 30°C. Scale bars (A–E): 4 μm.

We used gene replacement to generate single and triple chromosomal green fluorescent protein (GFP) fusions to examine the subcellular localization of endogenous Cyk3p. The fusion proteins were functional based on their ability to fully support Cyk3p function in a *cdc4-8* background. During vegetative growth, Cyk3p localized to three distinct sites: contractile rings, division septa, and cell tips (**Figure 2-3A**). The Cyk3p signal was most prominent at contractile rings. Time-lapse analysis revealed that Cyk3p joins the ring at the final stages of its assembly, is present at both rings and across growing septa during ring constriction, and remains as a band spanning the septum following ring disassembly (**Figure 2-3B**). This pattern was particularly clear when Cyk3p was colocalized with the myosin II regulatory light chain Rlc1p, which assembles earlier and disappears following ring contraction (**Figure 2-3C** and **Supplemental Movie 2-S1**).

On contractile ring disassembly, Cyk3p localization at the septum was relatively faint, but it became brighter a short time later, forming a tight spot at the center of the septum just before cell separation and remaining at the new cell poles following separation

66

(**Figure 2-3**, **A** and **D**). This unipolar tip localization became bipolar as Cyk3p accumulated at the old cell poles later in the cell cycle (**Figure 2-3D**). Although the bipolar tip localization was relatively faint when the tagged Cyk3p was expressed at endogenous levels, it became more conspicuous when Cyk3p-GFP was expressed from a multi-copy plasmid (**Figure 2-3E**).

In summary, Cyk3p localizes in a manner consistent with roles in cell morphogenesis during both division and polarized cell growth.

2.4.3 CYK3P IS A COMPONENT OF THE CONTRACTILE RING AND

PROMOTES RING DYNAMICS
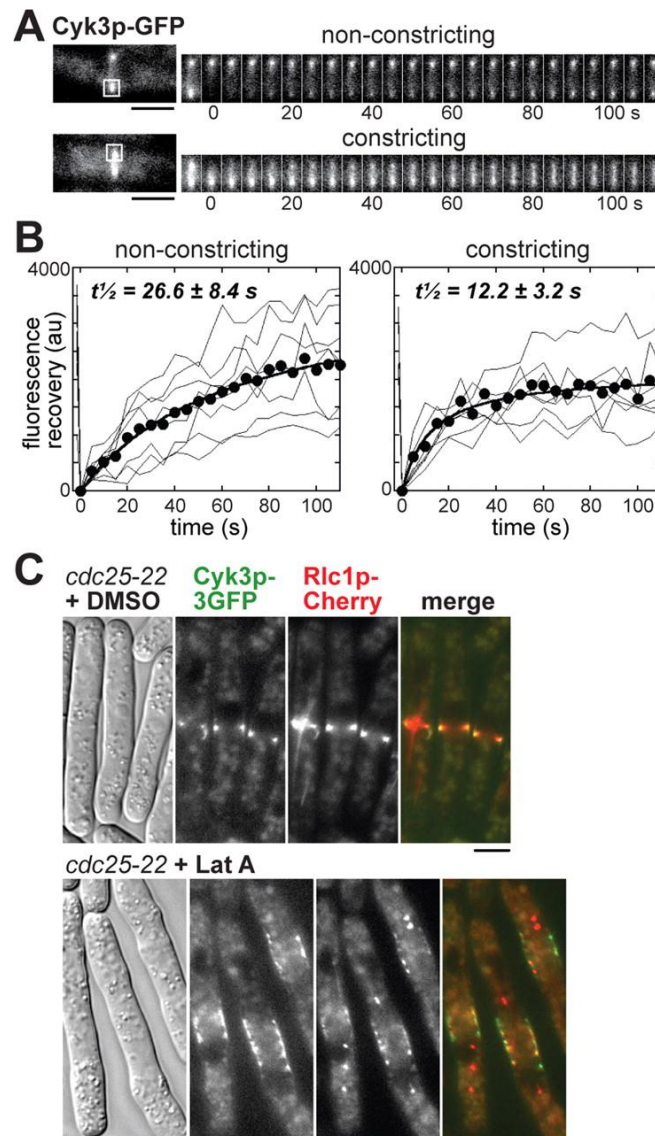
Figure 2-4: Cyk3p is a contractile ring component.
Cyk3p is a contractile ring component. (A and B) Measurement of Cyk3p exchange rates in contractile rings using FRAP. *cyk3-GFP* (MLP 15) cells were grown in YE5S medium at 25°C and examined at room temperature, as described in *Materials and Methods.* (A) Representative images comparing the recovery of Cyk3p-GFP fluorescence in nonconstricting (top) and constricting (bottom) rings. Left, cells before bleaching; the ROIs (white boxes) were then bleached at time zero. Right, recovery of signal over 110 s after bleaching. (B) Quantitation of FRAP in experiments like those in (A). Fluorescence intensities measured prebleach (−1.5 s) and postbleach (every 5 s for 0–110 s) are plotted.

Individual ROI traces (thin lines) are shown (n = 7–8) along with the averages (filled circles, thick line). (C) Cyk3p ring assembly relies on actin filaments. Cells (LP 116) were arrested at the G2 phase of the cell cycle by invoking the temperature-sensitivity of the *cdc25-22* mutation via 4 h of growth at 36°C. Cells were released from the arrest by growth at 25°C for 30 min in the presence of dimethyl sulfoxide (control) or 10 μM latrunculin A to prevent actin polymerization and contractile ring formation. In the presence of latrunculin, Cyk3p and myosin II (Rlc1p-Cherry) localize at the division site in (actin-independent) broad bands. Scale bars (A, C): 4 μm.

Given its prominent localization at the actomyosin ring, we tested whether Cyk3p was truly a component of this structure. Fluorescence recovery after photobleaching (FRAP) studies have shown that ring components exchange rapidly and that myosin II Myo2p exchanges with different kinetics in nonconstricting and constricting rings (Sladewski et al., 2009; Stark et al., 2010). Examination of Cyk3p-GFP exchange revealed almost identical kinetics to those of Myo2p in both nonconstricting ($t_{1/2} = 27$ s vs. ~37 s for Myo2p), and constricting ($t_{1/2} = 12$ s vs. ~13 s for Myo2p) rings (**Figure 2-4**, **A** and **B**; Sladewski *et al.*, 2009). Depolymerization of the actin cytoskeleton with latrunculin A blocked the formation of both myosin II and Cyk3p rings and led to a buildup of both proteins as ring precursors at the incipient medial division sites (**Figure 2-4C**). Taken together, these results suggest that Cyk3p is indeed a component of the actomyosin ring.
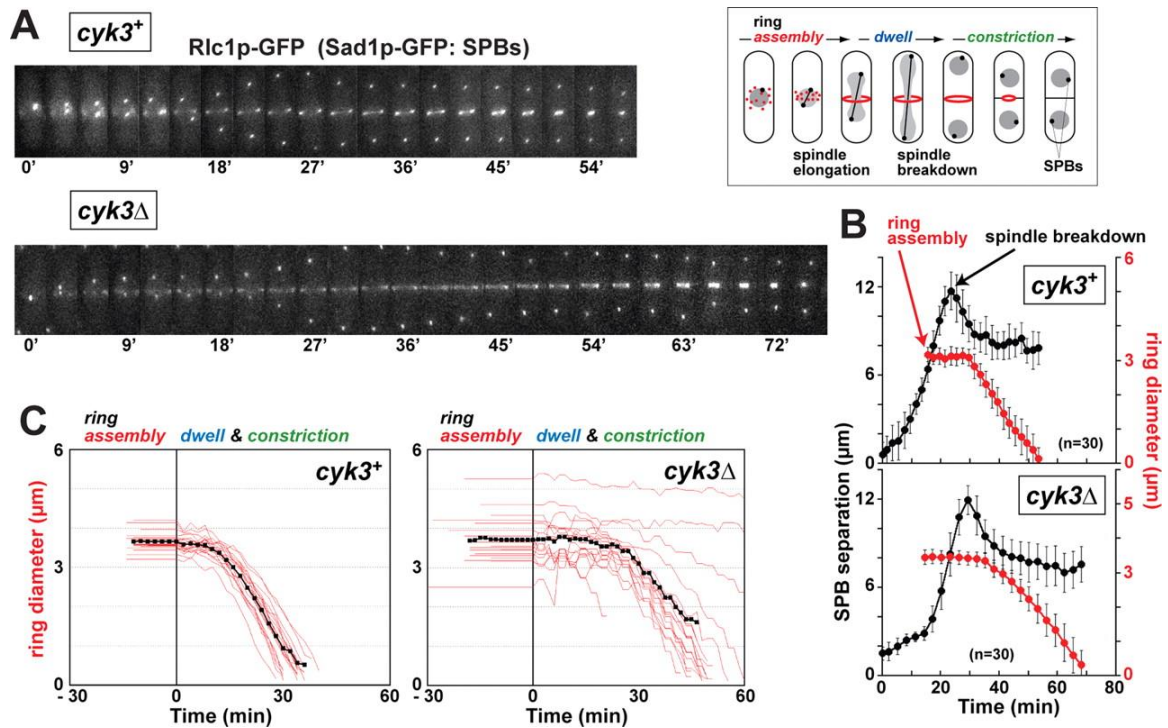
Figure 2-5: Cyk3p affects contractile ring dynamics.

Cyk3p affects contractile ring dynamics. Ring dynamics and mitotic spindle behavior were assessed by tracking Rlc1p-GFP and Sad1p-GFP, respectively. (A) Time-lapse observations (maximum projections from six Z-sections captured every 3 min) on representative wild-type (MLY 572) and *cyk3Δ* (MLY 657) cells grown in YE5S medium at 25°C. The observations begin immediately before SPB separation. Right, schematic shows the normal timing of ring (red) assembly, dwell, and constriction phases relative to mitotic progression based on SPB dynamics. (B) Plots summarizing the results from wild-type and *cyk3Δ* cells examined as in (B). For each strain, mean ring diameters (red) and SPB separation distances (black) were aligned based on the times at which each ring initiated constriction, and time zero was defined as the mean time from initial SPB separation to initiation of ring constriction. The times at which ring assembly was completed and spindle breakdown began are indicated by arrows; error bars show standard deviations. Dwell phases (horizontal portion of curve) and constriction phases (diagonal portion of curve) are evident. Table 1 contains average values and statistics. (C) Traces showing the ring assembly, dwell, and constriction phases for 20 individual cells (red) and the corresponding means (black) from wild-type (MLP 198) and *cyk3Δ* (MLY 655) cells examined by time-lapse microscopy in YE5S medium at 23°C after growth in the same medium at 36°C. Time zero is defined as the completion of ring assembly for each cell and thus represents the transition from assembly to dwell phases. SPB analysis was not performed in cells pregrown at 36°C, because Sad1p-GFP fails to mark SPBs under these conditions.

To test for a possible role of Cyk3p in contractile ring dynamics, we first monitored contractile ring behavior, using Rlc1p-GFP as a marker, in relation to mitotic progression, as judged by the spindle-pole body (SPB) protein Sad1p-GFP (**Figure 2-5A**, **left box**). Using the beginning of SPB separation as a reference point, we found that ring assembly time and constriction rate were affected little or not at all in a *cyk3Δ* mutant grown at 25°C, whereas the preconstriction "dwell" time was significantly lengthened (**Figure 2-5**, **A** and **B**, and **Table 2-1**). Interestingly, the delay was paralleled by a delay in the completion of spindle elongation: although ring constriction began ∼8–9 min following spindle breakdown in both wild-type and *cyk3Δ* cells, spindle breakdown (like ring constriction) was delayed ∼6 min in the mutant relative to wild-type (**Figure 2-5B**). The reason for this delay is not clear, but it appeared to be due mostly to a slower spindle elongation during the phase of contractile ring assembly (**Figure 2-5B**).

The ability of *cyk3Δ* cells to grow at 36°C allowed a further informative analysis in which cells grown at 36°C were subsequently imaged at 23°C. In this case, the assembly, dwell, and constriction phases were all significantly affected, with the largest effect on the dwell time (**Figure 2-5C** and **Table 2-1**), probably because the absence of Cyk3p during growth at 36°C produced changes in the levels of Cyk3p-interacting proteins that could affect ring dynamics even after a return to lower growth temperature. In summary, although Cyk3p appears to be involved in all phases of contractile ring function, its most important role seems to be in promoting ring constriction.

2.4.4. CYK3P PARTICIPATES IN CELL SEPARATION FOLLOWING

DISASSEMBLY OF THE CONTRACTILE RING
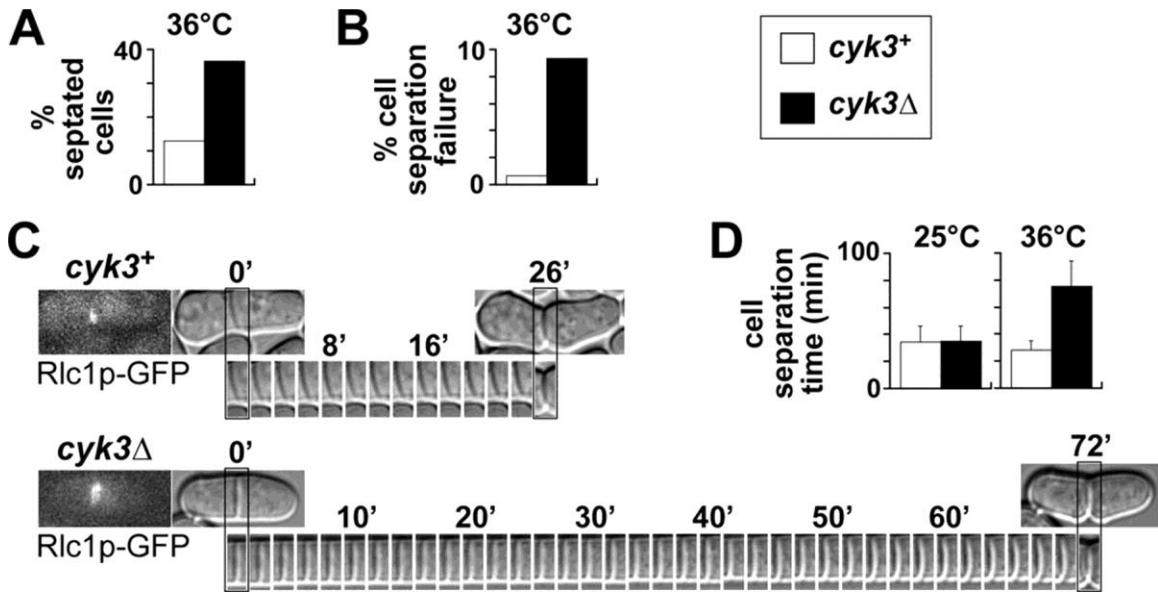
Figure 2-6: Cyk3p promotes cell separation.
Cyk3p promotes cell separation. The role of Cyk3p was examined by comparing the efficiencies with which wild-type (MLP 198) and *cyk3Δ* (MLY 655) cells transitioned from septation to separation during growth on YE5S medium. (A and B) Histograms comparing the percentages of (A) cells with visible septa (n = 500) and (B) cell separation failure (n = 128–146) following growth at 36°C. Separation failure was defined as the failure of a septated cell to separate during the course of the 3-h time-lapse movie. Because *cyk3Δ* cells averaged 75.6 min from septum completion to cell separation during growth at 36°C (D), we only scored a cell as failing when a septum had been present >76 min by the end of the movie. (C) Single-cell images tracking medial division sites from septum completion (0′) to cell separation (defined as the loss of continuity between daughter cells as they split apart; see far right panels) for representative cells grown at 36°C. Completion of septation coincides with completion of contractile ring constriction (indicated by the fluorescence images of the disassembling Rlc1p-GFP ring, which is transiently observed at mid-cell as a smear following constriction). (D) Summary of average separation intervals (± SD) from experiments like those in (C), performed at 25 and 36°C (n = 11–15).

The localization of Cyk3p to the septal region (**Figure 2-3**) and multi-septate

phenotype of *cyk3Δ* mutants (**Figure 2-2A**) suggested Cyk3p might play a role in the

maturation of the septum, its splitting at cell division, or both. Consistent with such a

72

role(s), *cyk3Δ* cells showed increased percentages of septated cells (**Figure 2-6A**) and of cells that apparently failed to separate (**Figure 2-6B**), as well as an increase in the average time from septum completion to cell separation (**Figure 2-6**, **C** and **D**), during growth at 36°C. These effects were not seen at 25°C (**Figure 2-6D**), and even at 36°C, septum completion appeared to coincide with the completion of contractile ring constriction, as in wild-type cells (**Figure 2-6C**). Thus, in addition to a role in actomyosin ring constriction, Cyk3p also contributes to cell separation.

2.4.5. CYK3 CONCENTRATES IN DYNAMIC CORTICAL PUNCTA DURING STATIONARY PHASE

When cells expressing Cyk3-GFP grew to stationary phase, they displayed a pattern of localization that appeared to be distinct from the division site and cell tip localization seen during vegetative growth. In particular, Cyk3p was found randomly throughout the cortex as discrete, dynamic puncta (**Figure 2-S2** and **Movies 2-S2** and **2-S3**). Although these puncta were similar in size and distribution to endocytic actin patches, Cyk3p did not colocalize with the actin-patch component Fim1p (fimbrin) during stationary phase (**Figure 2-S2**), and the Cyk3p puncta had a considerably longer average lifetime (~4 min) than did Fim1p or actin patches (~20 s; **Figure 2-S2**; Sirotkin et al*.,* 2010). In addition, unlike typical endocytic patches, the Cyk3p puncta did not depend on actin (**Figure 2-S2**) and often showed considerable lateral motility (Movies 2 and 3). These observations suggest that Cyk3p may play a more general role in cell-surface organization in addition to its roles at specific sites during the vegetative cell cycle.

73

2.4.6. OVEREXPRESSION OF CYK3P LEADS TO DEFECTS IN CYTOKINESIS AND CELL SHAPE
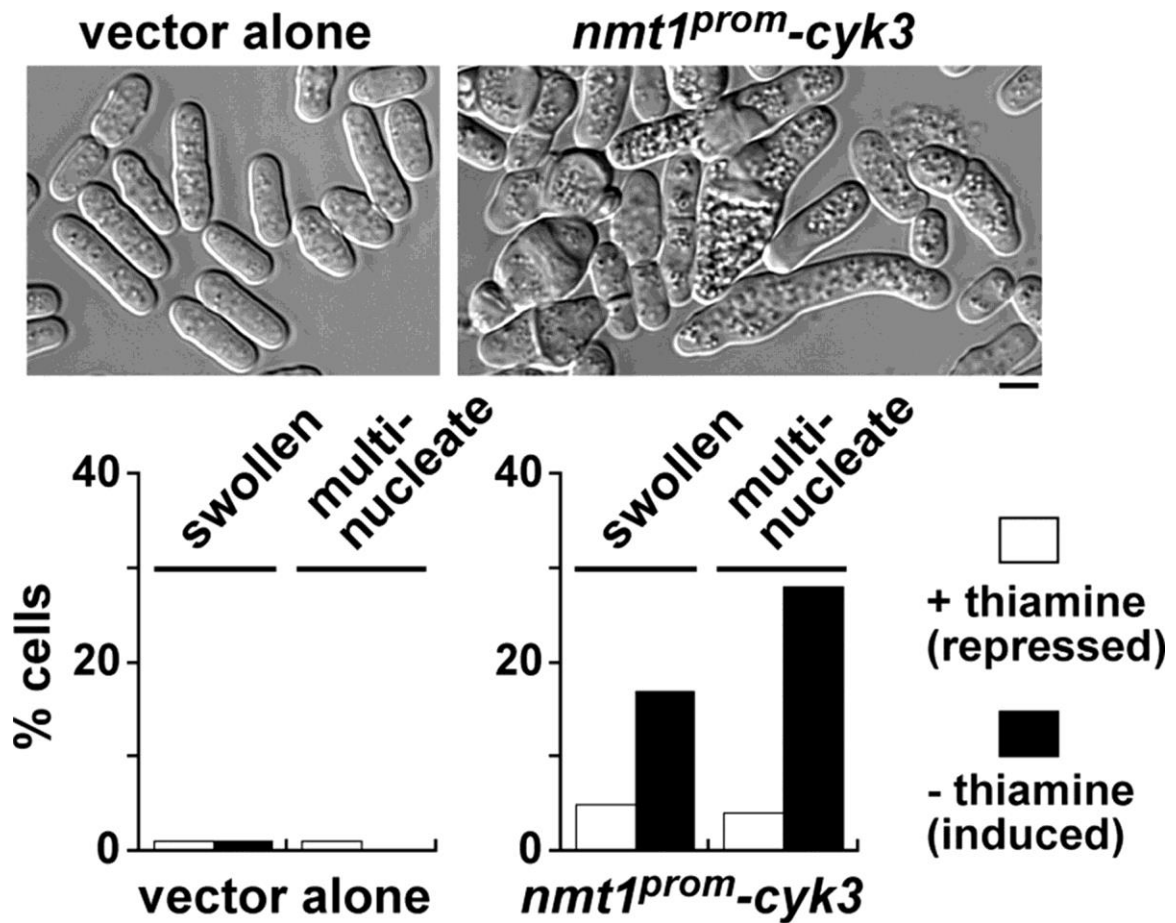
Figure 2-7: Cyk3p overexpression perturbs cell shape.
Cyk3p overexpression perturbs cell shape. Wild-type (MLP 11) cells were transformed with plasmid *nmt1prom* (control) or *nmt1prom-cyk3* (to overexpress Cyk3p from the full-strength *nmt1* promoter). Cells were grown initially on EMM-uracil plates containing 5 μg/ml thiamine, and were then resuspended in EMM- uracil liquid medium without thiamine and grown for 24 h to induce overexpression. Top, representative DIC images of control and Cyk3p-overexpressing cells. Bottom, such images were scored for the indicated abnormal cell morphologies (n = 500 for each count). Scale bars: 4 μm.

To explore further the roles of Cyk3p in vegetative cells, we overexpressed it in otherwise wild-type cells. On overexpression, cells displayed gross morphological defects

74

characterized by multinucleate cells with abnormal septa and rounded/swollen shapes that had lost the typical cigar shape of fission yeast (**Figures 2-7** and **2-S3**). A combination of both phenotypes was evident in some cells (**Figure 2-7**), but time-lapse observations revealed that the phenotypes were often independent of one another (Figure S3), so that cell swelling was not simply a secondary effect of cytokinetic failure. These phenotypes paralleled those of *cyk3Δ* cells (**Figure 2-2A**), presumably reflecting roles for Cyk3p in both cytokinesis and cell shape determination.

2.4.7. CYK3P FUNCTION DEPENDS ON ITS TRANSGLUTAMINASE DOMAIN

BUT NOT ITS SH3 DOMAIN
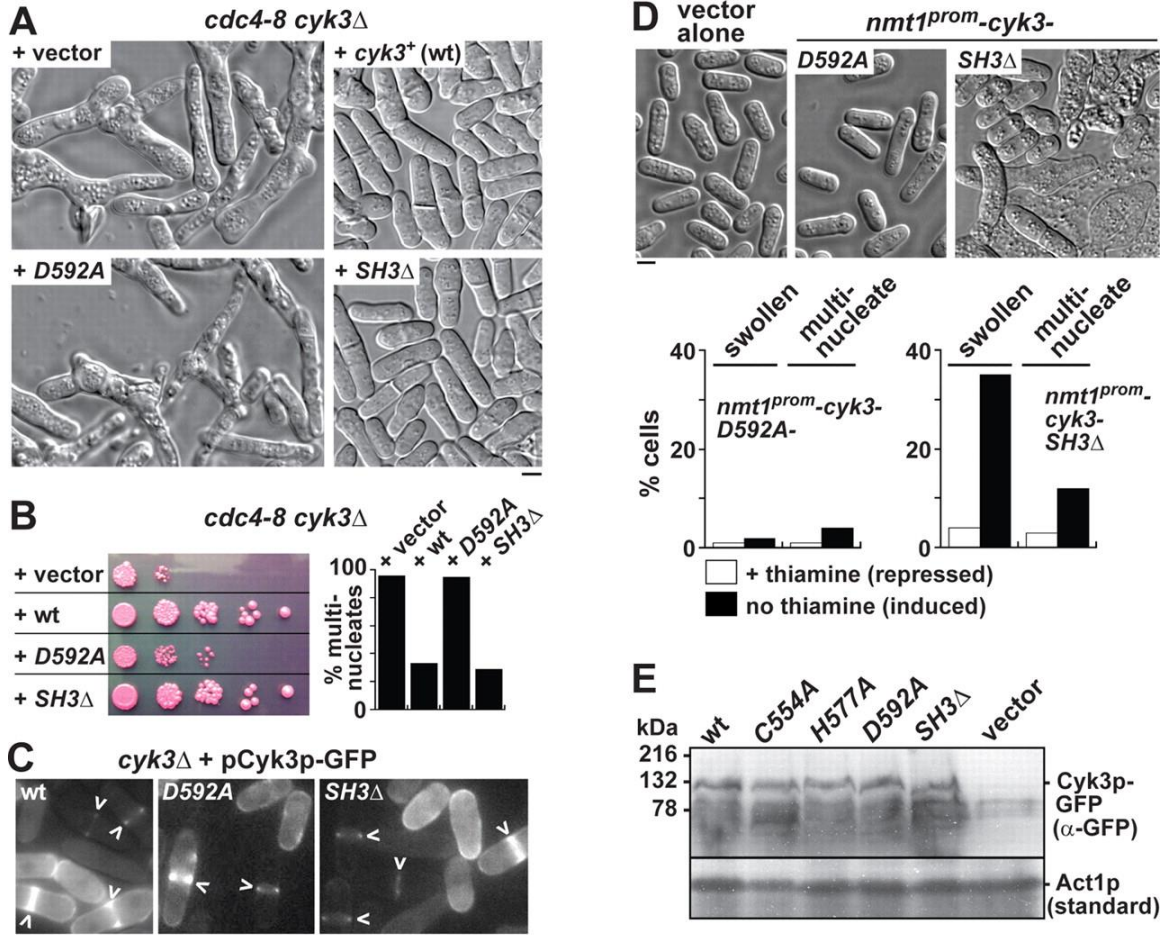
Figure 2-8: Cyk3p function depends on its transglutaminase domain but not its SH3 domain.

Cyk3p function depends on its transglutaminase domain but not its SH3 domain. (A and B) Rescue of the *cdc4-8 cyk3Δ* synthetic phenotype by plasmids expressing wild-type Cyk3p-GFP or Cyk3p-SH3Δ-GFP but not by vector alone or a plasmid expressing Cyk3p-Asp-592-Ala-GFP. *cdc4-8 cyk3Δ* cells (MLP 178) were transformed with plasmid *pGFP* (vector control), *cyk3-GFP*, *cyk3-SH3Δ-GFP*, or *cyk3-Asp-592-Ala-GFP* (see Table 3 and *Materials and Methods*). (A) Representative fields of cells were imaged by DIC microscopy after growth in EMM-uracil liquid medium at 32°C (used because the restrictive temperature of the *cdc4-8 cyk3Δ* double mutant is higher in minimal than in rich medium). (B) Left, 5-μl aliquots of cell suspensions (of identical optical density) were spotted along with four 10-fold serial dilutions of each onto EMM- uracil plates containing 5 μg/ml phloxin B and grown at 30°C. Right, the cultures described in (A) were scored for cytokinetic defects (as percentages of multinucleate cells; n = 500). (C) Normal localization

of wild-type and mutant forms of Cyk3p-GFP to contractile rings (arrowheads). *cyk3Δ* transformants were grown in EMM-uracil liquid medium at 25°C. The variable strength of the Cyk3p-GFP signal presumably reflects the variable copy number of fission yeast plasmids. (D) Effects of overexpressing mutant forms of Cyk3p. Wild-type strain MLP 11 was transformed with plasmid *nmt1^{prom}-cyk3-SH3Δ* or *nmt1^{prom}-cyk3-Asp-592-Ala* (Table 3), and were then grown and scored as described in Figure 7. Top, representative DIC images; bottom, quantification of morphological defects (n = 500). (E) Wild-type and mutant forms of Cyk3p-GFP are expressed at similar levels. *cyk3Δ* strain MLP 3 was transformed with plasmids expressing the indicated proteins and grown as in (C). Extracts were prepared, normalized for total protein, and evaluated by immunoblotting using anti-GFP or anti-actin (as a loading control) antibodies. The indicated band has the appropriate apparent molecular weight (~125 kDa) for a full-length Cyk3p-GFP fusion; as expected, the Cyk3p-SH3Δ-GFP fusion runs slightly faster. Scale bars: 4 μm.

To gain insight into Cyk3p function, we created plasmids expressing proteins that lacked the SH3 domain or contained mutations in the transglutaminase domain (see *Materials and Methods*). Surprisingly, Cyk3p-SH3Δ appeared to retain full function during cytokinesis (**Figure 2-8**, **A** and **B**) and to support normal polarized growth (**Figure 2-8A**). Moreover, like wild-type, this truncated form localized normally (**Figure 2-8C**), produced cytokinetic defects and morphological abnormalities when overexpressed (**Figure 2-8D**), and was expressed at normal levels (**Figure 2-8E**). In contrast, mutation of the conserved aspartate residue of the catalytic triad (in the TGase core) led to a seemingly complete loss of Cyk3p function (**Figure 2-8**, **A**, **B**, and **D**), even though the protein localized normally (**Figure 2-8C**) and was expressed at normal levels (**Figure 2-8E**). We further tested the importance of the TGase domain using another mutation (His-577-Ala) in the catalytic triad (**Figure 2-1**). This mutant protein was expressed effectively, localized normally, and rescued the growth of a *cdc4-8 cyk3Δ* mutant (**Figures 2-8E** and **2-S4**). However, closer inspection revealed that Cyk3p-His-577-Ala retained only partial function: it was unable

to fully relieve the morphological and cytokinetic defects associated with loss of Cyk3p, and it produced relatively mild morphological defects when overexpressed (**Figure 2-S4**). In summary, the TGase domain, but not the SH3 domain, is critical for Cyk3p function in fission yeast.

2.4.8. CYK3P LINKS THE CONTRACTILE RING AND DIVISION SEPTUM

DURING CYTOKINESIS
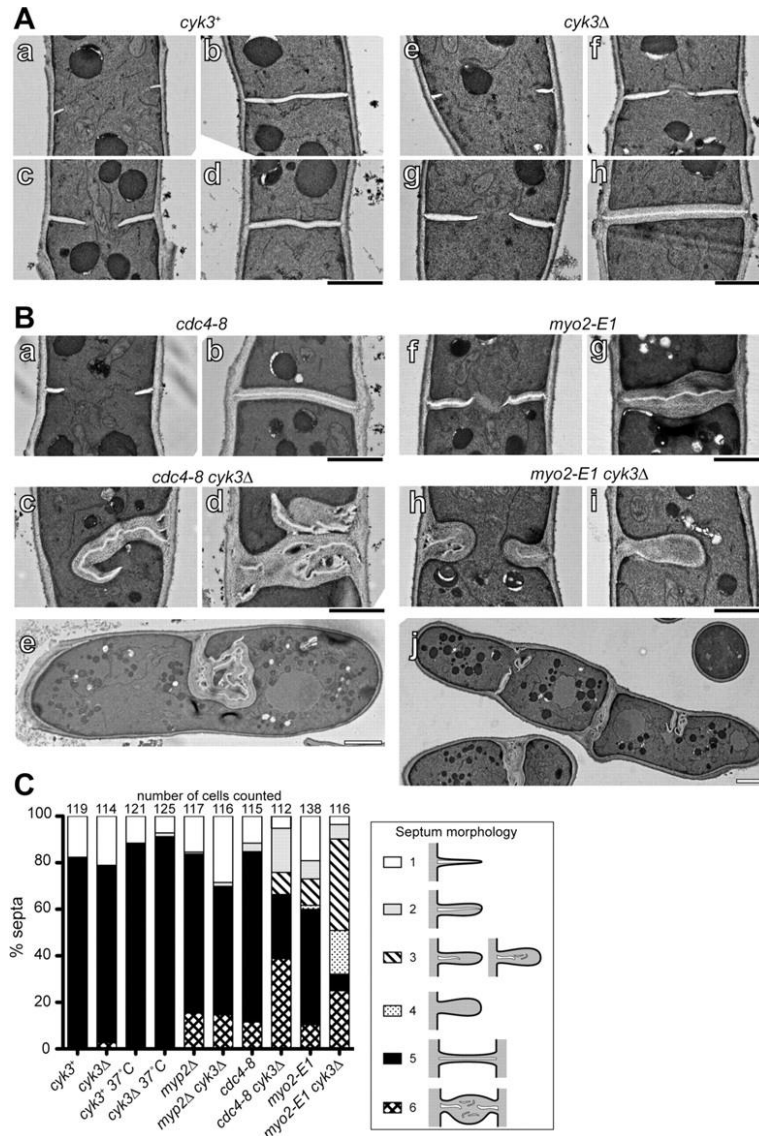
Figure 2-9: EM analysis of septation with and without Cyk3p.
EM analysis of septation with and without Cyk3p. (A) Deletion of *cyk3* alone has a mild effect on septum morphology. Representative electron micrographs of wild-type (a–d) and *cyk3Δ* (e–h) cells grown at 27.5°C in YE5S medium are shown. Cells in the initial (a and e) and late (b, c, f, and g) stages of septation are shown, as are cells with complete septa (d and h). Scale bars: 0.5 µm. (B) Deletion of *cyk3* exacerbates the septum morphology defects in *cdc4-8* (a–e) and *myo2-E1* (f–j) mutants. Cells were cultured as in (A); representative images are shown. Black scale bars: 0.5 µm; white scale bars (e and j): 2 µm. (C) Quantitative analysis of septum morphology in wild-type and mutant strains. Cells

were grown in YE5S medium at 27.5°C, except for two cultures that were incubated at 37°C for 4 h following overnight growth at 25°C. The septa observed by EM were classified as follows: 1, an incomplete sharp septum with an electron-translucent (white) band reaching its leading edge; 2, an incomplete bulged septum with a white band reaching its leading edge; 3, an incomplete bulged septum with a white band(s) not reaching its leading edge; 4, an incomplete bulged septum with no white band; 5, a complete septum across the division plane; 6, a complete but deformed septum with interrupted white bands.

Contractile ring constriction and septum formation are coupled in yeast. The unique localization of Cyk3p in both rings and septa prompted us to further examine its roles in these structures. Because *S. cerevisiae* Cyk3p division site localization depends on the MEN pathway (Meitinger et al., 2010), we tested whether the homologous pathway (the septation initiation network, or SIN) governed Cyk3p localization in fission yeast. The SIN is essential for initiating septum formation and ring constriction (McCollum and Gould, 2001). Use of a temperature-sensitive *sid2-250* mutant demonstrated that localization of Cyk3p to rings was not dependent on the SIN (**Figure 2-S5**). Thus, as with other contractile ring proteins, the formation of Cyk3p rings is actin-dependent (**Figure 2-4C**) but does not rely on septum formation. This indicates that Cyk3p is a core component of the ring that must interface with the leading edge of the trailing septum during cytokinesis, presumably leading to its incorporation across the septum (**Figure 2-3C**).

We turned to electron microscopy (EM) to directly assess Cyk3p's role in ring constriction and septation, and, in particular, how the contractile ring defects of *cyk3* mutants affected growth of the septum. Although septation was generally normal in the absence of Cyk3p (**Figure 2-9A**, compare **a–d** with **e–g**; **Figure 2-9C**), a few *cyk3Δ* cells (3 of 114 cells examined) contained an apparently complete septum with a gap in the

electron-translucent central layer (**Figures 2-9Ah** and **2-9C**) that was never observed in wild-type cells. Actomyosin ring mutants also displayed defects in septum structures (**Figure 2-9B**, **a**, **b**, **f**, and **g**), which became much more severe in double mutants lacking *cyk3Δ* (**Figure 2-9B**, **c–e** and **h–j**). Although these double mutants were viable, their septa were typically abnormally thickened and often appeared misdirected across the division plane (**Figure 2-9**, **B** and **C**). Consistent with the genetic data indicating that Cyk3p functions in the same pathway as Myp2p (**Figures 2-1E** and **2-S1**), the EM analysis revealed little or no exacerbation of the *myp2Δ* septation defect by loss of Cyk3p (**Figures 2-9C** and **2-S6**). Taken together with the localization of Cyk3p, these direct observations of the septa imply a role for Cyk3p in coupling ring constriction and septum growth during cytokinesis.

2.5. DISCUSSION

Our work highlights the role of a TGase-related protein in cell morphogenesis. Fission yeast Cyk3p participates in actomyosin ring constriction, septation, and cell separation during cytokinesis, and also plays a relatively minor role in cell shape and integrity during vegetative growth and stationary phase. Inactive TGases such as Cyk3p are found throughout eukaryotes and our results demonstrate that the TGase domains of such proteins can have key roles in the cell.

2.5.1. FISSION YEAST CYK3P FUNCTIONS IN CYTOKINESIS AND CELL WALL REMODELING

81

Cyk3p functions in cytokinesis, promoting ring constriction and subsequent cell separation. Correspondingly, Cyk3p appears in two distinct structures, the actomyosin ring and the division septum. Cyk3p is an integral component of the ring and is incorporated late in ring assembly. Around this time *cyk3Δ* cells exhibit a cell cycle delay reflected by a brief stall in anaphase B and a delay in the initiation of ring constriction. While the defects are subtle, *cyk3Δ* mutants (like other cytokinetic mutants) invoke lethality in the absence of the Cdc14 family phosphatase Clp1p/Flp1p (Mishra et al., 2004). When ring integrity is compromised Clp1p activates a cytokinetic checkpoint, during which Clp1p activity is also mobilized to stabilize ring structures (Mishra et al., 2004). Thus actomyosin rings lacking Cyk3p rely on compensatory maintenance to support cytokinesis and growth.

Although we do not yet understand the molecular mechanisms by which Cyk3p carries out its role at the ring, they probably involve three other factors: the F-BAR protein Cdc15p, the nonessential myosin II Myp2p, and the chitin synthase Chs2p. Cyk3p coprecipitates with Cdc15p from cell lysates and (along with other ring components) was found to accumulate at the division site upon premature self-assembly of a constitutively dephosphorylated form of Cdc15p (Roberts-Galbraith et al., 2010). Our genetic analysis showed that *myp2Δ* was epistatic to *cyk3Δ*. Myp2p stabilizes rings as they constrict and ensures normal septation (Bezanilla et al., 1997; Motegi et al., 1997; Mulvihill and Hyams, 2003). Correspondingly, direct analysis of septation by EM in *myo2-E1 cyk3Δ* and *cdc4-8 cyk3Δ* double mutants indicated a role for Cyk3p in coordinating septum deposition with ring constriction. Chs2p is a transmembrane protein involved in septum formation and maintaining contractile ring integrity during the latter stages of constriction (Martin-Garcia

et al., 2003; Martin-Garcia and Valdivieso, 2006). The ability of the *chs2Δ* mutation to suppress cytokinetic defects associated with loss of Cyk3p suggests that Chs2p and Cyk3p work in a specific pathway with Myp2p. The actin-independent accumulation of Cyk3p at the division site probably relies on Cdc15p at ring precursors (nodes), given that Myp2p and Chs2p only localize to the division site once rings have formed (Bezanilla et al., 2000; Martin-Garcia and Valdivieso, 2006).

The actomyosin ring disassembles once ring constriction and septum formation are completed (Rajagopalan et al., 2003). Completion of cytokinesis and cell separation occur a short time later upon septum maturation and subsequent digestion of the primary septum by the Eng1p and Agn1p endoglucanases (Martin-Cuadrado et al., 2003; Dekker et al., 2004). Cell separation was significantly slower in *cyk3Δ* cells, suggesting an important role throughout this process for Cyk3p, consistent with its accumulation across the trailing septum during ring constriction and its polarization at the center of the septum immediately prior to cell separation. Outside of cytokinesis, Cyk3p localized at growing cell tips and redistributed throughout the cortex during stationary phase. These localizations and other results suggest that Cyk3p is mobilized for polarized growth during cell elongation and maintenance of cortical integrity upon cell cycle arrest and entry into the dormant phase. One consistent feature of Cyk3p localization is its appearance at the cortex during cell wall remodeling, both in growing cells and during stationary phase (when reinforcement and thickening of the wall occur to maintain cell integrity; Herman, 2002; Rincon *et al.*, 2006). Thus we hypothesize that Cyk3p is generally involved in facilitating cell wall synthesis and remodeling at relevant sites on the cortex.

2.5.2 CYK3P: AN INACTIVE TRANSGLUTAMINASE WITH PHYSIOLOGICAL RELEVANCE

At a mechanistic level, how does Cyk3p contribute to morphogenesis? The SH3 domain of *S. cerevisiae* Cyk3p is important, mediating its localization and association with the C2-domain protein Inn1p at the division site (Jendretzki et al., 2009; Nishihama et al., 2009). Similarly, the SH3 domain of the *S. cerevisiae* F-BAR protein Hof1p also propagates an interaction with Inn1p (Jendretzki et al., 2009; Nishihama et al., 2009; Meitinger et al., 2010). However, whereas loss of Inn1p typically results in lethality or extremely poor growth (Sanchez-Diaz et al., 2008; Jendretzki et al., 2009; Nishihama et al., 2009), *cyk3Δ* or *hof1Δ* cells show relatively minor defects in cytokinesis and growth (Kamei et al., 1998; Lippincott and Li, 1998; Korinek et al., 2000). Moreover, reminiscent of the lethal phenotype of a *cyk3Δ hof1Δ* double mutant, a double mutant possessing truncated forms of both Cyk3p and Hof1p (lacking their SH3 domains) does not grow (Jendretzki et al., 2009). In contrast, in fission yeast, the Cyk3p SH3 domain is not critical for function and does not share a redundant role with the SH3 domains of the F-BAR proteins Cdc15p and Imp2p. Irrespective of the status of Cyk3p, removal of the SH3 domains from both F-BAR proteins is enough to prevent recruitment of the C2-domain protein Fic1p to the division site (Roberts-Galbraith et al., 2009).

Although its SH3 domain is dispensable, the fission yeast Cyk3p TGase domain is required for function (an issue that does not appear to have been investigated for the *S. cerevisiae* protein). Each of the conserved active-site residues cysteine, histidine, and

84

aspartic acid, which make up the catalytic triad at the core of TGases, is essential for enzymatic activity (Hettasch and Greenberg, 1994; Micanovic et al., 1994; Pedersen et al., 1994; Yee et al., 1994), and mutagenesis of the corresponding aspartic acid (Asp-592) or histidine (His-577) residues of fission yeast Cyk3p led to complete or partial loss of function, respectively. Although these results demonstrate the importance of the TGase domain, it cannot function enzymatically because it lacks the cysteine residue to complete the catalytic triad (**Figure 2-1A**). The nearest cysteine residue (Cys-554) is 18 amino acids downstream from where the catalytic cysteine would be expected (**Figure 2-1A**). Nonetheless, this cysteine is conserved among Cyk3p homologues (**Figure 2-1A**) and could theoretically form a catalytic triad with His-577 and Asp-592. However, analysis of a Cys-554-Ala point mutant indicated that this was not the case. The Cys-554-Ala protein was expressed normally and behaved just like wild-type Cyk3p in vivo (**Figures 2-8E** and **2-S4**). In addition, the fact Cyk3p-His-577-Ala (but not -Asp-592-Ala) retains partial function (as opposed to complete loss or full function) also argues against an enzymatic role for the TGase domain in Cyk3p function.

The inactive nature of the Cyk3p TGase domain may reflect a structural/cytoskeletal role for this domain in cell wall remodeling, in which the charged His-577 and Asp-592 residues could help mediate electrostatic interactions between the TGase domain and Cyk3p binding partners. Similarly, a structural role has been proposed for band 4.2, the inactive TGase implicated in human disease that functions at the membrane of red blood cells (Satchwell et al., 2009). Alternatively, the inactive Cyk3p TGase domain may be a mimic that functions as a dominant-negative regulator of other

TGases. In this case, the localization of Cyk3p to sites of cell wall remodeling may promote cell wall dynamics and plasticity by sequestering substrates and thus limiting their cross-linking and stabilization by active endogenous TGases. This hypothesis is supported by the observations that TGase-mediated cross-linking contributes to cell wall organization in *S. cerevisiae* (Iranzo et al., 2002), *C. albicans* (Ruiz-Herrera et al., 1995), and the green alga *Chlamydomonas reinhardtii* (Waffenschmidt et al., 1999). Inhibition of cell wall cross-linking by Cyk3p might explain why its overexpression leads to the loss of polarity and ballooning of cells that could accompany loss of rigidity/excessive plasticity within the cell wall.

In conclusion, our work on fission yeast Cyk3p highlights the importance of the inactive subclass of the TGases that are found throughout eukaryotes. Animal TGases are thought to have evolved from bacterial thiol proteases, because they utilize the same catalytic triad and share the same core structural fold (Pedersen et al., 1994; Yee et al., 1994). Thus, in addition to adaptations favoring substrate cross-linking (via a reversion of the proteolytic reaction), adaptations associated with loss of enzymatic activity also appear to have been selected during the course of evolution.

2.7. REFERENCES

Bahler, J., J.Q. Wu, M.S. Longtine, N.G. Shah, A. McKenzie, 3rd, A.B. Steever, A. Wach, P. Philippsen, and J.R. Pringle. 1998. Heterologous modules for efficient and versatile PCR-based gene targeting in Schizosaccharomyces pombe. *Yeast*. 14:943-951.

Bezanilla, M., S.L. Forsburg, and T.D. Pollard. 1997. Identification of a second myosin-II in Schizosaccharomyces pombe: Myp2p is conditionally required for cytokinesis. *Molecular biology of the cell*. 8:2693-2705.

Bezanilla, M., J.M. Wilson, and T.D. Pollard. 2000. Fission yeast myosin-II isoforms assemble into contractile rings at distinct times during mitosis. *Current biology*. 10:397-400.

Bruce, L.J., S. Ghosh, M.J. King, D.M. Layton, W.J. Mawby, G.W. Stewart, P.A. Oldenborg, J. Delaunay, and M.J. Tanner. 2002. Absence of CD47 in protein 4.2-deficient hereditary spherocytosis in man: an interaction between the Rh complex and the band 3 complex. *Blood*. 100:1878-1885.

Cohen, C.M., E. Dotimas, and C. Korsgren. 1993. Human erythrocyte membrane protein band 4.2 (pallidin). *Seminars in hematology*. 30:119-137.

Dahl, K.N., R. Parthasarathy, C.M. Westhoff, D.M. Layton, and D.E. Discher. 2004. Protein 4.2 is critical to CD47-membrane skeleton attachment in human red cells. *Blood*. 103:1131-1136.

Dekker, N., D. Speijer, C.H. Grun, M. van den Berg, A. de Haan, and F. Hochstenbach. 2004. Role of the alpha-glucanase Agn1p in fission-yeast cell separation. *Molecular biology of the cell*. 15:3903-3914.

Facchiano, F., A. Facchiano, and A.M. Facchiano. 2006. The role of transglutaminase-2 and its substrates in human diseases. *Frontiers in bioscience : a journal and virtual library*. 11:1758-1773.

Fankhauser, C., A. Reymond, L. Cerutti, S. Utzig, K. Hofmann, and V. Simanis. 1995. The S. pombe cdc15 gene is a key element in the reorganization of F-actin at mitosis. *Cell*. 82:435-444.

Fesus, L., and Z. Szondy. 2005. Transglutaminase 2 in the balance of cell death and survival. *FEBS letters*. 579:3297-3302.

Herman, P.K. 2002. Stationary phase in yeast. *Current opinion in microbiology*. 5:602-607.

Hettasch, J.M., and C.S. Greenberg. 1994. Analysis of the catalytic activity of human factor XIIIa by site-directed mutagenesis. *The Journal of biological chemistry*. 269:28309-28313.

Ho, S.N., H.D. Hunt, R.M. Horton, J.K. Pullen, and L.R. Pease. 1989. Site-directed mutagenesis by overlap extension using the polymerase chain reaction. *Gene*. 77:51-59.

Iranzo, M., C. Aguado, C. Pallotti, J.V. Canizares, and S. Mormeneo. 2002. Transglutaminase activity is involved in Saccharomyces cerevisiae wall construction. *Microbiology*. 148:1329-1334.

Jendretzki, A., I. Ciklic, R. Rodicio, H.P. Schmitz, and J.J. Heinisch. 2009. Cyk3 acts in actomyosin ring independent cytokinesis by recruiting Inn1 to the yeast bud neck. *Molecular genetics and genomics*. 282:437-451.

Kamei, T., K. Tanaka, T. Hihara, M. Umikawa, H. Imamura, M. Kikyo, K. Ozaki, and Y. Takai. 1998. Interaction of Bnr1p with a novel Src homology 3 domain-containing Hof1p. Implication in cytokinesis in Saccharomyces cerevisiae. *The Journal of biological chemistry*. 273:28341-28345.

Knox, P., S. Crooks, and C.S. Rimmer. 1986. Role of fibronectin in the migration of fibroblasts into plasma clots. *The Journal of cell biology*. 102:2318-2323.

Korinek, W.S., E. Bi, J.A. Epp, L. Wang, J. Ho, and J. Chant. 2000. Cyk3, a novel SH3-domain protein, affects cytokinesis in yeast. *Current biology : CB*. 10:947-950.

Korsgren, C., J. Lawler, S. Lambert, D. Speicher, and C.M. Cohen. 1990. Complete amino acid sequence and homologies of human erythrocyte membrane protein band 4.2. *Proceedings of the National Academy of Sciences of the United States of America*. 87:613-617.

Lippincott, J., and R. Li. 1998. Dual function of Cyk2, a cdc15/PSTPIP family protein, in regulating actomyosin ring dynamics and septin distribution. *The Journal of cell biology*. 143:1947-1960.

Makarova, K.S., L. Aravind, and E.V. Koonin. 1999. A superfamily of archaeal, bacterial, and eukaryotic proteins homologous to animal transglutaminases. *Protein science : a publication of the Protein Society*. 8:1714-1719.

Mangala, L.S., and K. Mehta. 2005. Tissue transglutaminase (TG2) in cancer biology. *Progress in experimental tumor research*. 38:125-138.

Martin-Cuadrado, A.B., E. Duenas, M. Sipiczki, C.R. Vazquez de Aldana, and F. del Rey. 2003. The endo-beta-1,3-glucanase eng1p is required for dissolution of the primary septum during cell separation in Schizosaccharomyces pombe. *Journal of cell science*. 116:1689-1698.

Martin-Garcia, R., A. Duran, and M.H. Valdivieso. 2003. In Schizosaccharomyces pombe chs2p has no chitin synthase activity but is related to septum formation. *FEBS letters*. 549:176-180.

Martin-Garcia, R., and M.H. Valdivieso. 2006. The fission yeast Chs2 protein interacts with the type-II myosin Myo3p and is required for the integrity of the actomyosin ring. *Journal of cell science*. 119:2768-2779.

McCollum, D., and K.L. Gould. 2001. Timing is everything: regulation of mitotic exit and cytokinesis by the MEN and SIN. *Trends in cell biology*. 11:89-95.

Mehta, K., A. Kumar, and H.I. Kim. 2010. Transglutaminase 2: a multi-tasking protein in the complex circuitry of inflammation and cancer. *Biochemical pharmacology*. 80:1921-1929.

Meitinger, F., B. Petrova, I.M. Lombardi, D.T. Bertazzi, B. Hub, H. Zentgraf, and G. Pereira. 2010. Targeted localization of Inn1, Cyk3 and Chs2 by the mitotic-exit network regulates cytokinesis in budding yeast. *Journal of cell science*. 123:1851-1861.

Micanovic, R., R. Procyk, W. Lin, and G.R. Matsueda. 1994. Role of histidine 373 in the catalytic activity of coagulation factor XIII. *The Journal of biological chemistry*. 269:9190-9194.

Mishra, M., J. Karagiannis, S. Trautmann, H. Wang, D. McCollum, and M.K. Balasubramanian. 2004. The Clp1p/Flp1p phosphatase ensures completion of cytokinesis in response to minor perturbation of the cell division machinery in Schizosaccharomyces pombe. *Journal of cell science*. 117:3897-3910.

Moreno, S., A. Klar, and P. Nurse. 1991. Molecular genetic analysis of fission yeast Schizosaccharomyces pombe. *Methods in enzymology*. 194:795-823.

Mosher, D.F., and P.E. Schad. 1979. Cross-linking of fibronectin to collagen by blood coagulation Factor XIIIa. *The Journal of clinical investigation*. 64:781-787.

Motegi, F., K. Nakano, C. Kitayama, M. Yamamoto, and I. Mabuchi. 1997. Identification of Myo3, a second type-II myosin heavy chain in the fission yeast Schizosaccharomyces pombe. *FEBS letters*. 420:161-166.

Mulvihill, D.P., and J.S. Hyams. 2003. Role of the two type II myosins, Myo2 and Myp2, in cytokinetic actomyosin ring formation and function in fission yeast. *Cell motility and the cytoskeleton*. 54:208-216.

Nishihama, R., J.H. Schreiter, M. Onishi, E.A. Vallen, J. Hanna, K. Moravcevic, M.F. Lippincott, H. Han, M.A. Lemmon, J.R. Pringle, and E. Bi. 2009. Role of Inn1 and its interactions with Hof1 and Cyk3 in promoting cleavage furrow and septum formation in S. cerevisiae. *The Journal of cell biology*. 185:995-1012.

Pedersen, L.C., V.C. Yee, P.D. Bishop, I. Le Trong, D.C. Teller, and R.E. Stenkamp. 1994. Transglutaminase factor XIII uses proteinase-like catalytic triad to crosslink macromolecules. *Protein science : a publication of the Protein Society*. 3:1131-1135.

Pisano, J.J., J.S. Finlayson, and M.P. Peyton. 1968. [Cross-link in fibrin polymerized by factor 13: epsilon-(gamma-glutamyl)lysine]. *Science (New York, N.Y.)*. 160:892-893.

Rajagopalan, S., V. Wachtler, and M. Balasubramanian. 2003. Cytokinesis in fission yeast: a story of rings, rafts and walls. *Trends in genetics : TIG*. 19:403-408.

Reijnst, P., S. Jorde, and J. Wendland. 2010. Candida albicans SH3-domain proteins involved in hyphal growth, cytokinesis, and vacuolar morphology. *Current genetics*. 56:309-319.

Rice, R.H., and H. Green. 1978. Relation of protein synthesis and transglutaminase activity to formation of the cross-linked envelope during terminal differentiation of the cultured human epidermal keratinocyte. *The Journal of cell biology*. 76:705-711.

Rincon, S.A., B. Santos, and P. Perez. 2006. Fission yeast Rho5p GTPase is a functional paralogue of Rho1p that plays a role in survival of spores and stationary-phase cells. *Eukaryotic cell*. 5:435-446.

Roberts-Galbraith, R.H., J.S. Chen, J. Wang, and K.L. Gould. 2009. The SH3 domains of two PCH family members cooperate in assembly of the Schizosaccharomyces pombe contractile ring. *The Journal of cell biology*. 184:113-127.

Roberts-Galbraith, R.H., M.D. Ohi, B.A. Ballif, J.S. Chen, I. McLeod, W.H. McDonald, S.P. Gygi, J.R. Yates, 3rd, and K.L. Gould. 2010. Dephosphorylation of F-BAR

protein Cdc15 modulates its conformation and stimulates its scaffolding activity at the cell division site. *Molecular cell*. 39:86-99.

Ruiz-Herrera, J., M. Iranzo, M.V. Elorza, R. Sentandreu, and S. Mormeneo. 1995. Involvement of transglutaminase in the formation of covalent cross-links in the cell wall of Candida albicans. *Archives of microbiology*. 164:186-193.

Sakata, Y., and N. Aoki. 1980. Cross-linking of alpha 2-plasmin inhibitor to fibrin by fibrin-stabilizing factor. *The Journal of clinical investigation*. 65:290-297.

Sambrook, J., E.F. Fritsch, and T. Maniatis. 1989. Molecular cloning : a laboratory manual. Cold Spring Harbor Laboratory, Cold Spring Harbor, N.Y.

Sanchez-Diaz, A., V. Marchesi, S. Murray, R. Jones, G. Pereira, R. Edmondson, T. Allen, and K. Labib. 2008. Inn1 couples contraction of the actomyosin ring to membrane ingression during cytokinesis in budding yeast. *Nature cell biology*. 10:395-406.

Satchwell, T.J., D.K. Shoemark, R.B. Sessions, and A.M. Toye. 2009. Protein 4.2: a complex linker. *Blood cells, molecules & diseases*. 42:201-210.

Schwartz, M.L., S.V. Pizzo, R.L. Hill, and P.A. McKee. 1973. Human Factor XIII from plasma and platelets. Molecular weights, subunit structures, proteolytic activation, and cross-linking of fibrinogen and fibrin. *The Journal of biological chemistry*. 248:1395-1407.

Sirotkin, V., J. Berro, K. Macmillan, L. Zhao, and T.D. Pollard. 2010. Quantitative analysis of the mechanism of endocytic actin patch assembly and disassembly in fission yeast. *Molecular biology of the cell*. 21:2894-2904.

Sladewski, T.E., M.J. Previs, and M. Lord. 2009. Regulation of fission yeast myosin-II function and contractile ring dynamics by regulatory light-chain and heavy-chain phosphorylation. *Molecular biology of the cell*. 20:3941-3952.

Stark, B.C., T.E. Sladewski, L.W. Pollard, and M. Lord. 2010. Tropomyosin and myosin-II cellular levels promote actomyosin ring assembly in fission yeast. *Molecular biology of the cell*. 21:989-1000.

Thacher, S.M., and R.H. Rice. 1985. Keratinocyte-specific transglutaminase of cultured human epidermal cells: relation to cross-linked envelope formation and terminal differentiation. *Cell*. 40:685-695.

Waffenschmidt, S., T. Kusch, and J.P. Woessner. 1999. A transglutaminase immunologically related to tissue transglutaminase catalyzes cross-linking of cell wall proteins in Chlamydomonas reinhardtii. *Plant physiology*. 121:1003-1015.

Yawata, Y. 1994. Band 4.2 abnormalities in human red cells. *The American journal of the medical sciences*. 307:190-203.

Yee, V.C., L.C. Pedersen, I. Le Trong, P.D. Bishop, R.E. Stenkamp, and D.C. Teller. 1994. Three-dimensional structure of a transglutaminase: human blood coagulation factor XIII. *Proceedings of the National Academy of Sciences of the United States of America*. 91:7296-7300.

Zemskov, E.A., A. Janiak, J. Hang, A. Waghray, and A.M. Belkin. 2006. The role of tissue transglutaminase in cell-matrix interactions. *Frontiers in bioscience : a journal and virtual library*. 11:1057-1076.
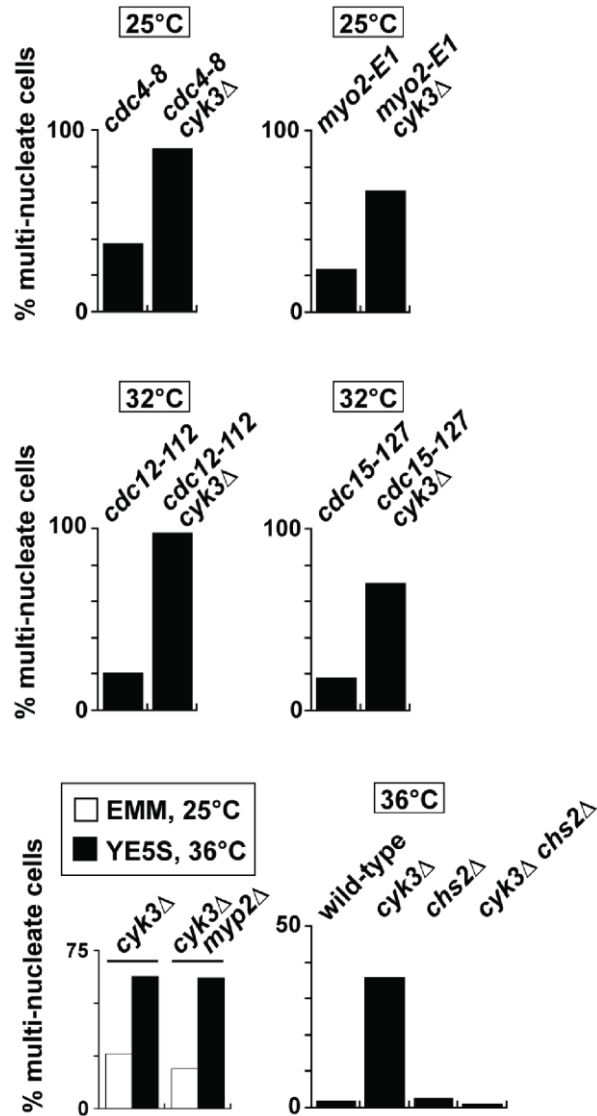
Figure 2-S1: Synthetic genetic interactions of a *cyk3* null with known cytokinesis mutants.

Plots comparing cell division defects (% multinucleate cells: 3+ nuclei/cell) for temperature sensitive (*cdc4-8*, TP 6; *myo2-E1*, TP 73; *cdc12-112*, TP 19; and *cdc15-127*, TP 30) and null (*myp2Δ*, MLP 34; *chs2Δ*, HVP 280) cytokinesis mutants alone and in combination with a *cyk3* null (strains MLP 178, MLP 17, MLP 323, MLP 326, MLP 35, and LP 112). Cells were grown on YE5S or EMM medium at the indicated temperatures. Over the 25-32°C temperature range the single *cyk3Δ* mutant does not exhibit morphological defects.
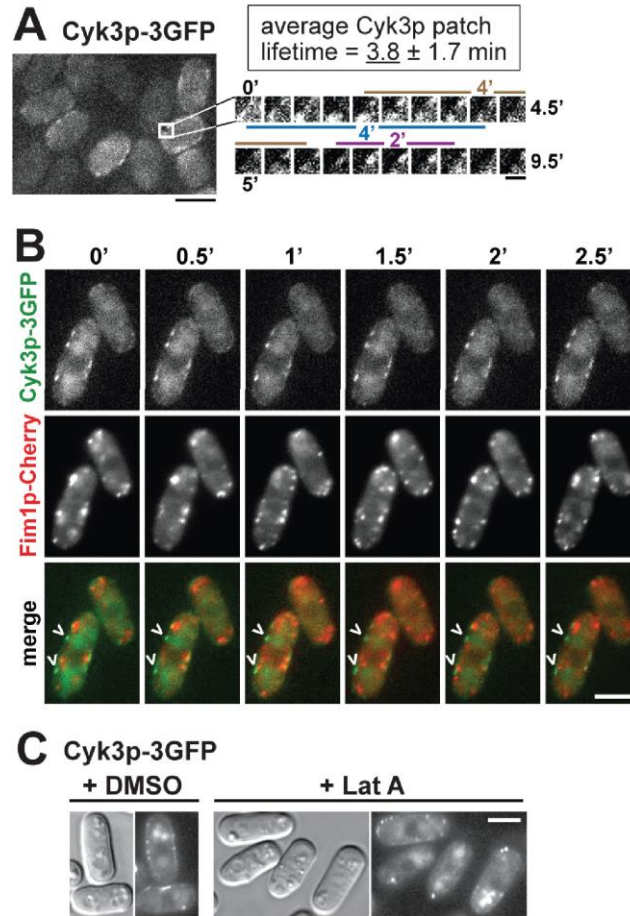
Figure 2-S2: Cyk3p localizes as cortical puncta that do not depend on actin in stationary phase cells.

(A) Wild-type strain LP 37 was grown overnight on YE5S plates and examined by time-lapse fluorescence microscopy. Left, a representative field of cells with more or less Cyk3p-3GFP puncta, presumably reflecting whether the individual cells are (or are not yet) in stationary phase. Right, time-lapse observations of three different Cyk3p puncta in a specific cortical region (white box). The overall average lifetime for the Cyk3p puncta is 3.8 ± 1.7 min (n=25). (B) Time-lapse montages showing localization of Cyk3p-3GFP punctae (upper panels), cortical Fim1p-Cherry at actin patches (center panels), and a merge of both (bottom panels) in a stationary phase cell (the lower of the two cells shown). Cells (LP 33) were grown overnight on YE5S plates at 32°C and then subjected to time-lapse epi-fluorescence microscopy. Arrowheads indicate the absence of Fim1p at Cyk3p puncta. (C) Cyk3p stationary phase cortical localization does not rely on actin filaments. Cells (LP 37) were grown to stationary phase in YE5S liquid media and treated with DMSO (control) or 10 μM Latrunculin A to depolymerize actin. In the presence of Latrunculin Cyk3p still localizes. Bars: 4 μm.
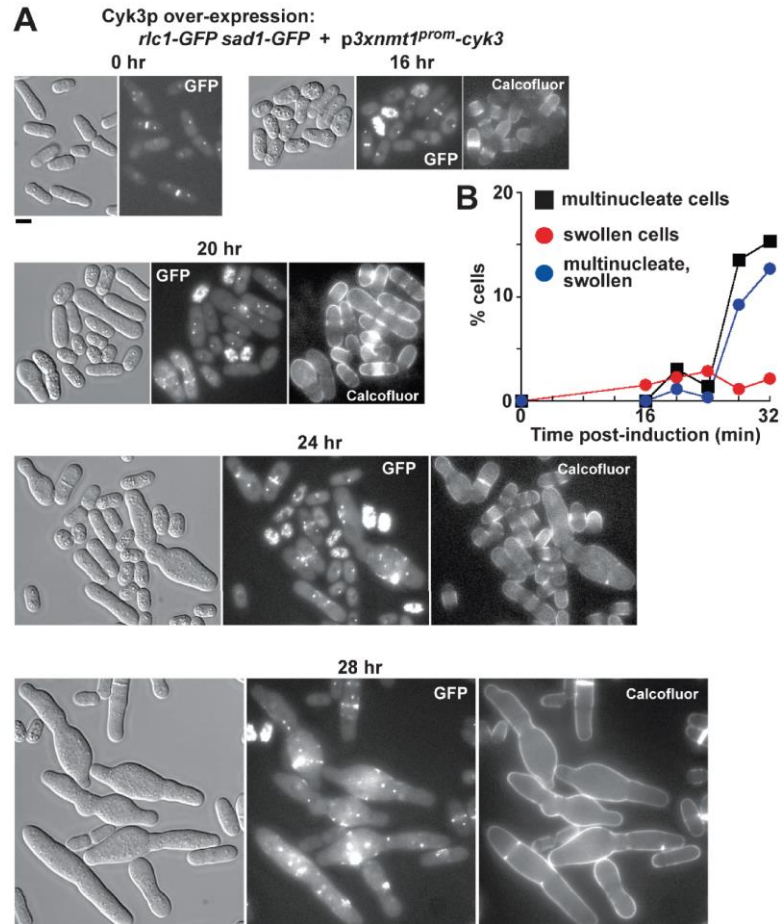
Figure 2-S3: Effect of Cyk3p over-expression on contractile rings, cytokinesis, and cell shape.

Cyk3p was over-expressed from a *ura4+* plasmid using the maximum strength *nmt1* promoter. *rlc1-mGFP sad1-mGFP* cells (MLY 572) harboring the *cyk3* plasmid were initially grown on EMM plates (lacking uracil, plus 5 µg/ml thiamine) before resuspending in EMM liquid media (lacking both uracil and thiamine) and further growth to induce over-expression. Cells were induced over a 32 hour time-course and imaged (following a 15 minute incubation in 200 µg/ml Calcofluor stain). (A) Representative 0-28 hour DIC and fluorescence (GFP; Calcofluor) images are shown. Contractile rings are marked with Rlc1p, and multinucleate cells inferred from SPB/nuclear Sad1p spots (GFP images); cell wall was detected by Calcofluor (DAPI channel). Bar: 4 µm. (B) Plots providing % counts of multi-nucleate (3+ nuclei/cell) and swollen-shaped (multi-nucleated and non-multinucleated) cells over the period of the time-course (n=94-347).
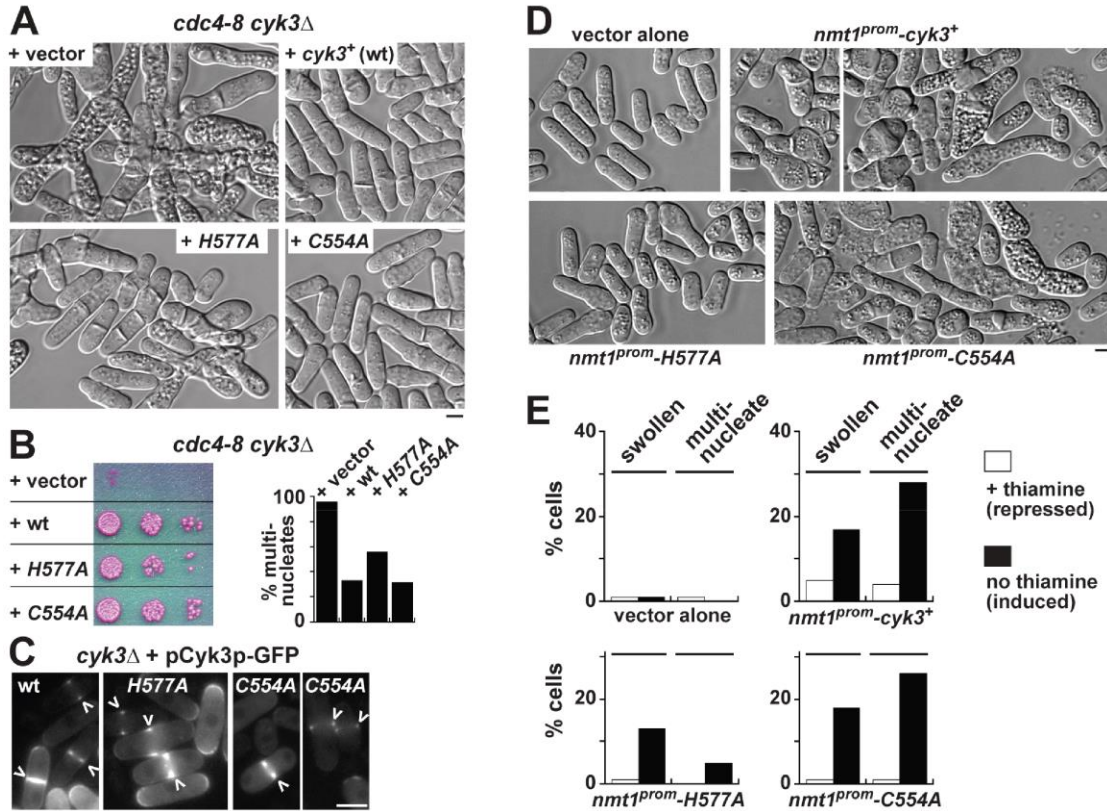
Figure 2-S4: Testing the importance of H577 and C554 for Cyk3p function.
(A) Representative fields of *cdc4-8 cyk3Δ* (MLP 178) plasmid transformants harboring vector alone (negative control), wild-type (*cyk3-GFP*, positive control), or mutant forms of *cyk3-GFP*. *H577A* and *C554A* are point mutants within the catalytic core of the TGase domain. Cells were imaged by DIC microscopy following growth at 32°C in EMM-Ura-liquid medium. (B) Comparing the growth and morphology of *cdc4-8 cyk3Δ* transformants. *Left*: 5 μl cell suspensions (of identical OD) were spotted (along with two ten-fold serial dilutions) on to EMMUra- (plus 5 μg/ml phloxin B) plates and grown at 30°C. *Right*: quantification of cytokinesis defects (multinucleate cells; n=500) following growth in liquid media (as described in A). (C) Localization of wild-type and mutant forms of Cyk3p-GFP at contractile rings (arrowheads). *cyk3Δ* cells (MLP 17 harboring the indicated *cyk3-GFP* plasmid) were grown at 25°C in EMMUra- liquid medium. The variable levels of Cyk3p-GFP at contractile rings reflects the multicopy nature of fission yeast plasmids. (D-E) Effects of over-expressing wild type and mutant (*H577A* and *C554A*) forms of Cyk3p on cell shape and cytokinesis. Wild-type cells (MLP 11) harboring a vector lacking *cyk3* (vector alone) were included as a control. (D) Representative DIC images of cells. (E) Quantification of swollen and multinucleate phenotypes (n=500). All Bars: 4 μm.

97
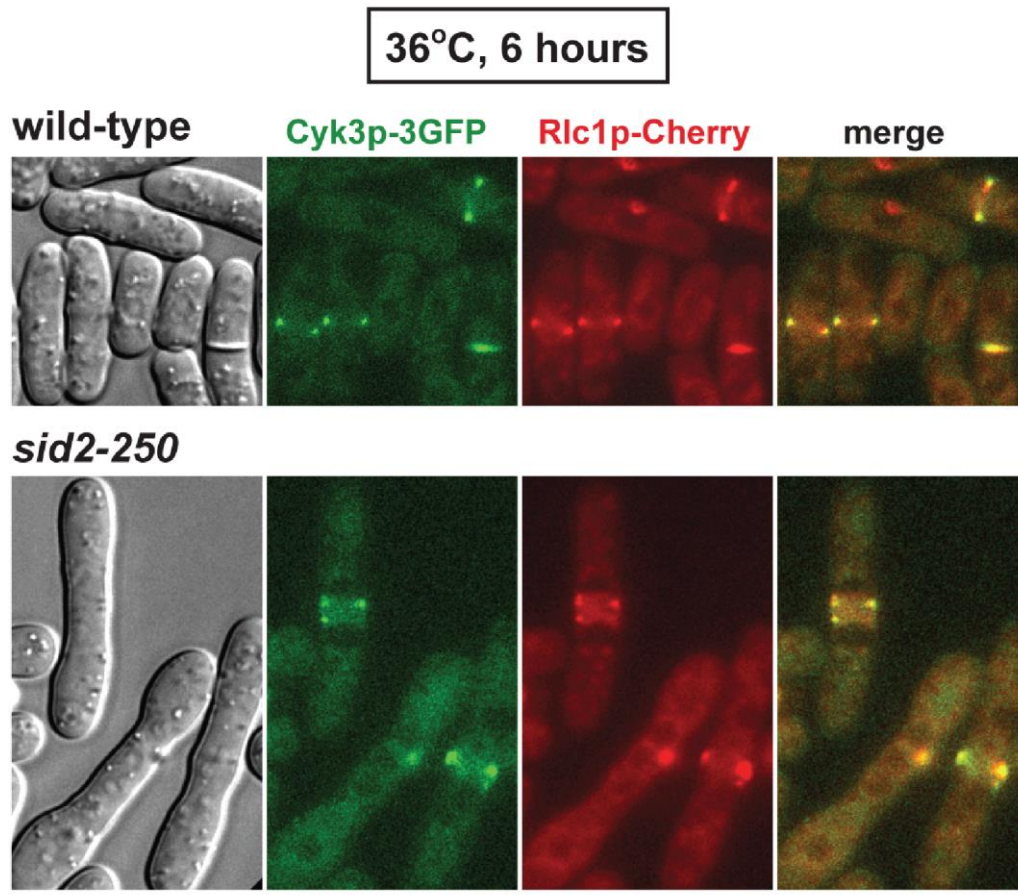
Figure 2-S5: Localization of Cyk3p at contractile rings does not require the initiation of septation.

Wild-type (MLY 757) and *sid2-250* (LP 69) cells expressing Cyk3p-3xGFP and Rlc1p-Cherry were grown at 25°C overnight and then shifted to the restrictive temperature (36°C) for 6 hours to attenuate SIN function. Representative DIC (left panels), GFP, Cherry, and merged GFP/Cherry images are shown indicating that Cyk3p still localizes at rings when septation is blocked. Bar: 4 μm.
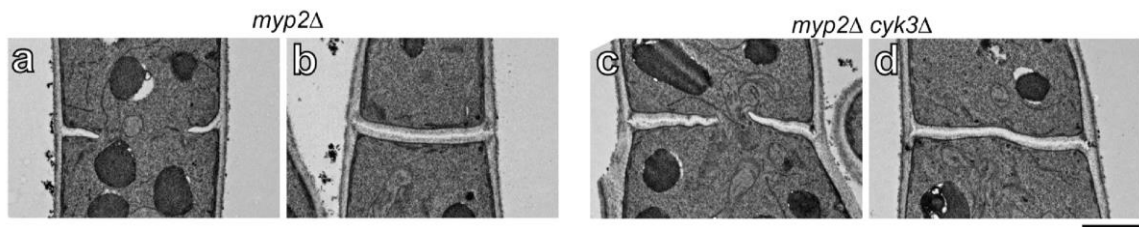
Figure 2-S6: Electron microscopy of *myp2Δ* and m*yp2Δ cyk3Δ* mutants.
Double-deletion of *myp2Δ* and *cyk3Δ* does not cause an additive phenotype in septum morphology. Representative electron micrographs of *myp2Δ* (MLP 34; a and b) and *myp2Δ cyk3Δ* (MLP 35; c and d) cells grown at 27.5°C in YE5S medium are shown. Bar: 0.5 μm.

2.8.1. MOVIE LEGENDS

Movies are available at

http://www.molbiolcell.org/content/23/13/2433/suppl/DC1

Movie 2-S1. Cyk3p and myosin-II (Rlc1p) co-localization at contractile rings. A representative time-lapse movie charting the co-localization of Cyk3p-3xGFP (green) and Rlc1p-mCherry (red). This field of cells (LP 116) is employed in Figure 3C. The movie was generated from images captured every 2 minutes and is played at frames 7 frames per second (sped up 840x).

Movie 2-S2. Cyk3p localization dynamics in stationary phase cells (2 minute intervals) Representative movie showing the sub-cellular localization of Cyk3p in stationary phase *cyk3-3GFP* (LP 37) cells. The movie was generated from images captured every 2 minutes for 14 minutes and is played at 8 frames per second (sped up 960x).

Movie 2-S3. Cyk3p localization dynamics in stationary phase cells (30 second intervals) Representative movie showing the sub-cellular localization of Cyk3p in stationary phase *cyk3-3GFP* cells (LP 37). The movie was generated from images captured every 30 seconds for 14.5 minutes and is played at 32 frames per second (sped up 960x).

CHAPTER 3: FISSION YEAST MYO2 FUNCTIONS AS AN UNUSUAL CLASS-II MYOSIN DURING CYTOKINESIS

Luther W. Pollard, Carol S. Bookwalter, Qing Tang, Elena Krementsova, Kathleen M. Trybus, and Susan Lowey

Department of Molecular Physiology & Biophysics, University of Vermont, Burlington, VT 05405.

Correspondence:
Susan Lowey
Health Science Research Facility 128
149 Beaumont Avenue
Department of Molecular Physiology & Biophysics
University of Vermont
Burlington, VT 05405
phone: 802-656-8091
susan.lowey@uvm.edu

Subject terms: Fission yeast, Cytokinesis, Myosin-II

3.1. ABSTRACT

Studies in the fission yeast system provide much of the basis for detailed models that account for the dynamics of the contractile ring that drives cytokinesis. Myo2, a class-II myosin, is the major source of motor activity in the contractile ring in fission yeast. However, it is poorly understood how Myo2 is anchored and regulated so that it can produce force in the contractile ring. Here, Myo2 was expressed in the baculovirus/*Sf*9 insect cell system with its two native light chains. Good yields of soluble Myo2 were obtained that exhibited enzymatic activity and motility. An unusual finding was that regulatory light chain phosphorylation reduced Myo2's affinity for actin, in contrast to animal nonmuscle myosins that require phosphorylation for an active state. Moreover, unlike other class-II myosins which form filamentous structures, Myo2 showed no inclination to self-assemble at physiological salt concentrations according to sedimentation velocity measurements. The lack of assembly implies that Myo2 depends on interactions at the cell cortex in structural units called nodes for force production during cytokinesis.

3.2. INTRODUCTION

Animals, amoebas, and fungi undergo cytokinesis through the formation of a cleavage furrow, which is guided by tension generated by an actomyosin contractile ring. Relatively little is known about the physical interactions and juxtaposition of proteins in the contractile ring in animal cells (Pollard, 2014; Cheffings et al., 2016). However, excellent classical and molecular genetics of the haploid fission yeast, *Schizosaccharomyces pombe*, has made it a well-established model for elucidating how contractile rings assemble and constrict. Elucidation of the inventory, timing, concentrations, and genetic interactions of cytokinesis proteins in the fission yeast contractile ring have led to computational models that account for many dynamical aspects of the contractile ring (Pollard, 2014). To expand upon these models, it is necessary to obtain better knowledge of the biophysical properties of the proteins involved. How Myo2, the essential class-II myosin in fission yeast, is regulated and functions in the contractile ring represents a major gap in understanding the forces contributing to contractile ring dynamics.

In addition to Myo2, two other myosins, class-II Myp2 and class-V Myo51, contribute differentially to contractile ring assembly and constriction in fission yeast (Laplante et al., 2015). Myo2 is required for cytokinesis and cell viability, whereas Myp2 and Myo51 can be deleted, which causes subtle defects in contractile ring dynamics (Bezanilla et al., 1997; Kitayama et al., 1997; Win et al., 2001; Laplante et al., 2015). Myo2 powers contractile ring assembly, which occurs by the coalescence of precursor nodes that

are modular units of the ring (Wu et al., 2006; Laporte et al., 2011; Laplante et al., 2015). The compaction of the ring is theorized to occur by a "Search, Capture, Pull, and Release" mechanism, where Myo2, incorporated into nodes, pulls on actin filaments that span between the nodes, bringing them together (Vavylonis et al., 2008; Pollard and Wu, 2010; Lee et al., 2012). The region that localizes Myo2 to nodes has been mapped to ~100-300 amino acids at the carboxy (C)-terminus through the expression of green fluorescent protein (GFP) fusion constructs with various sections of Myo2 (Mulvihill et al., 2001; Motegi et al., 2004). The binding partners of this region of Myo2 in the nodes are not established, but IQGAP Rng2 and anillin-like Mid1 have been implicated based on localization dependency and co-immunoprecipitation experiments (Laporte et al., 2011; Takaine et al., 2014). Unlike Myp2 and Myo51, Myo2 localization to the division site does not depend on actin filaments (Win et al., 2001; Takaine et al., 2014; Takaine et al., 2015). Although Myo2's interactions with other node proteins are unresolved at the molecular level, a plausible mechanism of Myo2 function is that it could form clusters by being stably anchored to nodes.

Unc45/Cro1/She4 (UCS) family chaperones work with heat shock protein (HSP)-90 to fold myosin (Lee et al., 2014; Ni and Odunuga, 2015). Consequently, the UCS chaperone, Rng3, and HSP90, Swo1, are required for cytokinesis in fission yeast (Wong et al., 2000; Mishra et al., 2005a). Rng3-defective, *rng3-65* fission yeast strains exhibit failed contractile ring assembly at high temperature (37°C), which is consistent with a loss of Myo2 function (Wong et al., 2000). GFP-tagged Rng3 is enriched ~70-fold in the contractile ring in *myo2-E1* mutant cells (Wong et al., 2000; Wu and Pollard, 2005). Yeast

with the *myo2-E1* allele harbor a mutation near the nucleotide binding pocket of the Myo2 motor domain, G345R, resulting in a total loss of motility and severely reduced ATPase (Lord and Pollard, 2004; Stark et al., 2013). Myo2-E1 is also more sensitive to limited proteolysis than the wildtype protein (Stark et al., 2013), which suggests that unfolded Myo2-E1 recruits Rng3 to the ring. Additionally, the *myo2-E1 rng3-65* double-mutant strains exhibit synthetically lethal cytokinesis defects (Wong et al., 2000). Overall, these findings are consistent with the role of fission yeast Rng3 as a conserved member of the UCS protein family, which functions to fold myosins. However, Rng3 has also been suggested to activate Myo2. This hypothesis comes from the first study to isolate Myo2 from fission yeast, where it was observed that purified Myo2 did not bind actin filaments in motility assays unless Rng3 was added (Lord and Pollard, 2004). Later studies, however, found that Rng3 did not affect ATPase rates and enhanced Myo2 motility only at low myosin concentrations (Lord et al., 2008), but it was not clear why this occurs. Here, we offer an explanation for why Rng3 appeared to enhance actin binding in motility assays.

Class-II myosins are conventionally composed of two globular head domains that bind to actin and hydrolyze ATP, and a rod-like, α-helical coiled-coil tail that assembles the molecules into bipolar filaments. Molecules typically consist of two ~1500-2000 amino acid heavy chains (HC), and two each of the essential (ELC) and regulatory (RLC) light chains. In animal cells, the nonmuscle myosins form minifilaments of ~30 molecules and ~300 nm in length (Billington et al., 2013), whereas the muscle thick filaments are 1.6 μm long and contain around 300 molecules. Myosin-II filament assembly is ancient, and conserved in amoebozoans such as *Acanthamoeba castellanii* and *Dictyostelium*

105

discoideum that form myosin filaments of variable size by unique rod-rod interactions (Mahajan and Pardee, 1996; Liu et al., 2013). In animal cells, smooth muscle and nonmuscle class-II myosins are regulated by RLC phosphorylation. When the RLC is unphosphorylated, these myosins are monomeric, inactive 10S conformers, which are folded and auto-inhibited by head-head interactions (Trybus et al., 1982; Craig et al., 1983; Trybus and Lowey, 1984; Wendt et al., 1999; Wendt et al., 2001). Phosphorylation of the RLC is necessary for smooth and nonmuscle myosins to unfold into active 6S monomers that self-assemble into filaments at physiological salt conditions (Craig et al., 1983; Billington et al., 2013). It is unclear how Myo2 is regulated by RLC phosphorylation or whether it assembles minifilaments because the yields of Myo2 from fission yeast have been insufficient to fully explore these mechanisms *in vitro*. Our study takes advantage of the baculovirus/*Sf*9 insect cell expression system to obtain better yields of Myo2 for molecular characterization. Employing recombinant Myo2, we examined the effects of RLC phosphorylation on enzymatic activity and motility as well as the propensity for Myo2 to self-assemble to address the question of how Myo2 is anchored for force production in the contractile ring.

3.3. MATERIALS AND METHODS

3.3.1. EXPRESSION AND PURIFICATION OF MYO2 AND RNG3

The coding sequence of the Myo2 heavy chain (HC) was cloned into the *Sf9*/baculovirus expression system vectors pAcSG2 (BD Biosciences, San Jose, CA) and

pFastBac-1 (Thermo Fisher Scientific). The light chains (LC), Cdc4 and Rlc1, were cloned into pAcUW51, a dual-promoter vector that drives expression of both LCs (BD Biosciences). The HC-coding sequence was linked at either the N- or the C-terminus by a FLAG tag (DYKDDDDK) to facilitate purification by affinity chromatography. Certain constructs additionally linked the HC-coding sequence to a C-terminal biotin tag (Cronan, 1990) for attachment to streptavidin-coated surfaces. *Sf9* cells were co-infected with recombinant baculovirus coding for the HC and LC constructs. After 72 h at 27°C, the cells were harvested by centrifugation at 5,000 x g for 10 min at 4°C. The cells were resuspended in ice-cold lysis buffer A (300 mM NaCl, 10 mM imidazole pH 7.4, 5 mM $MgCl_2$, and 1 mM ethylene glycol tetraacetic acid (EGTA)) supplemented with 2 mM dithiothreitol (DTT), 7% w/v sucrose, 0.5 mM 4 -(2-Aminoethyl) benzenesulfonyl fluoride hydrochloride (AEBSF) (Fisher, Fair Lawn, NJ), 5 µg/ml leupeptin (Acros Organics, NJ), 0.5 mM phenylmethylsulfonyl fluoride (PMSF) (MP Biomedical, Solon, OH), 0.5 mM Nα-Tosyl-L-lysine chloromethyl ketone hydrochloride (TLCK (Sigma-Aldrich, St. Louis, MO), 0.4 mg/ml benzamidine (Sigma), and protease inhibitor cocktail (P8340, Sigma), and lysed by sonication on an ice bath. Two mM MgATP was added, and cell debris was pelleted by centrifugation at 250,000 x g for 20 min at 4°C. The clarified supernatant was batch-incubated with FLAG-affinity resin (Sigma) for 1 h at 4°C. The resin was packed into a column and washed with lysis buffer before elution with 100 µg/mL FLAG peptide (Sigma) in lysis buffer A. The pooled elution fractions were concentrated by Amicon-Ultra filtration (EMD Millipore, Billerica, MA) and dialyzed at 4°C against storage buffer (300 mM NaCl, 10 mM imidazole pH 7.4, 1 mM EGTA, 1 mM NaN_3, 50% glycerol (vol/vol))

with 2 mM DTT and 1 µg/ml leupeptin) for storage at -20°C. Rng3 with a C-terminal FLAG tag was expressed in the *Sf9*-baculovirus system and purified in the same way. Average yields of Myo2 and Rng3 were approximately 1 mg per billion cells.

3.3.2. PURIFICATION OF OTHER PROTEINS

The p21/Cdc42-activated kinase (PAK), Pak1/Shk1/Orb2 , coding sequence was cloned into the pET19 (EMD Millipore) vector upstream of a C-terminal FLAG tag sequence. Pak1 expression in Rosetta (DE3) *Escherichia coli* (EMD Millipore) grown to OD_{600} 0.8-1.0 in Luria-Bertani (LB) broth was induced with 1 mM Isopropyl β-D-1-thiogalactopyranoside (IPTG) (Sigma) for 18h at room temperature. After the induction, cells were pelleted by centrifugation at 5,000 x g for 20 min. Cells were lysed by sonication on ice in lysis buffer A supplemented with 2 mM DTT, 7% sucrose, 10 mM Na pyrophosphate, 10 mM NaF, 0.5 mM AEBSF (Fisher), 5 µg/mL leupeptin (Acros), 0.5 mM PMSF (MP), and 5 mM benzamidine (Sigma). Following lysis, the lysate was clarified and FLAG-affinity chromatography was performed as outlined above.

Chicken skeletal actin was purified according to Spudich and Watt (1971). To purify Tpm, a bacterial expression construct pET3a (EMD Millipore) containing the coding sequence of fission yeast Cdc8 with N-terminal Ala-Ser (acetylation mimic) was transformed into BL21-DE3 *E. coli* (EMD Millipore). Transformed bacteria were grown in LB to OD_{600} 0.8-1.0 and induced with 0.4 mM IPTG for 5 h at 25°C. Cells were harvested by centrifugation and suspended in ice-cold lysis buffer B (20mM imidazole, pH 7.5, 10 mM NaCl, and 2mM EDTA) supplemented with 1mM DTT, 1 µg/mL leupeptin,

0.5 mM PMSF, and 0.4 mg/mL benzamidine and lysed by sonication on ice. Cell debris was pelleted by centrifugation at 30,000 g for 15 min at 4°C. The supernatants were boiled for 5 min while stirring, cooled to 25°C, and then denatured proteins were pelleted by centrifugation at 30,000 g for 15 min at 4°C. Tpm was precipitated by adjusting the pH of the supernatant to its isoelectric focusing point (pH 4.6), pelleted at 30,000 g for 15 min at 4°C, and dissolved by gentle agitation overnight at 4°C in lysis buffer B supplemented with 1 mM DTT and 1 μg/mL leupeptin. The dissolved Tpm was dialyzed against Tpm buffer (50 mM NaCl, 10 mM imidazole, pH 7.5, and 1 mM DTT)

3.3.3. RLC PHOSPHORYLATION

Myo2 was phosphorylated by adding 0.3 molar ratio of PAK in kinase buffer (150 mM NaCl, 10 mM imidazole pH 7.4, 5 mM $MgCl_2$ 1 mM EGTA, 1 mM NaN3 and 2 mM DTT) with 5 mM MgATP, and incubating at 30°C for 1 h. The control underwent the same treatment, but without Pak1. To evaluate phosphorylation levels, SDS-PAGE gels were stained with Pro Q Diamond Phosphoprotein Gel stain (Invitrogen, Eugene, OR) according to online protocol. Alternatively, samples were dissolved in 7.5 M urea and run on 40% glycerol gels (Trybus, 2000) to resolve the RLC based on charge. For ATPase and motility assays the RLC was 100% phosphorylated.

3.3.4. *IN VITRO* MOTILITY

To remove ATP-insensitive heads, Myo2 was subjected to centrifugation for 20 min at 400,000 x g in the presence of 2-fold excess F-actin and 2 mM MgATP in myosin

buffer (10 mM imidazole pH 7.4, 0.3 M NaCl, 5 mM $MgCl_2$, 1 mM EGTA, and 10 mM DTT). Nitrocellulose-coated flow cells were prepared with Neutravidin by the sequential addition of 0.5 mg/mL biotinylated BSA, 1 mg/mL BSA, and 10-50 μg/mL Neutravidin (Thermo Scientific) in Buffer A (25 mM imidazole pH 7.4, 0.15 M KCl, 4 mM $MgCl_2$, 1 mM EGTA, and 10 mM DTT), each followed by a 1 min incubation and 3 washes of buffer A. Myo2 was then applied in myosin buffer at 50 μg/mL (unless otherwise specified) for 1 min. ATP-insensitive heads were further blocked by two additions of 1μM vortexed F-actin in buffer B (25 mM imidazole pH 7.4, 50 mM KCl, 4 mM $MgCl_2$, 1 mM EGTA, and 10 mM DTT, 3 mg/mL glucose, 0.125 mg/mL glucose oxidase (Sigma-Aldrich), and 0.05 mg/mL catalase (Sigma-Aldrich)) over 1 min. Active heads were freed by three washes of buffer B with 1mM MgATP. The ATP was washed out with three more passes of buffer B and then 10nM F-actin labeled with 1.5-molar excess of rhodamine-phalloidin (Thermo Scientific) in buffer B was applied twice over 1 min. Buffer B with 0.5% methylcellulose and 1 mM MgATP was applied two times before imaging. When indicated, the KCl and methylcellulose was varied in the final buffer. To decorate actin with tropomyosin the AlaSer-Cdc8 acetyl mimic was added at 2μM with the labeled actin stock, and 2 μM tropomyosin was added to the final buffer. For experiments where Myo2 and Rng3 were attached to the coverslip surface, instead of preparing the flow cells with Neutravidin, combinations of Myo2 and Rng3 in myosin buffer were applied directly to the nitrocellulose-coated flow cells and then 1 mg/mL BSA was used to block the remaining surface.

Actin movement at 30°C was observed using an inverted microscope (Zeiss Axiovert 10) equipped with a heated objective, epifluorescence, and a Rolera MGi Plus digital camera. A dedicated computer with the Nikon NIS Elements software package was used to control the microscope and record the image data. Tiff stacks were processed in imageJ and analyzed using a filament tracking program described previously (Kinose et al., 1996).

3.3.5. ACTIN-ACTIVATED ATPASE ACTIVITY

ATPase assays were performed in 10 mM imidazole, pH 7.0, 50 mM NaCl, 1 mM $MgCl_2$, 1 mM Na azide, and 2mM DTT in separate 1.5 mL Eppendorf tubes in a 30°C water bath, while stirring. Myo2 was clarified by centrifugation for 20 min at 400,000 g in myosin buffer and then diluted to 2-fold concentration (final concentration: 25 μg/mL) in the assay buffer before being mixed 1:1 with skeletal actin at various concentrations. For Tpm-decoration, the actin stock was mixed 2:1 with AlaSer-Cdc8. Activity was initiated by the addition of 1mM MgATP and quenched with SDS at 5 min intervals over 25 min. Inorganic phosphate concentration was determined colorimetrically (Trybus, 2000).

3.3.6. ANALYTICAL ULTRACENTRIFUGATION

Myo2 was dialyzed for 18 h against buffers containing 10 mM imidazole, pH 7.0, 5 mM $MgCl_2$, 1 mM EGTA, and 1 mM DTT with varying concentrations of KCl. After dialysis, Myo2 was clarified by centrifugation at 200,000 g for 10 min at 4°C. Recovery of protein was 70-80% of the mass pre-dialysis. Precipitate was visible when Myo2 was dialyzed

against buffer containing 50 mM KCl. This sample was clarified by centrifugation at 20,000 g for 5 min at 4°C and ~50% of the protein was recovered. An Optima XL-1 analytical ultracentrifuge was employed to perform sedimentation velocity runs at 40,000 rpm and 20°C. Sedimentation coefficients were calculated using DCDT+ (v.2.4.3) software by John Philo and were corrected for temperature and buffer composition using Sednterp software.

3.4. RESULTS

3.4.1. PROPERTIES OF MYO2

We investigated Myo2's sequence and structure to obtain clues as to how it might be regulated and function during cytokinesis. The rod-like tail domain is a canonical feature of class-II myosins that dictates self-assembly. Based on domain analysis, Myo2 is similar to other class-II myosins except that the α-helical coiled-coil tail domain contains nine prolines distributed throughout its length (**Figure 3-1A**). Despite the presence of prolines, which disrupt coiled-coils, Myo2 has a rod-like tail and two heads (**Figure 3-1B**). However, the coiled-coil pattern of the Myo2 tail is highly disrupted, unlike the tails of other class-II myosins that self-assemble, where the coiled-coil is consistent throughout (**Figure 3-1C**). The disrupted coiled-coil of the rod is a unique feature of fungal class-II myosins that differentiates their functions and localizations in the cell (Bezanilla and Pollard, 2000; Lord et al., 2005; Fang et al., 2010).
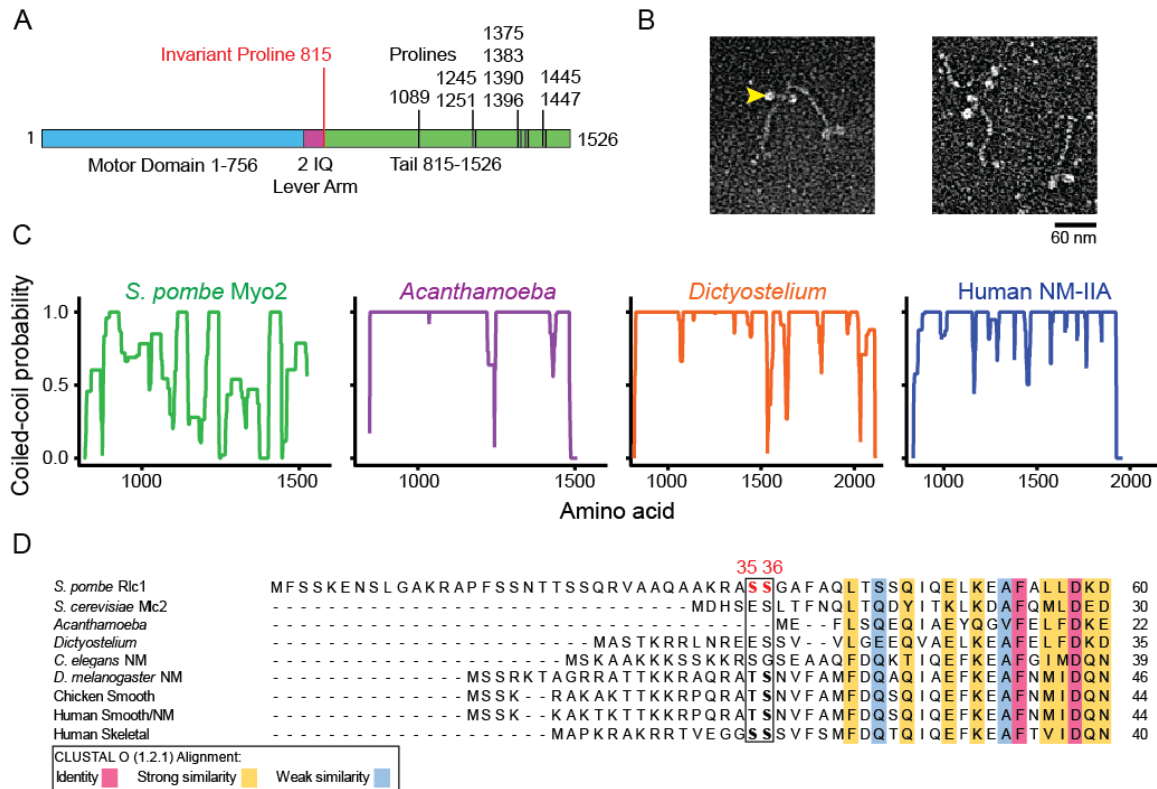
Figure 3-1: Unique features of fission yeast Myo2.
(A) Diagram illustrating the domain structure of Myo2, and the high number of Pro residues interspersed throughout the tail. The invariant proline marks the junction between the lever arm and the tail. (B) Electron micrographs of platinum shadowed Myo2 (C-Biotin-C-FLAG) molecules (courtesy of R. Craig) showing that Myo2 has two heads and an ~ 80 nm long tail. Filled yellow arrowhead points to a motor domain. (C) Coiled-coil predictions using Paircoil2 analysis comparing the tails of Myo2 and myosin-II from other species (*Acanthamoeba castellanii*, *Dictyostelium discoideum*, and human nonmuscle myosin-IIA). Plots begin with the invariant proline and end at the final residue. (D) A multiple sequence alignment of RLCs from different species using the CLUSTAL O (1.2.1) program. The N-terminal region is shown. The box indicates the conserved phosphorylation site(s) in other species align to Serines 35 and 36 in fission yeast RLC (red).

Studies in the fission yeast system by Loo and Balasubramanian (2008) provided evidence both *in vitro* and *in vivo* that fission yeast p21/Cdc42-activated kinase (PAK) can phosphorylate wild type RLC but not the Ser-35/36 double alanine mutant. Serines 35 and 36 of fission yeast RLC are conserved with Thr-18 and Ser-19 of the smooth/non-muscle

RLC in mammals (**Figure 3-1D**). However, it is unknown how phosphorylation by PAK

affects Myo2's enzymatic and motor activity.
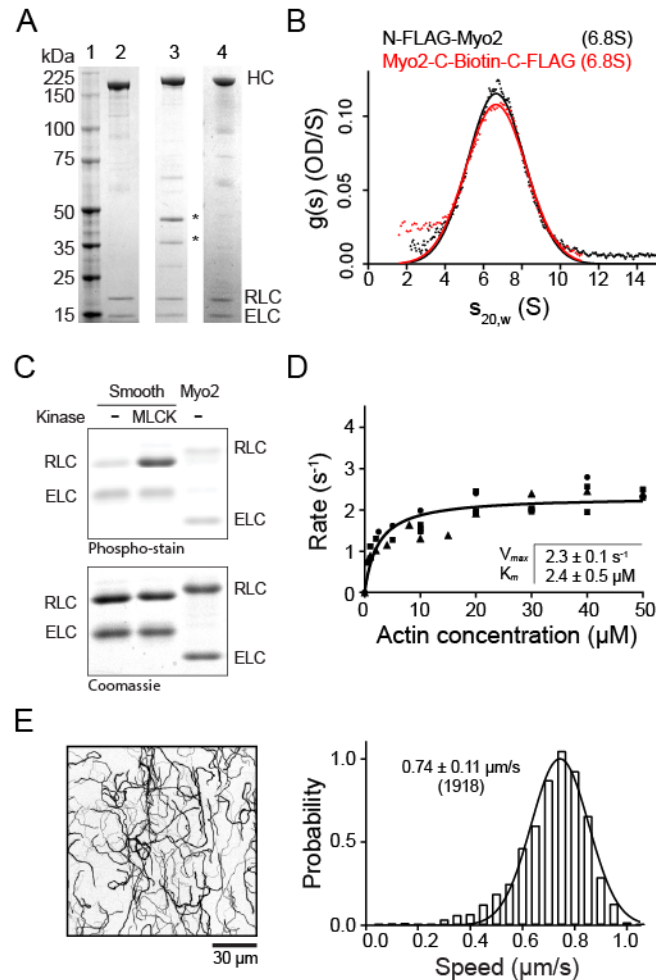
Figure 3-2: Unphosphorylated Myo2 has motor activity.
(A) SDS-gels of Myo2 heavy chain (HC) co-expressed with its native light chains, Rlc1 (RLC) and Cdc4 (ELC) in the baculovirus/insect cell expression system. (Lane 1), molecular mass standards, (lane 2) N-FLAG-Myo2, (lane 3) Myo2-C-Biotin-C-FLAG, and (lane 4) N-FLAG-Myo2-C-Biotin. Stars (*) indicate breakdown products of the myosin tail, identified by mass spectrometry, that co-purify on the FLAG-affinity resin. 4-12% SDS-PAGE gradient gels. (B) Sedimentation velocity of Myo2 by analytical ultracentrifugation. Conditions: 20°C, 40,000 rpm, 0.5M KCl, 5 mM $MgCl_2$, 1 mM EGTA, 1 mM DTT. The buffer was 10 mM potassium phosphate, pH 7.5 for the C-Biotin-FLAG construct, and 10 mM imidazole, pH7.0 for the N-FLAG construct. OD: optical density. (C) A 12% SDS-PAGE gel double-stained with Pro-Q Diamond phosphoprotein stain

(company) and then Coomassie Brilliant Blue. The light chains of unphosphorylated smooth muscle myosin, or phosphorylated with myosin light chain kinase (MLCK) (Trybus, 2000), are used as controls. Lane 3 shows that the RLC of expressed N-FLAG-Myo2-C-Biotin is unphosphorylated. (D) Rates of steady-state ATPase of Myo2 in the presence of various actin concentrations. Circles, squares, and triangles represent independent preparations of N-FLAG-Myo2-C-Biotin. Conditions: 30°C, 10 mM imidazole, pH 7.0, 50 mM NaCl, 1mM $MgCl_2$, 1 mM ATP, and 2 mM DTT. (E) In vitro motility assay. N-FLAG-Myo2-C-Biotin was attached to the coverslip with Neutravidin to ensure that all heads are available for interaction with actin. (Left) A maximum projection image of a representative field (128 μm x 128 μm x 50 s) showing trails of gliding actin filaments. (Right) Speeds of actin filament movement from two independent preparations of Myo2. Number of filaments tracked are indicated in parentheses. Error: ± SD.

It was anticipated that Myo2 folding in insect cells might require the co-expression

of a species-specific chaperone like certain unconventional myosins (Bird et al., 2014;

Bookwalter et al., 2014) because animals and fission yeast are separated by one billion

years of evolution (Pollard, 2014). Myo2 was co-expressed with its native light chains

Cdc4 (ELC) and Rlc1 (RLC). However, it was not necessary to co-express the native

chaperone Rng3 to obtain soluble Myo2 (**Figure 3-2A**). Sedimentation velocity in the

analytical ultracentrifuge showed symmetrical 7S peaks (**Figure 3-2B**), indicating that

Myo2 is a monodispersed, extended molecule. Phosphoprotein staining revealed that the

RLC of the recombinant Myo2 was unphosphorylated (**Figure 3-2C**). Despite lacking RLC

phosphorylation, recombinant Myo2 exhibited ATPase activity with a V_{max} of ~2.3 s^{-1}

(**Figure 3-2D**), which is consistent with the rates obtained with Myo2 purified from fission

yeast in previous studies (Lord and Pollard, 2004; Lord et al., 2008; Stark et al., 2010;

Clayton et al., 2015). Unphosphorylated Myo2 was also capable of sliding actin filaments

in motility assays with average rates around 0.7 μm/s at 30°C (**Figure 3-2E**).
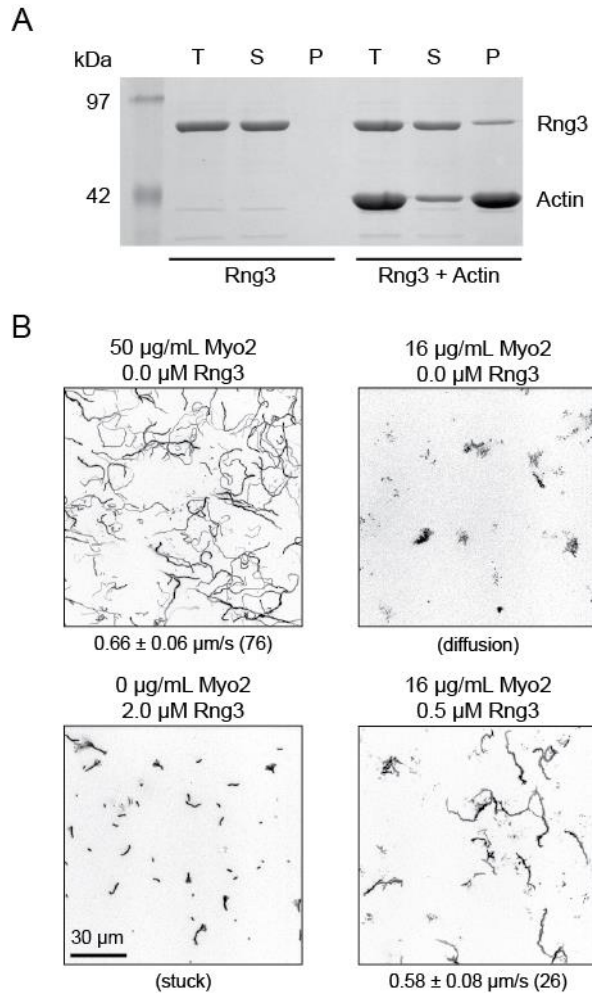
Figure 3-3: Rng3 promotes motility by binding actin filaments at low ionic strength. (A) A 12% SDS-PAGE gel showing (T) totals, (S) supernatants, and (P) pellets from a co-sedimentation assay in which 700 nM Rng3 and 75 μM actin were pelleted at 400,000 x g for 20 min in 25mM imidazole, pH 7.4, 46 mM KCl, 23 mM NaCl, 1 mM EGTA, 4 mM MgCl$_2$, and 2 mM DTT. Rng3 does not pellet in the absence of actin. (B) Panels showing maximum projections of representative fields (128 μm x 128 μm x 50 s) of motility in 50 mM KCl assay buffer performed in the absence of methylcellulose, to allow diffusion of actin away from the coverslip surface. Rng3 and Myo2 (N-FLAG-C-Biotin), were adhered non-specifically to nitrocellulose-coated flow cells (Lord and Pollard, 2004). Motility assay conditions: 30°C, 25 mM imidazole, pH 7.4, 50 mM KCl, 1 mM EGTA, 4 mM MgCl$_2$, 10 mM DTT, and 1 mM ATP. Mean speeds are indicated below each panel with numbers of tracked filaments in parentheses. Error: ± SD.

In earlier work, were Myo2 was isolated from fission yeast, it was observed that

Rng3 activated motility when the Myo2 concentration was low (Lord and Pollard, 2004;

Lord et al., 2008). Therefore, we probed into the mechanism of this apparent activation. Because a minimum number of myosin heads are required for motility, a plausible explanation for activation is that Rng3, when bound to nonspecifically to the nitrocellulose coated coverslip, may have tethered actin down to the surface. We preformed co-sedimentation assays to assess whether Rng3 binds to actin in low salt, similar to the motility assay conditions. A small portion of Rng3 pelleted with the actin (**Figure 3-3A**), indicating a weak interaction. We next examined whether Rng3 binds to actin in the motility assay. To assay relative actin binding, methylcellulose was omitted to allow the actin to freely diffuse away from the coverslip surface. Consistent with the dependence of motility on the number of myosin heads present, Myo2 alone applied to the chamber at 50 µg/mL exhibited robust motility with an average speed of ~0.7 µm/s, however no filament binding or motility was observed when the Myo2 concentration was reduced to 16 µg/mL (**Figure 3-3B**). Recapitulating the results of previous studies, the adhesion of Rng3 to the coverslip alongside 16 µg/mL Myo2 restored motility (**Figure 3-3B**). Additionally, Rng3 by itself was observed to recruit actin filaments near the coverslip surface (**Figure 3-3B**). Together, these data indicate that Rng3 binds to actin in the motility assay. Since we found Myo2 at sufficient concentrations to be fully active without adding Rng3 (**Figures 3-2D**, **3-2E**, and **3-3B**), the question remains whether Rng3's interaction with actin is relevant in a cellular context.

3.4.2. RLC PHOSPHORYLATION BY PAK LOWERS ACTOMYOSIN

AFFINITY

In order to examine the effects of RLC phosphorylation on Myo2, we phosphorylated the RLC *in vitro* using purified fission yeast PAK expressed in *E. coli* (**Figure 3-4A**). Phosphorylation correlated to a single shift on charge-separation gels (**Figure 3-4B**), indicating that the expressed PAK phosphorylates a single serine.
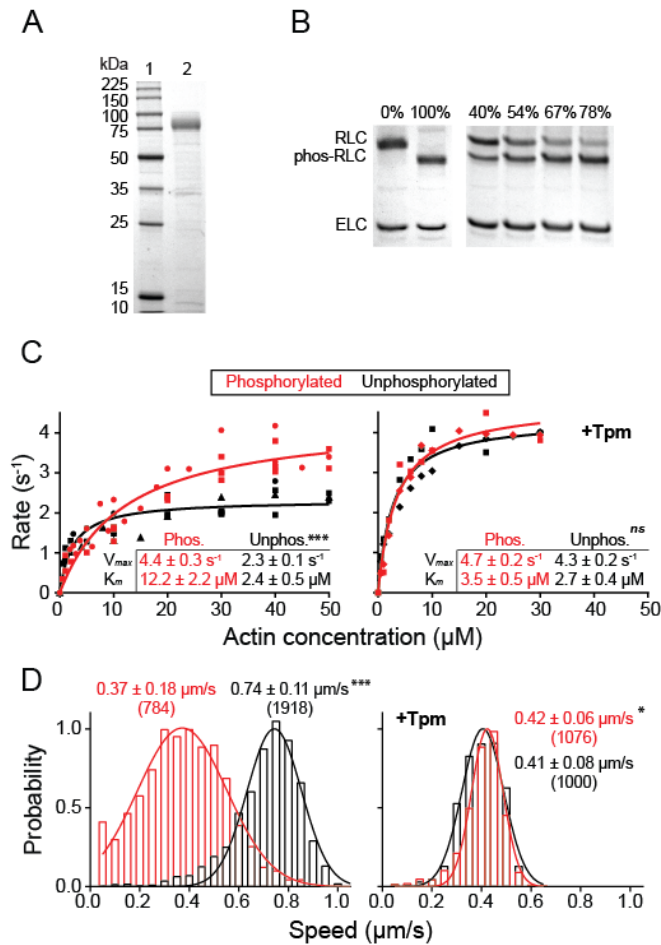
Figure 3-4: Effect of RLC phosphorylation on ATPase activity and motility.

118

(A) A 12% SDS-PAGE gel of (lane 1) molecular mass markers and (lane 2) purified recombinant fission yeast PAK. (B) Phosphorylated RLC migrates faster than unphosphorylated RLC on a 10% charge separation gel. Right panel shows a time course of phosphorylation, with percent phosphorylated indicated. (C) Steady-state ATPase of unphosphorylated or phosphorylated Myo2 in the absence or presence of tropomyosin (Tpm). Circles and squares represent independent preparations of N-FLAG-Myo2-C-Biotin. Diamonds represent N-FLAG-Myo2. Conditions: 30°C, 10 mM imidazole, pH 7.0, 50 mM NaCl, 1mM $MgCl_2$, 1 mM ATP, and 2 mM DTT. Tpm was added at a 2:1 Actin-Tpm molar ratio. Statistical significance was assessed by the Extra sum-of-squares F-test using GraphPad software. (D) In vitro motility speeds of unphosphorylated or phosphorylated Myo2, in the absence or presence of Tpm. Speeds represent motility data from two independent preparations of N-FLAG-Myo2-C-Biotin. To ensure that all heads were available for interaction with actin, Myo2 was attached to neutravidin-coated coverslips by a biotin tag at its C-terminus. Conditions: 30ºC, 0.5% methylcellulose, 25mM imidazole pH 7.4, 50 mM KCl, 4 mM $MgCl_2$, 1 mM EGTA, 1 mM ATP, and 10 mM DTT. When indicated, Tpm was added to a final concentration of 2 μM. Number of filaments tracked are indicated in the parentheses. Statistical significance was assessed d by Student's t-test, applying Welch's correction for unequal variance in the absence of Tpm. For all statistics: *$P < 0.05$, **$P < 0.001$, ***$P < 0.0001$, ns: no significance. Note: (C and D, left) Data for the unphosphorylated Myo2 are also represented in **Figures 3-2 D** and **E**.

Myo2 RLC phosphorylation was associated with a ~2-fold increase in actin-activated ATPase activity and a ~4-fold increase in K*m* (**Figure 3-4C**). Tropomyosin (Tpm)-decoration of actin also increased the Myo2 ATPase activity ~2-fold as shown previously (Stark et al., 2010; Clayton et al., 2015), however phosphorylation appeared to have little effect in the presence of Tpm (**Figure 3-4C**). Additionally, we examined the effects of phosphorylation on actin-gliding motility. To ensure equal availability of heads, Myo2 was attached to neutravidin-coated flow cells through the C-terminal biotin tag. Unphosphorylated Myo2 glided filaments at 0.74 ± 0.11 μm/s, whereas phosphorylated Myo2 had a speed of 0.34 ± 0.18 μm/s (**Figure 3-4D**). Similar to the ATPase result, Tpm masked the effect of phosphorylation and correlated with average speeds around 0.4 μm/s (**Figure 3-4D**). Tpm is thought to enhance actomyosin affinity in fission yeast and other

non-muscle systems (Stark et al., 2010; Barua et al., 2014). To examine the effects of phosphorylation and Tpm on actomyosin affinity, we conducted a series of motility assays designed to reduce actin binding incrementally by removing methylcellulose and increasing salt. Without methylcellulose, phosphorylated Myo2 bound fewer filaments compared to unphosphorylated (**Figure 3-5**). Tpm-decoration correlated with increased actin filament binding by Myo2, independent of phosphorylation, however phosphorylated Myo2 exhibited a more precipitous decrease in affinity with increasing salt (**Figure 3-5**). These data indicate that phosphorylation of the Myo2 RLC lowers the affinity for actin yet increases the V_{max} of ATPase, while Tpm has a dominant effect typified by an increase Myo2-actin binding.
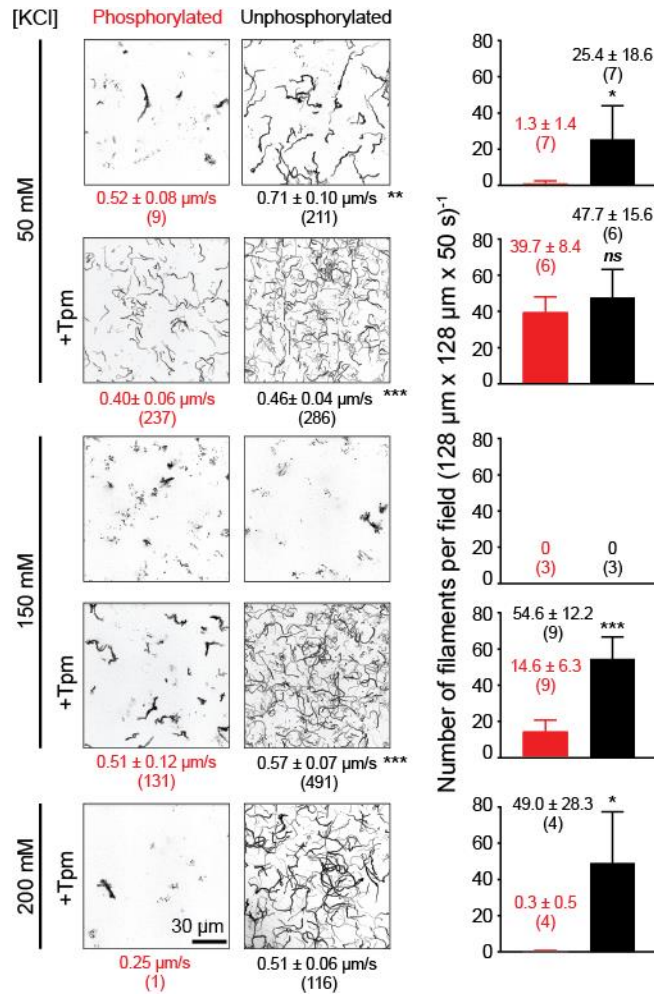
Figure 3-5: RLC phosphorylation reduces the number of Myo2 heads bound to actin filaments.

(Left) Panels showing maximum projections of representative fields (128 μm x 128 μm x 50 s). Speeds indicated with number of filaments tracked shown in parentheses. (Right) Quantification of panels to the left. Numbers of filaments ± SD identified by the analysis software (Kinose et al., 1996). Number of fields analyzed shown in parenthesis. Myo2 was attached to neutravidin-coated coverslips through the C-terminal biotin tag. Conditions: 30ºC, 25mM imidazole pH 7.4, KCl as indicated, 4 mM $MgCl_2$, 1 mM EGTA, 1 mM ATP, and 10 mM DTT. No methylcellulose was used to allow the diffusion of actin away from the surface. When indicated, Tpm was added to a final concentration of 2 μM. Data are from two independent preparations of Myo2 (N-FLAG-C-Biotin). Phosphorylation of the RLC was measured to be 100%. Error: ± SD. Significant difference was determined by Student's t-test, applying Welch's correction for unequal variance: *P < 0.05, **P < 0.001, ***P < 0.0001, ns: no significance.

3.4.3. MYO2 DOES NOT ASSEMBLE FILAMENTS IN PHYSIOLOGICAL SALT
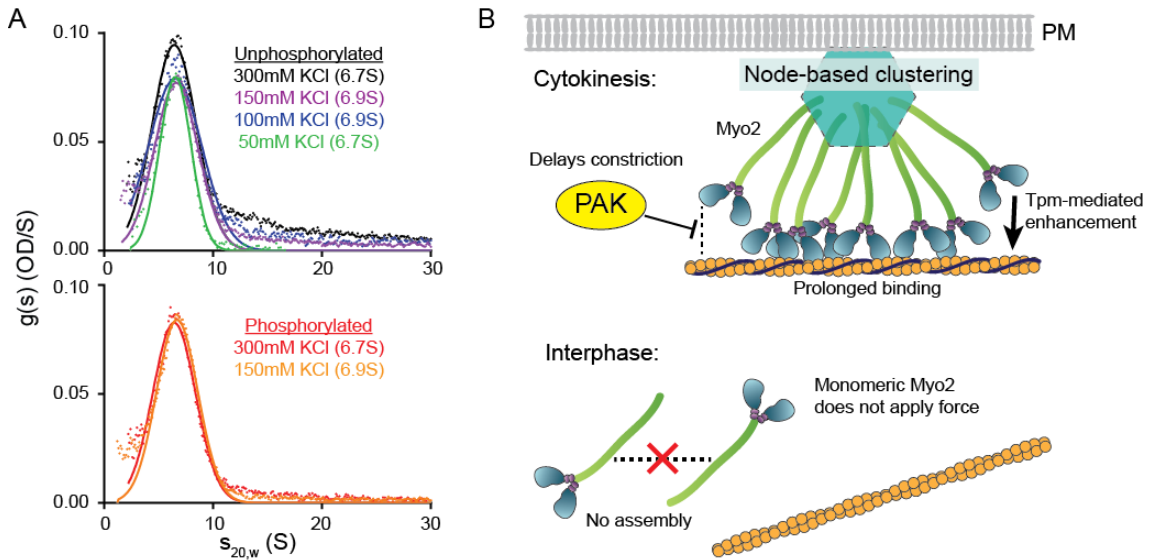
Figure 3-6: Lack of self-assembly suggests Myo2 function depends on anchorage into nodes.

(A) Sedimentation velocity of unphosphorylated or phosphorylated N-FLAG-Myo2 by analytical ultracentrifugation at varying KCl concentrations. Conditions: 20°C, 40,000 rpm, 10 mM imidazole, pH 7.0, 5 mM MgCl$_2$, 1 mM EGTA, 1 mM DTT (KCl as indicated). OD: optical density. (B) A model of Myo2 regulation during cytokinesis and interphase. During cytokinesis, clustering by the node anchors Myo2 for force-production in the contractile ring. RLC phosphorylation by PAK could delay contractile ring constriction (Loo and Balasubramanian, 2008) by reducing actomyosin affinity (this study). During interphase, unanchored Myo2 monomers in the cytosol would be unable to produce force. Plasma membrane: PM.

We examined whether Myo2 can self-assemble at various ionic strengths under such conditions that other class-II myosins assemble. Sedimentation velocities for all conditions tested were fit to single 7S species (**Figure 3-6A),** corresponding to the two-headed monomer. Myo2 was soluble down to 100 mM KCl, however we observed that approximately half of the material precipitated at 50 mM KCl (not shown). Despite Myo2's partial insolubility at 50 mM KCl, we did not observe any faster-sedimenting intermediate

species. Our observations fail to provide any evidence of Myo2 self-assembly, suggesting that Myo2 does not form minifilaments.

3.5. DISCUSSION

To better understand the mechanism of cytokinesis, we chose to investigate the function and regulation of Myo2, the myosin that is essential for cytokinesis in the well-established fission yeast model. Here, for the first time, we examined the molecular properties of recombinant Myo2, which lacked RLC phosphorylation and Rng3. Myo2 had enzymatic and motor activity without Rng3, and lacked auto-inhibition when unphosphorylated. Motility and ATPase assays revealed that Myo2 RLC phosphorylated *in vitro* by PAK exhibited a significantly lower affinity for actin. Furthermore, hydrodynamic measurements indicated that Myo2 also lacks self-assembly properties conserved with most myosins of class-II. Our findings underscore that Myo2 is an atypical class-II myosin in terms of molecular function and regulation, despite its conserved biological role during cytokinesis.

3.5.1. A LACK OF ASSEMBLY SUGGESTS MYO2 CLUSTERS IN NODES

It is generally thought that Myo2, like other class-II myosins, spends a low proportion of time in strong-binding states within its ATPase cycle, or has a low duty ratio. Duty ratio estimates, derived from ATPase and motility (Huxley, 1990), based on our data are consistent with Stark et al. (2010), ranging from 4-10%, depending on the presence of

Tpm. Class-II myosins in animal cells overcome their low duty ratio by forming filaments that contain from 30 to 300 molecules (Harrison et al., 1971; Billington et al., 2013). In order to maintain prolonged association with actin, a functional unit of Myo2 in the contractile ring is expected to consist of multiple molecules as well. However, the coiled-coil of the Myo2 tail is highly disrupted relative to the tails of other filament-forming myosins (**Figure 3-1C**). Consistently, Myo2 was not observed to form filaments or any higher-order structures under any condition tested (**Figure 3-6A**). Although the conditions examined were not exhaustive, it can be concluded that Myo2 does not self-assemble under physiological salt conditions. Without the ability to self-assemble, Myo2 may be assembled into clusters through the association of the Myo2 tail with other proteins of the contractile ring nodes (**Figure 3-6B**). Recently, super-resolution studies by Laplante et al. (2016) support aspects of this model, such as the arrangement of Myo2 tails collected together near plasma membrane while the heads are splayed out toward the cytoplasm. Additionally, each node was estimated to contain around ten Myo2 molecules (Laplante et al., 2016), which would ensure a constant (100%) association with actin-Tpm, given a duty ratio of 10%. Our lack of evidence for Myo2 self-assembly supports the model that Myo2 is clustered together by proteins of the node complex.

3.5.2. MYO2 DOES NOT NEED RNG3 FOR ACTIVITY

Our findings show that Rng3 is not needed for Myo2 motor activity. Active recombinant Myo2 was obtained without co-expression of Rng3 (**Figure 3-2A**). Therefore, the insect homolog of Rng3, Unc45, must be sufficient to chaperone Myo2 into its native

conformation. Our data suggest Rng3 binds actin in the motility assay, which could plausibly be misinterpreted as increased actomyosin binding (**Figure 3-3B**). Since we found that recombinant Myo2 is fully active, the effect of Rng3 tethering actin, when bound nonspecifically to the coverslip, could be an *in vitro* artefact. In general, the cellular role of UCS proteins as actin-tethers has not been suggested in any other studies, whereas there is evidence for UCS proteins' involvement in unfolding-response and protein turnover (Etard et al., 2008; Melkani et al., 2010; Melkani et al., 2011). UCS proteins are widely known to be chaperones that assist in the folding of myosin (Hutagalung et al., 2002). Evidence suggests that Rng3 too is essential for chaperoning myosin in fission yeast (Stark et al., 2013) and for cytokinesis (Wong et al., 2000). The hypothesis that Rng3 activates motility stemmed, in part, from the observation that low concentrations (~60 molecules) of Rng3 localize to the contractile ring in wildtype cells (Lord and Pollard, 2004; Wu and Pollard, 2005). However, given the low abundance of Rng3 at the contractile ring it is possible that a subpopulation of Myo2 can sometimes bring Rng3 along during the process of folding as Myo2 is incorporated into nodes, since motor function is not required for the division site recruitment of Myo2 (Wong et al., 2000; Mulvihill et al., 2001; Motegi et al., 2004).

3.5.3. RLC PHOSPHORYLATION DECREASES MYO2'S FORCE

PAK was observed to phosphorylate a single residue of RLC *in vitro* (**Figure 3-4B**). Similarly, Chew et al. (1998), employing reconstituted mammalian proteins, described that PAK phosphorylated Ser19 but not Thr18 on the RLC. However, myosin

light chain kinase (MLCK) preferentially phosphorylates Ser19, but also phosphorylates Thr18. Based on alignment, Ser36 of fission yeast is the residue homologous to Ser19 (**Figure 3-1D**), which we predict to represent the conserved site for PAK across species.

We showed for the first time that Myo2 is active when the RLC is unphosphorylated, unlike vertebrate nonmuscle myosins (**Figure 3-2**, **C-E**). However, our results indicate that RLC phosphorylation leads to weaker actin-binding, which is consistent with *in vivo* studies suggesting that RLC phosphorylation delays ring constriction and dephosphorylation upregulates cytokinesis (Loo and Balasubramanian, 2008). Loo and Balasubramanian (2008) reported that the phospho-null RLC (Ser35,36Ala) mutation in fission yeast resulted in premature constriction, which sometimes led to aneuploidies. We found that phosphorylation increased actin-activated ATPase V_{max} and slowed motility, and was associated with a ~4-fold increase in the K_m and weaker actin-binding in the motility assay (**Figures 3-4** and **3-5**), which could explain a delay in constriction. In contrast to our findings, Sladewski et al. (2009), employing Myo2 purified from fission yeast, reported that the S35,36A mutant had 4-fold slower motility than the wild-type and phospho-mimetic, while ATPase rates were unaffected. The implication being that phosphorylation enhances the motility speed of Myo2 leading to increased rates of contractile ring constriction. The 2009 study did not report the phosphorylation state of the wild-type Myo2 isolated from fission yeast. Our study was able to control the phosphorylation state of the RLC associated with Myo2, which was not possible previously with the yields of Myo2 that can be purified from the yeast. Furthermore, it is likely that the phospho-mimetic and -null mutants do not fully simulate

126

the native serine with or without phosphorylation. We also show that Tpm strongly enhances Myo2's affinity for actin and opposes the effect of phosphorylation in motility and ATPase assays (**Figures 3-4** and **3-5**). Therefore, the increased ATPase V$_{max}$ and K$_m$ when Myo2 is phosphorylated (**Figure 3-4C**) may be due to faster transitioning into weak actin-binding states. In contrast, Tpm has been shown to prolong the strong-binding states of budding yeast myosin-V (Hodges et al., 2012) and has been suggested to do similarly for fission yeast Myo2 (Stark et al., 2010). The opposing effects between phosphorylation and Tpm in motility assays suggest that phosphorylation may reduce force production by lowering actin affinity

Our study shows that the functional consequences of phosphorylating the RLC of fission yeast Myo2 are the opposite of animal nonmuscle myosins, where phosphorylation is required for activity. One striking feature of fission yeast RLC is an extended N-terminus that is distinct from RLCs of other species (**Figure 3-1D**), which may be responsible for its unique regulatory properties. The structural basis of how RLC phosphorylation affects myosin function is not completely understood, but it is thought that stiffness of the lever arm could be altered by conformational changes in the RLC. Furthermore, interactions between the RLC N-terminus and the ELC likely have an important role in shaping the lever arm (Taylor et al., 2014). If RLC phosphorylation reduces the force output of Myo2, it could be due to some novel interactions that occur between the extended N-terminus and other parts of the molecule. Myo2's particular RLC regulatory mechanism may be pertinent in understanding the structural differences that lead to functional variation across species and disease states.

3.5.4. CONCLUSIONS AND PERSPECTIVES

Our observations indicate that the Myo2 tail may represent a fungal adaptation to cluster myosin in the nodes. This raises the question of whether animal cells also build contractile rings from nodes or by some other mechanism, especially since nonmuscle myosins function as minifilaments. It remains unknown what components of the node are the direct binding partners of the Myo2 tail. This question requires *in vitro* reconstitution, for which our study lays the foundation. Characterizing Myo2's biochemistry builds upon the current models of cytokinesis, which are based on work in the fission yeast system.

3.6. REFERENCES

Barua, B., A. Nagy, J.R. Sellers, and S.E. Hitchcock-DeGregori. 2014. Regulation of Nonmuscle Myosin II by Tropomyosin. *Biochemistry*. 53:4015-4024.

Bezanilla, M., S.L. Forsburg, and T.D. Pollard. 1997. Identification of a second myosin-II in Schizosaccharomyces pombe: Myp2p is conditionally required for cytokinesis. *Molecular biology of the cell*. 8:2693-2705.

Bezanilla, M., and T.D. Pollard. 2000. Myosin-II tails confer unique functions in Schizosaccharomyces pombe: characterization of a novel myosin-II tail. *Molecular biology of the cell*. 11:79-91.

Billington, N., A. Wang, J. Mao, R.S. Adelstein, and J.R. Sellers. 2013. Characterization of three full-length human nonmuscle myosin II paralogs. *The Journal of biological chemistry*. 288:33398-33410.

Bird, J.E., Y. Takagi, N. Billington, M.P. Strub, J.R. Sellers, and T.B. Friedman. 2014. Chaperone-enhanced purification of unconventional myosin 15, a molecular motor specialized for stereocilia protein trafficking. *Proceedings of the National Academy of Sciences of the United States of America*. 111:12390-12395.

Bookwalter, C.S., A. Kelsen, J.M. Leung, G.E. Ward, and K.M. Trybus. 2014. A Toxoplasma gondii class XIV myosin, expressed in Sf9 cells with a parasite co-chaperone, requires two light chains for fast motility. *The Journal of biological chemistry*. 289:30832-30841.

Cheffings, T.H., N.J. Burroughs, and M.K. Balasubramanian. 2016. Actomyosin Ring Formation and Tension Generation in Eukaryotic Cytokinesis. *Current biology : CB*. 26:R719-737.

Chew, T.L., R.A. Masaracchia, Z.M. Goeckeler, and R.B. Wysolmerski. 1998. Phosphorylation of non-muscle myosin II regulatory light chain by p21-activated kinase (gamma-PAK). *Journal of muscle research and cell motility*. 19:839-854.

Clayton, J.E., L.W. Pollard, G.G. Murray, and M. Lord. 2015. Myosin motor isoforms direct specification of actomyosin function by tropomyosins. *Cytoskeleton (Hoboken, N.J.)*. 72:131-145.

Craig, R., R. Smith, and J. Kendrick-Jones. 1983. Light-chain phosphorylation controls the conformation of vertebrate non-muscle and smooth muscle myosin molecules. *Nature*. 302:436-439.

Cronan, J.E., Jr. 1990. Biotination of proteins in vivo. A post-translational modification to label, purify, and study proteins. *The Journal of biological chemistry*. 265:10327-10333.

Etard, C., U. Roostalu, and U. Strahle. 2008. Shuttling of the chaperones Unc45b and Hsp90a between the A band and the Z line of the myofibril. *The Journal of cell biology*. 180:1163-1175.

Fang, X., J. Luo, R. Nishihama, C. Wloka, C. Dravis, M. Travaglia, M. Iwase, E.A. Vallen, and E. Bi. 2010. Biphasic targeting and cleavage furrow ingression directed by the tail of a myosin II. *The Journal of cell biology*. 191:1333-1350.

Harrison, R.G., S. Lowey, and C. Cohen. 1971. Assembly of myosin. *J Mol Biol*. 59:531-535.

Hodges, A.R., E.B. Krementsova, C.S. Bookwalter, P.M. Fagnant, T.E. Sladewski, and K.M. Trybus. 2012. Tropomyosin is essential for processive movement of a class V myosin from budding yeast. *Current biology : CB*. 22:1410-1416.

Hutagalung, A.H., M.L. Landsverk, M.G. Price, and H.F. Epstein. 2002. The UCS family of myosin chaperones. *Journal of cell science*. 115:3983-3990.

Huxley, H.E. 1990. Sliding filaments and molecular motile systems. *The Journal of biological chemistry*. 265:8347-8350.

Kinose, F., S.X. Wang, U.S. Kidambi, C.L. Moncman, and D.A. Winkelmann. 1996. Glycine 699 is pivotal for the motor activity of skeletal muscle myosin. *The Journal of cell biology*. 134:895-909.

Kitayama, C., A. Sugimoto, and M. Yamamoto. 1997. Type II myosin heavy chain encoded by the myo2 gene composes the contractile ring during cytokinesis in Schizosaccharomyces pombe. *The Journal of cell biology*. 137:1309-1319.

Laplante, C., J. Berro, E. Karatekin, A. Hernandez-Leyva, R. Lee, and T.D. Pollard. 2015. Three myosins contribute uniquely to the assembly and constriction of the fission yeast cytokinetic contractile ring. *Current biology : CB*. 25:1955-1965.

Laplante, C., F. Huang, I.R. Tebbs, J. Bewersdorf, and T.D. Pollard. 2016. Molecular organization of cytokinesis nodes and contractile rings by super-resolution fluorescence microscopy of live fission yeast. *Proceedings of the National Academy of Sciences of the United States of America*. 113:E5876-e5885.

Laporte, D., V.C. Coffman, I.J. Lee, and J.Q. Wu. 2011. Assembly and architecture of precursor nodes during fission yeast cytokinesis. *The Journal of cell biology*. 192:1005-1021.

Lee, C.F., G.C. Melkani, and S.I. Bernstein. 2014. The UNC-45 myosin chaperone: from worms to flies to vertebrates. *International review of cell and molecular biology*. 313:103-144.

Lee, I.J., V.C. Coffman, and J.Q. Wu. 2012. Contractile-ring assembly in fission yeast cytokinesis: Recent advances and new perspectives. *Cytoskeleton (Hoboken, N.J.)*. 69:751-763.

Liu, X., M.S. Hong, S. Shu, S. Yu, and E.D. Korn. 2013. Regulation of the filament structure and assembly of Acanthamoeba myosin II by phosphorylation of serines in the heavy-chain nonhelical tailpiece. *Proceedings of the National Academy of Sciences of the United States of America*. 110:E33-40.

Loo, T.H., and M. Balasubramanian. 2008. Schizosaccharomyces pombe Pak-related protein, Pak1p/Orb2p, phosphorylates myosin regulatory light chain to inhibit cytokinesis. *The Journal of cell biology*. 183:785-793.

Lord, M., E. Laves, and T.D. Pollard. 2005. Cytokinesis depends on the motor domains of myosin-II in fission yeast but not in budding yeast. *Molecular biology of the cell*. 16:5346-5355.

Lord, M., and T.D. Pollard. 2004. UCS protein Rng3p activates actin filament gliding by fission yeast myosin-II. *The Journal of cell biology*. 167:315-325.

Lord, M., T.E. Sladewski, and T.D. Pollard. 2008. Yeast UCS proteins promote actomyosin interactions and limit myosin turnover in cells. *Proceedings of the National Academy of Sciences of the United States of America*. 105:8014-8019.

Mahajan, R.K., and J.D. Pardee. 1996. Assembly mechanism of Dictyostelium myosin II: regulation by K+, Mg2+, and actin filaments. *Biochemistry*. 35:15504-15514.

Melkani, G.C., R. Bodmer, K. Ocorr, and S.I. Bernstein. 2011. The UNC-45 chaperone is critical for establishing myosin-based myofibrillar organization and cardiac contractility in the Drosophila heart model. *PloS one*. 6:e22579.

Melkani, G.C., C.F. Lee, A. Cammarato, and S.I. Bernstein. 2010. Drosophila UNC-45 prevents heat-induced aggregation of skeletal muscle myosin and facilitates refolding of citrate synthase. *Biochemical and biophysical research communications*. 396:317-322.

Mishra, M., M. D'Souza V, K.C. Chang, Y. Huang, and M.K. Balasubramanian. 2005. Hsp90 protein in fission yeast Swo1p and UCS protein Rng3p facilitate myosin II assembly and function. *Eukaryotic cell*. 4:567-576.

Motegi, F., M. Mishra, M.K. Balasubramanian, and I. Mabuchi. 2004. Myosin-II reorganization during mitosis is controlled temporally by its dephosphorylation and spatially by Mid1 in fission yeast. *The Journal of cell biology*. 165:685-695.

Mulvihill, D.P., C. Barretto, and J.S. Hyams. 2001. Localization of fission yeast type II myosin, Myo2, to the cytokinetic actin ring is regulated by phosphorylation of a C-terminal coiled-coil domain and requires a functional septation initiation network. *Molecular biology of the cell*. 12:4044-4053.

Ni, W., and O.O. Odunuga. 2015. UCS proteins: chaperones for myosin and co-chaperones for Hsp90. *Sub-cellular biochemistry*. 78:133-152.

Pollard, T.D. 2014. The value of mechanistic biophysical information for systems-level understanding of complex biological processes such as cytokinesis. *Biophysical journal*. 107:2499-2507.

Pollard, T.D., and J.Q. Wu. 2010. Understanding cytokinesis: lessons from fission yeast. *Nat Rev Mol Cell Biol*. 11:149-155.

Stark, B.C., M.L. James, L.W. Pollard, V. Sirotkin, and M. Lord. 2013. UCS protein Rng3p is essential for myosin-II motor activity during cytokinesis in fission yeast. *PloS one*. 8:e79593.

Stark, B.C., T.E. Sladewski, L.W. Pollard, and M. Lord. 2010. Tropomyosin and myosin-II cellular levels promote actomyosin ring assembly in fission yeast. *Molecular biology of the cell*. 21:989-1000.

Takaine, M., O. Numata, and K. Nakano. 2014. Fission yeast IQGAP maintains F-actin-independent localization of myosin-II in the contractile ring. *Genes to cells : devoted to molecular & cellular mechanisms*. 19:161-176.

Takaine, M., O. Numata, and K. Nakano. 2015. An actin-myosin-II interaction is involved in maintaining the contractile ring in fission yeast. *Journal of cell science*. 128:2903-2918.

Taylor, K.A., M. Feig, C.L. Brooks, 3rd, P.M. Fagnant, S. Lowey, and K.M. Trybus. 2014. Role of the essential light chain in the activation of smooth muscle myosin by regulatory light chain phosphorylation. *Journal of structural biology*. 185:375-382.

Trybus, K.M. 2000. Biochemical studies of myosin. *Methods (San Diego, Calif.)*. 22:327-335.

Trybus, K.M., T.W. Huiatt, and S. Lowey. 1982. A bent monomeric conformation of myosin from smooth muscle. *Proceedings of the National Academy of Sciences of the United States of America*. 79:6151-6155.

Trybus, K.M., and S. Lowey. 1984. Conformational states of smooth muscle myosin. Effects of light chain phosphorylation and ionic strength. *The Journal of biological chemistry*. 259:8564-8571.

Vavylonis, D., J.Q. Wu, S. Hao, B. O'Shaughnessy, and T.D. Pollard. 2008. Assembly mechanism of the contractile ring for cytokinesis by fission yeast. *Science (New York, N.Y.)*. 319:97-100.

Wendt, T., D. Taylor, T. Messier, K.M. Trybus, and K.A. Taylor. 1999. Visualization of head-head interactions in the inhibited state of smooth muscle myosin. *The Journal of cell biology*. 147:1385-1390.

Wendt, T., D. Taylor, K.M. Trybus, and K. Taylor. 2001. Three-dimensional image reconstruction of dephosphorylated smooth muscle heavy meromyosin reveals asymmetry in the interaction between myosin heads and placement of subfragment 2. *Proceedings of the National Academy of Sciences of the United States of America*. 98:4361-4366.

Win, T.Z., Y. Gachet, D.P. Mulvihill, K.M. May, and J.S. Hyams. 2001. Two type V myosins with non-overlapping functions in the fission yeast Schizosaccharomyces pombe: Myo52 is concerned with growth polarity and cytokinesis, Myo51 is a component of the cytokinetic actin ring. *Journal of cell science*. 114:69-79.

Wong, K.C., N.I. Naqvi, Y. Iino, M. Yamamoto, and M.K. Balasubramanian. 2000. Fission yeast Rng3p: an UCS-domain protein that mediates myosin II assembly during cytokinesis. *Journal of cell science*. 113 (Pt 13):2421-2432.

Wu, J.Q., and T.D. Pollard. 2005. Counting cytokinesis proteins globally and locally in fission yeast. *Science (New York, N.Y.)*. 310:310-314.

Wu, J.Q., V. Sirotkin, D.R. Kovar, M. Lord, C.C. Beltzner, J.R. Kuhn, and T.D. Pollard. 2006. Assembly of the cytokinetic contractile ring from a broad band of nodes in fission yeast. *The Journal of cell biology*. 174:391-402.

CHAPTER 4: DISCUSSION

4.1. LESSONS ON CYTOKINESIS FROM FISSION YEAST

Tension in the contractile ring is an important physical aspect of cytokinesis that is not well understood. Measuring the kinetic rates and understanding the physical geometry of the myosins allows for the development of more accurate biophysical models that can explain the contractile ring's dynamics. Currently, biophysical models of cytokinesis are well-established in fission yeast (Pollard, 2014). To build upon these models it is critical to understand how the essential myosin, Myo2, functions in the contractile ring. As introduced in **Chapter one**, the most likely ways that Myo2 could plausibly anchor into the ring are represented by two models. Model one suggests that Myo2 could function similarly to animal nonmuscle myosins that form minifilaments and are regulated by RLC phosphorylation. Model two, which is based on *in vivo* studies showing that Myo2 functions in nodes, suggests that Myo2 is anchored to the nodes. We investigated model one by probing Myo2's propensity to self-assemble and measuring how RLC phosphorylation affects its enzymatic and motor activity (**Chapter three**). As discussed in **Section 4.1.1.**, our evidence failed to support the model that Myo2 functions similarly to animal nonmuscle myosins that form minifilaments, which helps to validate the second model where Myo2 is clustered by the nodes.

How does the tension of the ring lead to cytokinesis? In animal cells, the contractile ring is predicted to guide cytokinesis through directing passive forces (Poirier et al., 2012) and regulating other cellular processes (**Section 4.1.2**). The major force producer that drives cytokinesis in fission yeast is probably not the contractile ring but, rather, the cell

134

wall-based septum (Proctor et al., 2012). To fill some of the mechanistic gaps within the complex contractile ring-based signaling pathways that drive septum formation, we examined the contractile ring protein Cyk3, whose function was unknown. Our results indicated that Cyk3 functions as a catalytically inactive transglutaminase to regulate the cell wall (**Chapter two**). **Section 4.1.2**. discusses how Cyk3's transglutaminase-related activity may serve to directly regulate Rho1, which is centrally involved in the activation of septum-synthesizing enzymes.

4.1.1 NODE-BASED CONTRACTILE RING ASSEMBLY

Myo2 has a well-established role as the essential myosin isoform in the fission yeast contractile ring, which functions alongside auxiliary myosins Myp2 and Myo51. Based on the conventional mechanism of class-II myosin function, it was conceivable that Myo2 could form minifilaments to provide tension in the contractile ring. However, the study presented in **Chapter three**, which examined the ability of Myo2 to self-assemble, found that it does not form filaments like other class-II myosins. The conclusion is that Myo2 may be clustered together through node-binding in order to maintain its association with actin filaments. Recently, super resolution fluorescence microscopy studies of Myo2 tagged at either end with the photoconvertable fluorescent protein Eos found that the C-terminus of the Myo2 tail occupies a zone closer to the plasma membrane than the heads (Laplante et al., 2016), which suggests that the node scaffolding proteins bind the tails and point the heads towards the cytosol (**Figure 4-1**). Consistently, Myo2 does not rely on actin filaments for localization, but appears to depend on distal portions of its tail as well as

135

IQGAP^{Rng2} (Laporte et al., 2011; Takaine et al., 2014). Nonmuscle class-II myosin self-assembly collects around 30 molecules so that at least a few heads per minifilament maintain the association with actin filaments over multiple ATPase cycles (Billington et al., 2013). Therefore, it is generally assumed that the subcellular localizations of metazoan nonmuscle class-II myosins depend on local activation by phosphorylation, which directs the myosins to self-assemble and bind nearby actin filaments. Thus, it would seem that the mechanism where nodes anchor myosin-II to the membrane could be unique to Myo2 and similar fungal myosins. Perhaps the node is an adaptation to account for the cell wall that is a feature of fungi but not of animals and amoebas.
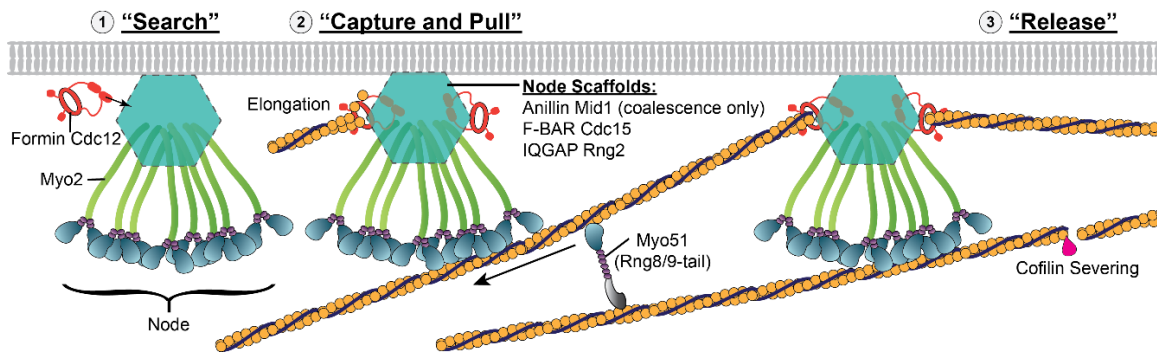
Figure 4-1: Myo2 clustered by nodes power "Search, Capture, Pull, and Release" (SCPR).

During the search phase, Myo2 and formin are recruited into the nodes. Once, nucleation and elongation of actin filaments occurs, Myo2 captures actin and pulls the adjacent node closer. Myo51 contributes to the node coalescence by anchoring to actin-tropomyosin filaments through the tail-binding partners Rng8 and Rng9 and pulling on nearby actin (Tang et al., 2016). Release occurs through filament severing or by myosin dissociation. Cycles of SCPR maintain the nodes as a tight ring at an optimal distance, while providing a steady-state tension (Vavylonis et al., 2008; Pollard and Wu, 2010; Lee et al., 2012).

Figure 4-1 depicts a SCPR model, which describes a node-based mechanism of contractile ring assembly, where Myo2 is clustered in nodes. This arrangement is

136

reasonable when considering how Myo2 motor activity makes the nodes dynamic for ring coalescence. Additionally, Myo51 has been proposed to contribute to ring coalescence (Laplante et al., 2015). New data suggest that Myo51 is stabilized as a single-headed motor by binding partners Rng8 and Rng9, which adapt the tail for ATP-insensitive binding to tropomyosin-decorated actin filaments (Tang et al., 2016). Therefore, in contrast to Myo2 that is two-headed and clustered by the node, many single-headed Myo51 molecules could anchor along the length of actin filaments in order to contribute to node coalescence (**Figure 4-1**). The third myosin, Myp2, does not enter the contractile ring until after coalescence (Bezanilla et al., 2000), and relies on actin to localize to the division site (Takaine et al., 2015). Myp2's primary role is to contribute force during ring constriction (Mishra et al., 2013; Laplante et al., 2015), but the mechanism of Myp2's function is unclear. Initial characterizations of Myp2's tail indicated that the N-terminal half formed an antiparallel coiled-coil with the C-terminal half (Bezanilla and Pollard, 2000), which suggests that Myp2 is single-headed. Since it depends on actin for localization, one speculation is that Myp2 self-clusters by some unforeseen manner.

4.1.2. REGULATION OF THE CLEAVAGE FURROW

The contractile ring functions as a guideline for cytokinesis in fission yeast, ensuring that the cleavage furrow follows a straight and even path at the cell equator through the regulation of membrane trafficking and cell wall synthesis (Thiyagarajan et al., 2015; Zhou et al., 2015). Vesicle trafficking at the division site is also important for animal cells to extend the plasma membrane inward from the cortex while maintaining the cell at

a constant volume (Albertson et al., 2005). The cleavage furrow in fission yeast requires the delivery of vesicles that carry the transmembrane enzymes that synthesize the septum cell wall. Evidence suggests that F-BAR[Cdc15] in the contractile ring ensures the efficient delivery of the β-glucan synthase Bgs1, which synthesizes the primary septum at the division site (Cortes et al., 2007; Arasada and Pollard, 2014). It is unclear how F-BAR[Cdc15] helps in recruiting vesicles containing Bgs1, but evidence indicates that F-BAR[Cdc15] coordinates another F-BAR protein Imp2 to organize a network of proteins that are generally involved with regulating cell wall (Ren et al., 2015). Some proteins of the F-BAR-associated network, such as Rho-GEF Rgf3 and paxillin Pxl1, affect cell wall synthesis through the activation or inhibition of the GTPase Rho1, which in turn activates Bgs1 (Arellano et al., 1996; Tajadura et al., 2004; Pinar et al., 2008; Ren et al., 2015).

Cyk3 is another member of the F-BAR[Cdc15] network (Roberts-Galbraith et al., 2010). **Chapter two** of this dissertation describes work indicating that Cyk3 is a transglutaminase-like regulator of septation/cell wall shape, which lacks a Cys residue necessary for catalytic activity. We found that Cyk3-mutant or -overexpressing yeast cells exhibited defects in the septum and cell shape in a manner dependent on conserved residues within the inactive transglutaminase domain. Additional localization studies of GFP-tagged Cyk3 in the cell indicated that it was a component of the contractile ring during cytokinesis and the cell cortex during interphase. Together, this evidence made a case for Cyk3 as a founding member of a new branch of transglutaminase-like proteins that regulates the integrity of the septum and cell wall. The importance of the inactive transglutaminase domain in cell wall remodeling was corroborated by studies of Cyk3 in

the budding yeast *Saccharomyces cerevisiae* that suggested that this domain inhibits Rho1 (Onishi et al., 2013). Onishi et al. (2013) reported that Cyk3-mutant cells exhibit increased Rho1 activity, and that Cyk3 interacts with Rho1 in pull down assays. Cyk3's genetic and physical interactions with Rho1 exhibited a dependency on the transglutaminase-like domain (Onishi et al., 2013). Fission yeast Cyk3 could likely inhibit Rho1 as well, since both yeast homologs of Cyk3 appear to share the same domain structures and cellular functions. Transglutaminases like Cyk3 may be able to bind to the same site on Rho1 as GEFs, which activate Rho, and prevent activity by competition, as proposed by Onishi et al. (2013), but more work will be required to support or refute this hypothesis. Other types of inactive transglutaminases that regulate RhoA could potentially exist in animals, but none have been identified so far.

4.2. FUTURE DIRECTIONS

4.2.1. RECONSTITUTING THE CONTRACTILE RING

Currently, how the Myo2 tail binds to the node is not known. It may bind directly to IQGAP^{Rng2} or there could another protein else that mediates this interaction. How IQGAP^{Rng2}, F-BAR^{Cdc15}, and formin^{Cdc12} fit together into the node, especially once Mid1 dissociates, is another unanswered question. In order to have a better picture of the node, it will be necessary to build the node *in vitro* by reconstituting these components one by one. Seeing if and how Myo2 and IQGAP^{Rng2} fit together and function would be a good start. Potentially, IQGAP^{Rng2} could tether Myo2 to actin, membrane-bound proteins, or

both. Studying IQGAP's interactions would provide deep insights into cytokinesis because it is a ubiquitous component of the contractile ring across eukaryotes (Shannon, 2012). Eventually, the minimal node complex could be built onto synthetic membranes, similar to studies of class-I myosin by the Ostap Laboratory (Pyrpassopoulos et al., 2016). They examined the forces applied by myosin-IC on actin filaments when bound to fluid lipid bilayers. Node complexes may function in some ways like class-I myosin owing to their attachment to the plasma membrane. It would be valuable measure the forces applied by Myo2 clusters in membrane-bound nodes to elucidate the effects of membrane fluidity on the tension of the contractile ring. Node reconstitution should elucidate many novel aspects about the physical interactions and regulatory mechanisms of the node, as well as biophysical principles underlying cytokinesis.

In addition to the bottom-up approach of *in vitro* reconstitution, some laboratories have taken the top-down genetics approach a step further by isolating whole contractile rings from cells (Mishra et al., 2013; Huang et al., 2016). These isolated rings are able to contract in the presence of ATP. Additionally, both Myo2 and Myp2 appear to contribute to the contraction of these *in vitro* rings (Mishra et al., 2013). Since we observed that RLC phosphorylation reduced actomyosin affinity in motility assays (**Chapter three**), it will be interesting to examine how RLC phosphorylation affects the contraction of the isolated ring system. Myo2 and Myp2 share the RLC, and thus phosphorylation could have a strong effect on contraction of *in vitro* rings. Experiments modifying Myo2 and Myp2 in different ways and observing changes in the contraction of *in vitro* rings may be ideal for

investigating some of the predictions of how class-II myosins are regulated during cytokinesis in the fission yeast system.

4.2.2. MECHANISTIC STUDIES OF MYOSIN

Unique structural features of Myo2 cause RLC phosphorylation to reduce Myo2's affinity for actin, whereas the same modification on other class-II myosins activates or enhances motility (**Chapter three**). Which differences between the myosins cause the disparities in regulation are unknown. Stopped flow experiments could be used to examine how phosphorylation affects the rates at which Myo2 transitions through different steps of the ATPase cycle. Measurements of transient kinetics are necessary to understand how myosins transition through the strong and weak actin-binding states. For example, stopped flow kinetics showed that tropomyosin prolonged the strong-binding states of budding yeast myosin-V, which explains how it enabled the myosin to walk along actin filaments (Hodges et al., 2012). RLC phosphorylation of Myo2 may result in a faster transition through the strong-binding states causing it to have lower affinity for actin. Examining what structural and kinetic differences makes Myo2 unique compared to other class-II myosins could yield novel insights into the underlying nature of myosin regulation in general.

Nothing is known about the structure of Myp2 molecules. Hydrodynamic measurements and electron microscopy (EM) images of recombinant Myp2 tails indicated that Myp2 tails formed a hairpin-like antiparallel coiled-coil (Bezanilla and Pollard, 2000). This finding suggested that Myp2 could be single-headed. However, Bezanilla and Pollard

(2000) had to re-solubilize the tails from the bacterial inclusion bodies, which may have impacted the structures they observed. Hypothetically, the antiparallel association they observed could exist in the full length molecule, but rather between two heavy chains. The result would be a molecule with a single head at either end of the rod, which would be a unique structure for a myosin of any class. Furthermore, Myp2 may also self-assemble and function more like a conventional myosin than previously thought. Conjecture aside, in order to understand Myp2's function during cytokinesis, recombinant Myp2 could be purified from the *Sf*9/baculovirus expression system so that its structure can be examined by EM and analytical ultracentrifugation.

4.2.3. IMAGING CONTRACTILE RINGS IN SUPER RESOLUTION

Studies in yeast cells will be all the more advantageous with current super resolution microscopic techniques, such as structured illumination (Chen et al., 2014), fPALM (fluorescence photoactivated localization microscopy) (Laplante et al., 2016), and STORM (stochastic optical reconstruction microscopy) (Veeraraghavan and Gourdie, 2016), that can resolve the subcellular localization of labeled molecules on the scale of tens of nanometers. Future studies of Myp2 and Myo51, as well as other contractile ring proteins, tagged with photoactivatable or photoswitchable fluorescent markers and imaged with super resolution microscopy should provide important information about the geometry of the contractile ring and supporting evidence for physical interactions established by *in vitro* reconstitution assays.

4.3. SUMMARY

The work described in this dissertation elucidates some mechanisms that lead to the self-assembly of the contractile ring and the regulation of cytokinesis in fission yeast. We found that Myo2 functions differently than conventional class-II myosins and likely anchors to the nodes at the plasma membrane to provide force in the contractile ring, which drives node coalescence. Additionally, Cyk3 was found to contribute to the contractile ring's regulation of septum formation, which drives constriction and cytokinesis. The common theme of this work is the importance of the node scaffolding complex due to its ability to recruit Myo2 and other factors to regulate cytokinesis. One future direction of this work is to further examine the interactions amongst the essential node proteins, such as IQGAP and F-BAR, by *in vitro* reconstitution. Additionally, it will be important to examine the structure and function of the nonessential class-II myosin, Myp2, to better understand the various forces that affect contractile ring dynamics. In conclusion, our work contributes to the thorough mechanistic characterization of the contractile ring in a simple organism. Such knowledge is necessary to build computational models to explain the mechanics of how contractile rings drive cytokinesis in general (Pollard, 2014).

4.4. REFERENCES

Albertson, R., B. Riggs, and W. Sullivan. 2005. Membrane traffic: a driving force in cytokinesis. *Trends in cell biology*. 15:92-101.

Arasada, R., and T.D. Pollard. 2014. Contractile ring stability in S. pombe depends on F-BAR protein Cdc15p and Bgs1p transport from the Golgi complex. *Cell reports*. 8:1533-1544.

Arellano, M., A. Duran, and P. Perez. 1996. Rho 1 GTPase activates the (1-3)beta-D-glucan synthase and is involved in Schizosaccharomyces pombe morphogenesis. *The EMBO journal*. 15:4584-4591.

Bezanilla, M., and T.D. Pollard. 2000. Myosin-II tails confer unique functions in Schizosaccharomyces pombe: characterization of a novel myosin-II tail. *Molecular biology of the cell*. 11:79-91.

Bezanilla, M., J.M. Wilson, and T.D. Pollard. 2000. Fission yeast myosin-II isoforms assemble into contractile rings at distinct times during mitosis. *Current biology : CB*. 10:397-400.

Billington, N., A. Wang, J. Mao, R.S. Adelstein, and J.R. Sellers. 2013. Characterization of three full-length human nonmuscle myosin II paralogs. *The Journal of biological chemistry*. 288:33398-33410.

Chen, B.C., W.R. Legant, K. Wang, L. Shao, D.E. Milkie, M.W. Davidson, C. Janetopoulos, X.S. Wu, J.A. Hammer, 3rd, Z. Liu, B.P. English, Y. Mimori-Kiyosue, D.P. Romero, A.T. Ritter, J. Lippincott-Schwartz, L. Fritz-Laylin, R.D. Mullins, D.M. Mitchell, J.N. Bembenek, A.C. Reymann, R. Bohme, S.W. Grill, J.T. Wang, G. Seydoux, U.S. Tulu, D.P. Kiehart, and E. Betzig. 2014. Lattice light-sheet microscopy: imaging molecules to embryos at high spatiotemporal resolution. *Science (New York, N.Y.)*. 346:1257998.

Cortes, J.C., M. Konomi, I.M. Martins, J. Munoz, M.B. Moreno, M. Osumi, A. Duran, and J.C. Ribas. 2007. The (1,3)beta-D-glucan synthase subunit Bgs1p is responsible for the fission yeast primary septum formation. *Molecular microbiology*. 65:201-217.

Hodges, A.R., E.B. Krementsova, C.S. Bookwalter, P.M. Fagnant, T.E. Sladewski, and K.M. Trybus. 2012. Tropomyosin is essential for processive movement of a class V myosin from budding yeast. *Current biology : CB*. 22:1410-1416.

Huang, J., T.G. Chew, Y. Gu, S. Palani, A. Kamnev, D.S. Martin, N.J. Carter, R.A. Cross, S. Oliferenko, and M.K. Balasubramanian. 2016. Curvature-induced expulsion of actomyosin bundles during cytokinetic ring contraction. *eLife*. 5.

Laplante, C., J. Berro, E. Karatekin, A. Hernandez-Leyva, R. Lee, and T.D. Pollard. 2015. Three myosins contribute uniquely to the assembly and constriction of the fission yeast cytokinetic contractile ring. *Current biology : CB*. 25:1955-1965.

Laplante, C., F. Huang, I.R. Tebbs, J. Bewersdorf, and T.D. Pollard. 2016. Molecular organization of cytokinesis nodes and contractile rings by super-resolution fluorescence microscopy of live fission yeast. *Proceedings of the National Academy of Sciences of the United States of America*. 113:E5876-e5885.

Laporte, D., V.C. Coffman, I.J. Lee, and J.Q. Wu. 2011. Assembly and architecture of precursor nodes during fission yeast cytokinesis. *The Journal of cell biology*. 192:1005-1021.

Lee, I.J., V.C. Coffman, and J.Q. Wu. 2012. Contractile-ring assembly in fission yeast cytokinesis: Recent advances and new perspectives. *Cytoskeleton (Hoboken, N.J.)*. 69:751-763.

Mishra, M., J. Kashiwazaki, T. Takagi, R. Srinivasan, Y. Huang, M.K. Balasubramanian, and I. Mabuchi. 2013. In vitro contraction of cytokinetic ring depends on myosin II but not on actin dynamics. *Nature cell biology*. 15:853-859.

Onishi, M., N. Ko, R. Nishihama, and J.R. Pringle. 2013. Distinct roles of Rho1, Cdc42, and Cyk3 in septum formation and abscission during yeast cytokinesis. *The Journal of cell biology*. 202:311-329.

Pinar, M., P.M. Coll, S.A. Rincon, and P. Perez. 2008. Schizosaccharomyces pombe Pxl1 is a paxillin homologue that modulates Rho1 activity and participates in cytokinesis. *Molecular biology of the cell*. 19:1727-1738.

Poirier, C.C., W.P. Ng, D.N. Robinson, and P.A. Iglesias. 2012. Deconvolution of the cellular force-generating subsystems that govern cytokinesis furrow ingression. *PLoS computational biology*. 8:e1002467.

Pollard, T.D. 2014. The value of mechanistic biophysical information for systems-level understanding of complex biological processes such as cytokinesis. *Biophysical journal*. 107:2499-2507.

Pollard, T.D., and J.Q. Wu. 2010. Understanding cytokinesis: lessons from fission yeast. *Nat Rev Mol Cell Biol*. 11:149-155.

Proctor, S.A., N. Minc, A. Boudaoud, and F. Chang. 2012. Contributions of turgor pressure, the contractile ring, and septum assembly to forces in cytokinesis in fission yeast. *Current biology : CB*. 22:1601-1608.

Pyrpassopoulos, S., G. Arpag, E.A. Feeser, H. Shuman, E. Tuzel, and E.M. Ostap. 2016. Force Generation by Membrane-Associated Myosin-I. *Scientific reports*. 6:25524.

Ren, L., A.H. Willet, R.H. Roberts-Galbraith, N.A. McDonald, A. Feoktistova, J.S. Chen, H. Huang, R. Guillen, C. Boone, S.S. Sidhu, J.R. Beckley, and K.L. Gould. 2015. The Cdc15 and Imp2 SH3 domains cooperatively scaffold a network of proteins that redundantly ensure efficient cell division in fission yeast. *Molecular biology of the cell*. 26:256-269.

Roberts-Galbraith, R.H., M.D. Ohi, B.A. Ballif, J.S. Chen, I. McLeod, W.H. McDonald, S.P. Gygi, J.R. Yates, 3rd, and K.L. Gould. 2010. Dephosphorylation of F-BAR protein Cdc15 modulates its conformation and stimulates its scaffolding activity at the cell division site. *Molecular cell*. 39:86-99.

Shannon, K.B. 2012. IQGAP Family Members in Yeast, Dictyostelium, and Mammalian Cells. *International journal of cell biology*. 2012:894817.

Tajadura, V., B. Garcia, I. Garcia, P. Garcia, and Y. Sanchez. 2004. Schizosaccharomyces pombe Rgf3p is a specific Rho1 GEF that regulates cell wall beta-glucan biosynthesis through the GTPase Rho1p. *Journal of cell science*. 117:6163-6174.

Takaine, M., O. Numata, and K. Nakano. 2014. Fission yeast IQGAP maintains F-actin-independent localization of myosin-II in the contractile ring. *Genes to cells : devoted to molecular & cellular mechanisms*. 19:161-176.

Takaine, M., O. Numata, and K. Nakano. 2015. An actin-myosin-II interaction is involved in maintaining the contractile ring in fission yeast. *Journal of cell science*. 128:2903-2918.

Tang, Q., N. Billington, E.B. Krementsova, C.S. Bookwalter, M. Lord, and K.M. Trybus. 2016. A single-headed fission yeast myosin V transports actin in a tropomyosin-dependent manner. *The Journal of cell biology*. 214:167-179.

Thiyagarajan, S., E.L. Munteanu, R. Arasada, T.D. Pollard, and B. O'Shaughnessy. 2015. The fission yeast cytokinetic contractile ring regulates septum shape and closure. *Journal of cell science*. 128:3672-3681.

Vavylonis, D., J.Q. Wu, S. Hao, B. O'Shaughnessy, and T.D. Pollard. 2008. Assembly mechanism of the contractile ring for cytokinesis by fission yeast. *Science (New York, N.Y.)*. 319:97-100.

Veeraraghavan, R., and R.G. Gourdie. 2016. Stochastic optical reconstruction microscopy-based relative localization analysis (STORM-RLA) for quantitative nanoscale assessment of spatial protein organization. *Molecular biology of the cell*. 27:3583-3590.

Zhou, Z., E.L. Munteanu, J. He, T. Ursell, M. Bathe, K.C. Huang, and F. Chang. 2015. The contractile ring coordinates curvature-dependent septum assembly during fission yeast cytokinesis. *Molecular biology of the cell*. 26:78-90.

LITERATURE CITED

Albertson, R., B. Riggs, and W. Sullivan. 2005. Membrane traffic: a driving force in cytokinesis. *Trends in cell biology*. 15:92-101.

Almonacid, M., S. Celton-Morizur, J.L. Jakubowski, F. Dingli, D. Loew, A. Mayeux, J.S. Chen, K.L. Gould, D.M. Clifford, and A. Paoletti. 2011. Temporal control of contractile ring assembly by Plo1 regulation of myosin II recruitment by Mid1/anillin. *Current biology : CB*. 21:473-479.

Almonacid, M., J.B. Moseley, J. Janvore, A. Mayeux, V. Fraisier, P. Nurse, and A. Paoletti. 2009. Spatial control of cytokinesis by Cdr2 kinase and Mid1/anillin nuclear export. *Current biology : CB*. 19:961-966.

Arasada, R., and T.D. Pollard. 2014. Contractile ring stability in S. pombe depends on F-BAR protein Cdc15p and Bgs1p transport from the Golgi complex. *Cell reports*. 8:1533-1544.

Arellano, M., A. Duran, and P. Perez. 1996. Rho 1 GTPase activates the (1-3)beta-D-glucan synthase and is involved in Schizosaccharomyces pombe morphogenesis. *The EMBO journal*. 15:4584-4591.

Bahler, J., A.B. Steever, S. Wheatley, Y. Wang, J.R. Pringle, K.L. Gould, and D. McCollum. 1998a. Role of polo kinase and Mid1p in determining the site of cell division in fission yeast. *The Journal of cell biology*. 143:1603-1616.

Bahler, J., J.Q. Wu, M.S. Longtine, N.G. Shah, A. McKenzie, 3rd, A.B. Steever, A. Wach, P. Philippsen, and J.R. Pringle. 1998b. Heterologous modules for efficient and versatile PCR-based gene targeting in Schizosaccharomyces pombe. *Yeast (Chichester, England)*. 14:943-951.

Balasubramanian, M.K., D.M. Helfman, and S.M. Hemmingsen. 1992. A new tropomyosin essential for cytokinesis in the fission yeast S. pombe. *Nature*. 360:84-87.

Balasubramanian, M.K., D. McCollum, L. Chang, K.C. Wong, N.I. Naqvi, X. He, S. Sazer, and K.L. Gould. 1998. Isolation and characterization of new fission yeast cytokinesis mutants. *Genetics*. 149:1265-1275.

Barral, J.M., C.C. Bauer, I. Ortiz, and H.F. Epstein. 1998. Unc-45 mutations in Caenorhabditis elegans implicate a CRO1/She4p-like domain in myosin assembly. *The Journal of cell biology*. 143:1215-1225.

Barral, J.M., A.H. Hutagalung, A. Brinker, F.U. Hartl, and H.F. Epstein. 2002. Role of the myosin assembly protein UNC-45 as a molecular chaperone for myosin. *Science (New York, N.Y.)*. 295:669-671.

Barua, B., A. Nagy, J.R. Sellers, and S.E. Hitchcock-DeGregori. 2014. Regulation of Nonmuscle Myosin II by Tropomyosin. *Biochemistry*. 53:4015-4024.

Barua, B., D.A. Winkelmann, H.D. White, and S.E. Hitchcock-DeGregori. 2012. Regulation of actin-myosin interaction by conserved periodic sites of tropomyosin. *Proceedings of the National Academy of Sciences of the United States of America*. 109:18425-18430.

Bembenek, J., and H. Yu. 2003. Regulation of CDC14: pathways and checkpoints of mitotic exit. *Frontiers in bioscience : a journal and virtual library*. 8:d1275-1287.

Bezanilla, M., S.L. Forsburg, and T.D. Pollard. 1997. Identification of a second myosin-II in Schizosaccharomyces pombe: Myp2p is conditionally required for cytokinesis. *Molecular biology of the cell*. 8:2693-2705.

Bezanilla, M., and T.D. Pollard. 2000. Myosin-II tails confer unique functions in Schizosaccharomyces pombe: characterization of a novel myosin-II tail. *Molecular biology of the cell*. 11:79-91.

Bezanilla, M., J.M. Wilson, and T.D. Pollard. 2000. Fission yeast myosin-II isoforms assemble into contractile rings at distinct times during mitosis. *Current biology : CB*. 10:397-400.

Bhutta, M.S., C.J. McInerny, and G.W. Gould. 2014. ESCRT function in cytokinesis: location, dynamics and regulation by mitotic kinases. *International journal of molecular sciences*. 15:21723-21739.

Billington, N., A. Wang, J. Mao, R.S. Adelstein, and J.R. Sellers. 2013. Characterization of three full-length human nonmuscle myosin II paralogs. *The Journal of biological chemistry*. 288:33398-33410.

Bird, J.E., Y. Takagi, N. Billington, M.P. Strub, J.R. Sellers, and T.B. Friedman. 2014. Chaperone-enhanced purification of unconventional myosin 15, a molecular motor specialized for stereocilia protein trafficking. *Proceedings of the National Academy of Sciences of the United States of America*. 111:12390-12395.

Bohnert, K.A., A.P. Grzegorzewska, A.H. Willet, C.W. Vander Kooi, D.R. Kovar, and K.L. Gould. 2013. SIN-dependent phosphoinhibition of formin multimerization controls fission yeast cytokinesis. *Genes & development*. 27:2164-2177.

Bookwalter, C.S., A. Kelsen, J.M. Leung, G.E. Ward, and K.M. Trybus. 2014. A Toxoplasma gondii class XIV myosin, expressed in Sf9 cells with a parasite co-chaperone, requires two light chains for fast motility. *The Journal of biological chemistry*. 289:30832-30841.

Bruce, L.J., S. Ghosh, M.J. King, D.M. Layton, W.J. Mawby, G.W. Stewart, P.A. Oldenborg, J. Delaunay, and M.J. Tanner. 2002. Absence of CD47 in protein 4.2-deficient hereditary spherocytosis in man: an interaction between the Rh complex and the band 3 complex. *Blood*. 100:1878-1885.

Bujalowski, P.J., P. Nicholls, J.M. Barral, and A.F. Oberhauser. 2015. Thermally-induced structural changes in an armadillo repeat protein suggest a novel thermosensor mechanism in a molecular chaperone. *FEBS letters*. 589:123-130.

Bujalowski, P.J., P. Nicholls, and A.F. Oberhauser. 2014. UNC-45B chaperone: the role of its domains in the interaction with the myosin motor domain. *Biophysical journal*. 107:654-661.

Chang, F., D. Drubin, and P. Nurse. 1997. cdc12p, a protein required for cytokinesis in fission yeast, is a component of the cell division ring and interacts with profilin. *The Journal of cell biology*. 137:169-182.

Chang, F., A. Woollard, and P. Nurse. 1996. Isolation and characterization of fission yeast mutants defective in the assembly and placement of the contractile actin ring. *Journal of cell science*. 109 (Pt 1):131-142.

Cheffings, T.H., N.J. Burroughs, and M.K. Balasubramanian. 2016. Actomyosin Ring Formation and Tension Generation in Eukaryotic Cytokinesis. *Current biology : CB*. 26:R719-737.

Chen, B.C., W.R. Legant, K. Wang, L. Shao, D.E. Milkie, M.W. Davidson, C. Janetopoulos, X.S. Wu, J.A. Hammer, 3rd, Z. Liu, B.P. English, Y. Mimori-Kiyosue, D.P. Romero, A.T. Ritter, J. Lippincott-Schwartz, L. Fritz-Laylin, R.D. Mullins, D.M. Mitchell, J.N. Bembenek, A.C. Reymann, R. Bohme, S.W. Grill, J.T. Wang, G. Seydoux, U.S. Tulu, D.P. Kiehart, and E. Betzig. 2014. Lattice light-sheet microscopy: imaging molecules to embryos at high spatiotemporal resolution. *Science (New York, N.Y.)*. 346:1257998.

Chen, C.T., A. Feoktistova, J.S. Chen, Y.S. Shim, D.M. Clifford, K.L. Gould, and D. McCollum. 2008. The SIN kinase Sid2 regulates cytoplasmic retention of the S. pombe Cdc14-like phosphatase Clp1. *Current biology : CB*. 18:1594-1599.

Chen, J.S., M.R. Broadus, J.R. McLean, A. Feoktistova, L. Ren, and K.L. Gould. 2013. Comprehensive proteomics analysis reveals new substrates and regulators of the

fission yeast clp1/cdc14 phosphatase. *Molecular & cellular proteomics : MCP*. 12:1074-1086.

Chen, Q., and T.D. Pollard. 2011. Actin filament severing by cofilin is more important for assembly than constriction of the cytokinetic contractile ring. *The Journal of cell biology*. 195:485-498.

Chew, T.L., R.A. Masaracchia, Z.M. Goeckeler, and R.B. Wysolmerski. 1998. Phosphorylation of non-muscle myosin II regulatory light chain by p21-activated kinase (gamma-PAK). *Journal of muscle research and cell motility*. 19:839-854.

Clayton, J.E., L.W. Pollard, G.G. Murray, and M. Lord. 2015. Myosin motor isoforms direct specification of actomyosin function by tropomyosins. *Cytoskeleton (Hoboken, N.J.)*. 72:131-145.

Clayton, J.E., L.W. Pollard, M. Sckolnick, C.S. Bookwalter, A.R. Hodges, K.M. Trybus, and M. Lord. 2014. Fission yeast tropomyosin specifies directed transport of myosin-V along actin cables. *Molecular biology of the cell*. 25:66-75.

Clayton, J.E., M.R. Sammons, B.C. Stark, A.R. Hodges, and M. Lord. 2010. Differential regulation of unconventional fission yeast myosins via the actin track. *Current biology : CB*. 20:1423-1431.

Clifford, D.M., B.A. Wolfe, R.H. Roberts-Galbraith, W.H. McDonald, J.R. Yates, 3rd, and K.L. Gould. 2008. The Clp1/Cdc14 phosphatase contributes to the robustness of cytokinesis by association with anillin-related Mid1. *The Journal of cell biology*. 181:79-88.

Cohen, C.M., E. Dotimas, and C. Korsgren. 1993. Human erythrocyte membrane protein band 4.2 (pallidin). *Seminars in hematology*. 30:119-137.

Cortes, J.C., M. Konomi, I.M. Martins, J. Munoz, M.B. Moreno, M. Osumi, A. Duran, and J.C. Ribas. 2007. The (1,3)beta-D-glucan synthase subunit Bgs1p is responsible for the fission yeast primary septum formation. *Molecular microbiology*. 65:201-217.

Coulton, A.T., D.A. East, A. Galinska-Rakoczy, W. Lehman, and D.P. Mulvihill. 2010. The recruitment of acetylated and unacetylated tropomyosin to distinct actin polymers permits the discrete regulation of specific myosins in fission yeast. *Journal of cell science*. 123:3235-3243.

Coureux, P.D., H.L. Sweeney, and A. Houdusse. 2004. Three myosin V structures delineate essential features of chemo-mechanical transduction. *The EMBO journal*. 23:4527-4537.

Craig, R., and J. Megerman. 1977. Assembly of smooth muscle myosin into side-polar filaments. *The Journal of cell biology*. 75:990-996.

Craig, R., R. Smith, and J. Kendrick-Jones. 1983. Light-chain phosphorylation controls the conformation of vertebrate non-muscle and smooth muscle myosin molecules. *Nature*. 302:436-439.

Cronan, J.E., Jr. 1990. Biotination of proteins in vivo. A post-translational modification to label, purify, and study proteins. *The Journal of biological chemistry*. 265:10327-10333.

Dahl, K.N., R. Parthasarathy, C.M. Westhoff, D.M. Layton, and D.E. Discher. 2004. Protein 4.2 is critical to CD47-membrane skeleton attachment in human red cells. *Blood*. 103:1131-1136.

De La Cruz, E.M., and E.M. Ostap. 2004. Relating biochemistry and function in the myosin superfamily. *Current opinion in cell biology*. 16:61-67.

De La Cruz, E.M., A.L. Wells, S.S. Rosenfeld, E.M. Ostap, and H.L. Sweeney. 1999. The kinetic mechanism of myosin V. *Proceedings of the National Academy of Sciences of the United States of America*. 96:13726-13731.

Dekker, N., D. Speijer, C.H. Grun, M. van den Berg, A. de Haan, and F. Hochstenbach. 2004. Role of the alpha-glucanase Agn1p in fission-yeast cell separation. *Molecular biology of the cell*. 15:3903-3914.

Doyle, A., R. Martin-Garcia, A.T. Coulton, S. Bagley, and D.P. Mulvihill. 2009. Fission yeast Myo51 is a meiotic spindle pole body component with discrete roles during cell fusion and spore formation. *Journal of cell science*. 122:4330-4340.

Dudin, O., L. Merlini, and S.G. Martin. 2016. Spatial focalization of pheromone/MAPK signaling triggers commitment to cell-cell fusion. *Genes & development*. 30:2226-2239.

Etard, C., U. Roostalu, and U. Strahle. 2008. Shuttling of the chaperones Unc45b and Hsp90a between the A band and the Z line of the myofibril. *The Journal of cell biology*. 180:1163-1175.

Facchiano, F., A. Facchiano, and A.M. Facchiano. 2006. The role of transglutaminase-2 and its substrates in human diseases. *Frontiers in bioscience : a journal and virtual library*. 11:1758-1773.

Fang, X., J. Luo, R. Nishihama, C. Wloka, C. Dravis, M. Travaglia, M. Iwase, E.A. Vallen, and E. Bi. 2010. Biphasic targeting and cleavage furrow ingression directed by the tail of a myosin II. *The Journal of cell biology*. 191:1333-1350.

Fankhauser, C., A. Reymond, L. Cerutti, S. Utzig, K. Hofmann, and V. Simanis. 1995. The S. pombe cdc15 gene is a key element in the reorganization of F-actin at mitosis. *Cell*. 82:435-444.

Fesus, L., and Z. Szondy. 2005. Transglutaminase 2 in the balance of cell death and survival. *FEBS letters*. 579:3297-3302.

Finer, J.T., R.M. Simmons, and J.A. Spudich. 1994. Single myosin molecule mechanics: piconewton forces and nanometre steps. *Nature*. 368:113-119.

Garcia Cortes, J.C., M. Ramos, M. Osumi, P. Perez, and J.C. Ribas. 2016. The Cell Biology of Fission Yeast Septation. *Microbiology and molecular biology reviews : MMBR*. 80:779-791.

Gazda, L., W. Pokrzywa, D. Hellerschmied, T. Lowe, I. Forne, F. Mueller-Planitz, T. Hoppe, and T. Clausen. 2013. The myosin chaperone UNC-45 is organized in tandem modules to support myofilament formation in C. elegans. *Cell*. 152:183-195.

Gordon, A.M., E. Homsher, and M. Regnier. 2000. Regulation of contraction in striated muscle. *Physiol Rev*. 80:853-924.

Green, R.A., E. Paluch, and K. Oegema. 2012. Cytokinesis in animal cells. *Annual review of cell and developmental biology*. 28:29-58.

Gunning, P.W., E.C. Hardeman, P. Lappalainen, and D.P. Mulvihill. 2015. Tropomyosin - master regulator of actin filament function in the cytoskeleton. *Journal of cell science*. 128:2965-2974.

Guzman-Vendrell, M., S. Baldissard, M. Almonacid, A. Mayeux, A. Paoletti, and J.B. Moseley. 2013. Blt1 and Mid1 provide overlapping membrane anchors to position the division plane in fission yeast. *Molecular and cellular biology*. 33:418-428.

Hachet, O., and V. Simanis. 2008. Mid1p/anillin and the septation initiation network orchestrate contractile ring assembly for cytokinesis. *Genes & development*. 22:3205-3216.

Hansen, L., S. Comyn, Y. Mang, A. Lind-Thomsen, L. Myhre, F. Jean, H. Eiberg, N. Tommerup, T. Rosenberg, and D. Pilgrim. 2014. The myosin chaperone UNC45B

is involved in lens development and autosomal dominant juvenile cataract. *European journal of human genetics : EJHG*. 22:1290-1297.

Harris, D.E., and D.M. Warshaw. 1993. Smooth and skeletal muscle myosin both exhibit low duty cycles at zero load in vitro. *The Journal of biological chemistry*. 268:14764-14768.

Harrison, R.G., S. Lowey, and C. Cohen. 1971. Assembly of myosin. *J Mol Biol*. 59:531-535.

Heissler, S.M., and D.J. Manstein. 2013. Nonmuscle myosin-2: mix and match. *Cellular and molecular life sciences : CMLS*. 70:1-21.

Herman, P.K. 2002. Stationary phase in yeast. *Current opinion in microbiology*. 5:602-607.

Hettasch, J.M., and C.S. Greenberg. 1994. Analysis of the catalytic activity of human factor XIIIa by site-directed mutagenesis. *The Journal of biological chemistry*. 269:28309-28313.

Ho, S.N., H.D. Hunt, R.M. Horton, J.K. Pullen, and L.R. Pease. 1989. Site-directed mutagenesis by overlap extension using the polymerase chain reaction. *Gene*. 77:51-59.

Hodges, A.R., E.B. Krementsova, C.S. Bookwalter, P.M. Fagnant, T.E. Sladewski, and K.M. Trybus. 2012. Tropomyosin is essential for processive movement of a class V myosin from budding yeast. *Current biology : CB*. 22:1410-1416.

Horiguchi, Y., N. Inoue, M. Masuda, T. Kashimoto, J. Katahira, N. Sugimoto, and M. Matsuda. 1997. Bordetella bronchiseptica dermonecrotizing toxin induces reorganization of actin stress fibers through deamidation of Gln-63 of the GTP-binding protein Rho. *Proceedings of the National Academy of Sciences of the United States of America*. 94:11623-11626.

Huang, J., T.G. Chew, Y. Gu, S. Palani, A. Kamnev, D.S. Martin, N.J. Carter, R.A. Cross, S. Oliferenko, and M.K. Balasubramanian. 2016. Curvature-induced expulsion of actomyosin bundles during cytokinetic ring contraction. *eLife*. 5.

Huang, Y., H. Yan, and M.K. Balasubramanian. 2008. Assembly of normal actomyosin rings in the absence of Mid1p and cortical nodes in fission yeast. *The Journal of cell biology*. 183:979-988.

Hutagalung, A.H., M.L. Landsverk, M.G. Price, and H.F. Epstein. 2002. The UCS family of myosin chaperones. *Journal of cell science*. 115:3983-3990.

154

Huxley, H.E. 1990. Sliding filaments and molecular motile systems. *The Journal of biological chemistry*. 265:8347-8350.

Iranzo, M., C. Aguado, C. Pallotti, J.V. Canizares, and S. Mormeneo. 2002. Transglutaminase activity is involved in Saccharomyces cerevisiae wall construction. *Microbiology (Reading, England)*. 148:1329-1334.

Jendretzki, A., I. Ciklic, R. Rodicio, H.P. Schmitz, and J.J. Heinisch. 2009. Cyk3 acts in actomyosin ring independent cytokinesis by recruiting Inn1 to the yeast bud neck. *Molecular genetics and genomics : MGG*. 282:437-451.

Johnson, M., D.A. East, and D.P. Mulvihill. 2014. Formins determine the functional properties of actin filaments in yeast. *Current biology : CB*. 24:1525-1530.

Kaiser, C.M., P.J. Bujalowski, L. Ma, J. Anderson, H.F. Epstein, and A.F. Oberhauser. 2012. Tracking UNC-45 chaperone-myosin interaction with a titin mechanical reporter. *Biophysical journal*. 102:2212-2219.

Kamei, T., K. Tanaka, T. Hihara, M. Umikawa, H. Imamura, M. Kikyo, K. Ozaki, and Y. Takai. 1998. Interaction of Bnr1p with a novel Src homology 3 domain-containing Hof1p. Implication in cytokinesis in Saccharomyces cerevisiae. *The Journal of biological chemistry*. 273:28341-28345.

Karabina, A., K. Kazmierczak, D. Szczesna-Cordary, and J.R. Moore. 2015. Myosin regulatory light chain phosphorylation enhances cardiac beta-myosin in vitro motility under load. *Archives of biochemistry and biophysics*. 580:14-21.

Kinose, F., S.X. Wang, U.S. Kidambi, C.L. Moncman, and D.A. Winkelmann. 1996. Glycine 699 is pivotal for the motor activity of skeletal muscle myosin. *The Journal of cell biology*. 134:895-909.

Kintses, B., M. Gyimesi, D.S. Pearson, M.A. Geeves, W. Zeng, C.R. Bagshaw, and A. Malnasi-Csizmadia. 2007. Reversible movement of switch 1 loop of myosin determines actin interaction. *The EMBO journal*. 26:265-274.

Kitayama, C., A. Sugimoto, and M. Yamamoto. 1997. Type II myosin heavy chain encoded by the myo2 gene composes the contractile ring during cytokinesis in Schizosaccharomyces pombe. *The Journal of cell biology*. 137:1309-1319.

Klein, J.C., A.R. Burr, B. Svensson, D.J. Kennedy, J. Allingham, M.A. Titus, I. Rayment, and D.D. Thomas. 2008. Actin-binding cleft closure in myosin II probed by site-directed spin labeling and pulsed EPR. *Proceedings of the National Academy of Sciences of the United States of America*. 105:12867-12872.

Knox, P., S. Crooks, and C.S. Rimmer. 1986. Role of fibronectin in the migration of fibroblasts into plasma clots. *The Journal of cell biology*. 102:2318-2323.

Korinek, W.S., E. Bi, J.A. Epp, L. Wang, J. Ho, and J. Chant. 2000. Cyk3, a novel SH3-domain protein, affects cytokinesis in yeast. *Current biology : CB*. 10:947-950.

Korsgren, C., J. Lawler, S. Lambert, D. Speicher, and C.M. Cohen. 1990. Complete amino acid sequence and homologies of human erythrocyte membrane protein band 4.2. *Proceedings of the National Academy of Sciences of the United States of America*. 87:613-617.

Kovar, D.R., J.R. Kuhn, A.L. Tichy, and T.D. Pollard. 2003. The fission yeast cytokinesis formin Cdc12p is a barbed end actin filament capping protein gated by profilin. *The Journal of cell biology*. 161:875-887.

Kovar, D.R., V. Sirotkin, and M. Lord. 2011. Three's company: the fission yeast actin cytoskeleton. *Trends in cell biology*. 21:177-187.

Krementsova, E.B., A.R. Hodges, C.S. Bookwalter, T.E. Sladewski, M. Travaglia, H.L. Sweeney, and K.M. Trybus. 2011. Two single-headed myosin V motors bound to a tetrameric adapter protein form a processive complex. *The Journal of cell biology*. 195:631-641.

Kull, F.J., E.P. Sablin, R. Lau, R.J. Fletterick, and R.D. Vale. 1996. Crystal structure of the kinesin motor domain reveals a structural similarity to myosin. *Nature*. 380:550-555.

Lacroix, B., and A.S. Maddox. 2012. Cytokinesis, ploidy and aneuploidy. *The Journal of pathology*. 226:338-351.

Laplante, C., J. Berro, E. Karatekin, A. Hernandez-Leyva, R. Lee, and T.D. Pollard. 2015. Three myosins contribute uniquely to the assembly and constriction of the fission yeast cytokinetic contractile ring. *Current biology : CB*. 25:1955-1965.

Laplante, C., F. Huang, I.R. Tebbs, J. Bewersdorf, and T.D. Pollard. 2016. Molecular organization of cytokinesis nodes and contractile rings by super-resolution fluorescence microscopy of live fission yeast. *Proceedings of the National Academy of Sciences of the United States of America*. 113:E5876-e5885.

Laporte, D., V.C. Coffman, I.J. Lee, and J.Q. Wu. 2011. Assembly and architecture of precursor nodes during fission yeast cytokinesis. *The Journal of cell biology*. 192:1005-1021.

Laporte, D., N. Ojkic, D. Vavylonis, and J.Q. Wu. 2012. alpha-Actinin and fimbrin cooperate with myosin II to organize actomyosin bundles during contractile-ring assembly. *Molecular biology of the cell*. 23:3094-3110.

Lee, C.F., A.V. Hauenstein, J.K. Fleming, W.C. Gasper, V. Engelke, B. Sankaran, S.I. Bernstein, and T. Huxford. 2011a. X-ray crystal structure of the UCS domain-containing UNC-45 myosin chaperone from Drosophila melanogaster. *Structure (London, England : 1993)*. 19:397-408.

Lee, C.F., G.C. Melkani, and S.I. Bernstein. 2014. The UNC-45 myosin chaperone: from worms to flies to vertebrates. *International review of cell and molecular biology*. 313:103-144.

Lee, C.F., G.C. Melkani, Q. Yu, J.A. Suggs, W.A. Kronert, Y. Suzuki, L. Hipolito, M.G. Price, H.F. Epstein, and S.I. Bernstein. 2011b. Drosophila UNC-45 accumulates in embryonic blastoderm and in muscles, and is essential for muscle myosin stability. *Journal of cell science*. 124:699-705.

Lee, I.J., V.C. Coffman, and J.Q. Wu. 2012. Contractile-ring assembly in fission yeast cytokinesis: Recent advances and new perspectives. *Cytoskeleton (Hoboken, N.J.)*. 69:751-763.

Lee, W.L., M. Bezanilla, and T.D. Pollard. 2000. Fission yeast myosin-I, Myo1p, stimulates actin assembly by Arp2/3 complex and shares functions with WASp. *The Journal of cell biology*. 151:789-800.

Li, R. 2007. Cytokinesis in development and disease: variations on a common theme. *Cellular and molecular life sciences : CMLS*. 64:3044-3058.

Lippincott, J., and R. Li. 1998. Dual function of Cyk2, a cdc15/PSTPIP family protein, in regulating actomyosin ring dynamics and septin distribution. *The Journal of cell biology*. 143:1947-1960.

Liu, L., R. Srikakulam, and D.A. Winkelmann. 2008. Unc45 activates Hsp90-dependent folding of the myosin motor domain. *The Journal of biological chemistry*. 283:13185-13193.

Liu, X., M.S. Hong, S. Shu, S. Yu, and E.D. Korn. 2013. Regulation of the filament structure and assembly of Acanthamoeba myosin II by phosphorylation of serines in the heavy-chain nonhelical tailpiece. *Proceedings of the National Academy of Sciences of the United States of America*. 110:E33-40.

Loo, T.H., and M. Balasubramanian. 2008. Schizosaccharomyces pombe Pak-related protein, Pak1p/Orb2p, phosphorylates myosin regulatory light chain to inhibit cytokinesis. *The Journal of cell biology*. 183:785-793.

Lord, M., E. Laves, and T.D. Pollard. 2005. Cytokinesis depends on the motor domains of myosin-II in fission yeast but not in budding yeast. *Molecular biology of the cell*. 16:5346-5355.

Lord, M., and T.D. Pollard. 2004. UCS protein Rng3p activates actin filament gliding by fission yeast myosin-II. *The Journal of cell biology*. 167:315-325.

Lord, M., T.E. Sladewski, and T.D. Pollard. 2008. Yeast UCS proteins promote actomyosin interactions and limit myosin turnover in cells. *Proceedings of the National Academy of Sciences of the United States of America*. 105:8014-8019.

Mahajan, R.K., and J.D. Pardee. 1996. Assembly mechanism of Dictyostelium myosin II: regulation by K+, Mg2+, and actin filaments. *Biochemistry*. 35:15504-15514.

Makarova, K.S., L. Aravind, and E.V. Koonin. 1999. A superfamily of archaeal, bacterial, and eukaryotic proteins homologous to animal transglutaminases. *Protein science : a publication of the Protein Society*. 8:1714-1719.

Mangala, L.S., and K. Mehta. 2005. Tissue transglutaminase (TG2) in cancer biology. *Progress in experimental tumor research*. 38:125-138.

Martin-Cuadrado, A.B., E. Duenas, M. Sipiczki, C.R. Vazquez de Aldana, and F. del Rey. 2003. The endo-beta-1,3-glucanase eng1p is required for dissolution of the primary septum during cell separation in Schizosaccharomyces pombe. *Journal of cell science*. 116:1689-1698.

Martin-Garcia, R., A. Duran, and M.H. Valdivieso. 2003. In Schizosaccharomyces pombe chs2p has no chitin synthase activity but is related to septum formation. *FEBS letters*. 549:176-180.

Martin-Garcia, R., and M.H. Valdivieso. 2006. The fission yeast Chs2 protein interacts with the type-II myosin Myo3p and is required for the integrity of the actomyosin ring. *Journal of cell science*. 119:2768-2779.

Martin, S.G., and M. Berthelot-Grosjean. 2009. Polar gradients of the DYRK-family kinase Pom1 couple cell length with the cell cycle. *Nature*. 459:852-856.

McCollum, D., and K.L. Gould. 2001. Timing is everything: regulation of mitotic exit and cytokinesis by the MEN and SIN. *Trends in cell biology*. 11:89-95.

McDonald, N.A., C.W. Vander Kooi, M.D. Ohi, and K.L. Gould. 2015. Oligomerization but Not Membrane Bending Underlies the Function of Certain F-BAR Proteins in Cell Motility and Cytokinesis. *Developmental cell*. 35:725-736.

McLachlan, A.D., and J. Karn. 1982. Periodic charge distributions in the myosin rod amino acid sequence match cross-bridge spacings in muscle. *Nature*. 299:226-231.

Mehta, A.D., R.S. Rock, M. Rief, J.A. Spudich, M.S. Mooseker, and R.E. Cheney. 1999. Myosin-V is a processive actin-based motor. *Nature*. 400:590-593.

Mehta, K., A. Kumar, and H.I. Kim. 2010. Transglutaminase 2: a multi-tasking protein in the complex circuitry of inflammation and cancer. *Biochemical pharmacology*. 80:1921-1929.

Meitinger, F., B. Petrova, I.M. Lombardi, D.T. Bertazzi, B. Hub, H. Zentgraf, and G. Pereira. 2010. Targeted localization of Inn1, Cyk3 and Chs2 by the mitotic-exit network regulates cytokinesis in budding yeast. *Journal of cell science*. 123:1851-1861.

Melkani, G.C., R. Bodmer, K. Ocorr, and S.I. Bernstein. 2011. The UNC-45 chaperone is critical for establishing myosin-based myofibrillar organization and cardiac contractility in the Drosophila heart model. *PloS one*. 6:e22579.

Melkani, G.C., C.F. Lee, A. Cammarato, and S.I. Bernstein. 2010. Drosophila UNC-45 prevents heat-induced aggregation of skeletal muscle myosin and facilitates refolding of citrate synthase. *Biochemical and biophysical research communications*. 396:317-322.

Mesentean, S., S. Koppole, J.C. Smith, and S. Fischer. 2007. The principal motions involved in the coupling mechanism of the recovery stroke of the myosin motor. *J Mol Biol*. 367:591-602.

Micanovic, R., R. Procyk, W. Lin, and G.R. Matsueda. 1994. Role of histidine 373 in the catalytic activity of coagulation factor XIII. *The Journal of biological chemistry*. 269:9190-9194.

Mishra, M., M. D'Souza V, K.C. Chang, Y. Huang, and M.K. Balasubramanian. 2005a. Hsp90 protein in fission yeast Swo1p and UCS protein Rng3p facilitate myosin II assembly and function. *Eukaryotic cell*. 4:567-576.

Mishra, M., J. Karagiannis, M. Sevugan, P. Singh, and M.K. Balasubramanian. 2005b. The 14-3-3 protein rad24p modulates function of the cdc14p family phosphatase clp1p/flp1p in fission yeast. *Current biology : CB*. 15:1376-1383.

Mishra, M., J. Karagiannis, S. Trautmann, H. Wang, D. McCollum, and M.K. Balasubramanian. 2004. The Clp1p/Flp1p phosphatase ensures completion of cytokinesis in response to minor perturbation of the cell division machinery in Schizosaccharomyces pombe. *Journal of cell science*. 117:3897-3910.

Mishra, M., J. Kashiwazaki, T. Takagi, R. Srinivasan, Y. Huang, M.K. Balasubramanian, and I. Mabuchi. 2013. In vitro contraction of cytokinetic ring depends on myosin II but not on actin dynamics. *Nature cell biology*. 15:853-859.

Moreno, S., A. Klar, and P. Nurse. 1991. Molecular genetic analysis of fission yeast Schizosaccharomyces pombe. *Methods in enzymology*. 194:795-823.

Morrell, J.L., C.B. Nichols, and K.L. Gould. 2004. The GIN4 family kinase, Cdr2p, acts independently of septins in fission yeast. *Journal of cell science*. 117:5293-5302.

Moseley, J.B., A. Mayeux, A. Paoletti, and P. Nurse. 2009. A spatial gradient coordinates cell size and mitotic entry in fission yeast. *Nature*. 459:857-860.

Mosher, D.F., and P.E. Schad. 1979. Cross-linking of fibronectin to collagen by blood coagulation Factor XIIIa. *The Journal of clinical investigation*. 64:781-787.

Motegi, F., M. Mishra, M.K. Balasubramanian, and I. Mabuchi. 2004. Myosin-II reorganization during mitosis is controlled temporally by its dephosphorylation and spatially by Mid1 in fission yeast. *The Journal of cell biology*. 165:685-695.

Motegi, F., K. Nakano, C. Kitayama, M. Yamamoto, and I. Mabuchi. 1997. Identification of Myo3, a second type-II myosin heavy chain in the fission yeast Schizosaccharomyces pombe. *FEBS letters*. 420:161-166.

Mulvihill, D.P., C. Barretto, and J.S. Hyams. 2001. Localization of fission yeast type II myosin, Myo2, to the cytokinetic actin ring is regulated by phosphorylation of a C-terminal coiled-coil domain and requires a functional septation initiation network. *Molecular biology of the cell*. 12:4044-4053.

Mulvihill, D.P., and J.S. Hyams. 2003. Role of the two type II myosins, Myo2 and Myp2, in cytokinetic actomyosin ring formation and function in fission yeast. *Cell motility and the cytoskeleton*. 54:208-216.

Nakano, K., R. Arai, and I. Mabuchi. 1997. The small GTP-binding protein Rho1 is a multifunctional protein that regulates actin localization, cell polarity, and septum formation in the fission yeast Schizosaccharomyces pombe. *Genes to cells : devoted to molecular & cellular mechanisms*. 2:679-694.

Ni, W., and O.O. Odunuga. 2015. UCS proteins: chaperones for myosin and co-chaperones for Hsp90. *Sub-cellular biochemistry*. 78:133-152.

Nishihama, R., J.H. Schreiter, M. Onishi, E.A. Vallen, J. Hanna, K. Moravcevic, M.F. Lippincott, H. Han, M.A. Lemmon, J.R. Pringle, and E. Bi. 2009. Role of Inn1 and its interactions with Hof1 and Cyk3 in promoting cleavage furrow and septum formation in S. cerevisiae. *The Journal of cell biology*. 185:995-1012.

Odronitz, F., and M. Kollmar. 2007. Drawing the tree of eukaryotic life based on the analysis of 2,269 manually annotated myosins from 328 species. *Genome biology*. 8:R196.

Onishi, M., N. Ko, R. Nishihama, and J.R. Pringle. 2013. Distinct roles of Rho1, Cdc42, and Cyk3 in septum formation and abscission during yeast cytokinesis. *The Journal of cell biology*. 202:311-329.

Padmanabhan, A., K. Bakka, M. Sevugan, N.I. Naqvi, V. D'Souza, X. Tang, M. Mishra, and M.K. Balasubramanian. 2011. IQGAP-related Rng2p organizes cortical nodes and ensures position of cell division in fission yeast. *Current biology : CB*. 21:467-472.

Paoletti, A., and F. Chang. 2000. Analysis of mid1p, a protein required for placement of the cell division site, reveals a link between the nucleus and the cell surface in fission yeast. *Molecular biology of the cell*. 11:2757-2773.

Pasternak, C., P.F. Flicker, S. Ravid, and J.A. Spudich. 1989. Intermolecular versus intramolecular interactions of Dictyostelium myosin: possible regulation by heavy chain phosphorylation. *The Journal of cell biology*. 109:203-210.

Pedersen, L.C., V.C. Yee, P.D. Bishop, I. Le Trong, D.C. Teller, and R.E. Stenkamp. 1994. Transglutaminase factor XIII uses proteinase-like catalytic triad to crosslink macromolecules. *Protein science : a publication of the Protein Society*. 3:1131-1135.

Pinar, M., P.M. Coll, S.A. Rincon, and P. Perez. 2008. Schizosaccharomyces pombe Pxl1 is a paxillin homologue that modulates Rho1 activity and participates in cytokinesis. *Molecular biology of the cell*. 19:1727-1738.

Pisano, J.J., J.S. Finlayson, and M.P. Peyton. 1968. [Cross-link in fibrin polymerized by factor 13: epsilon-(gamma-glutamyl)lysine]. *Science (New York, N.Y.)*. 160:892-893.

Poirier, C.C., W.P. Ng, D.N. Robinson, and P.A. Iglesias. 2012. Deconvolution of the cellular force-generating subsystems that govern cytokinesis furrow ingression. *PLoS computational biology*. 8:e1002467.

Pollard, L.W., and M. Lord. 2014. Getting myosin-V on the right track: Tropomyosin sorts transport in yeast. *Bioarchitecture*. 4:35-38.

Pollard, T.D. 2014. The value of mechanistic biophysical information for systems-level understanding of complex biological processes such as cytokinesis. *Biophysical journal*. 107:2499-2507.

Pollard, T.D., and J.Q. Wu. 2010. Understanding cytokinesis: lessons from fission yeast. *Nat Rev Mol Cell Biol*. 11:149-155.

Price, M.G., M.L. Landsverk, J.M. Barral, and H.F. Epstein. 2002. Two mammalian UNC-45 isoforms are related to distinct cytoskeletal and muscle-specific functions. *Journal of cell science*. 115:4013-4023.

Proctor, S.A., N. Minc, A. Boudaoud, and F. Chang. 2012. Contributions of turgor pressure, the contractile ring, and septum assembly to forces in cytokinesis in fission yeast. *Current biology : CB*. 22:1601-1608.

Pyrpassopoulos, S., G. Arpag, E.A. Feeser, H. Shuman, E. Tuzel, and E.M. Ostap. 2016. Force Generation by Membrane-Associated Myosin-I. *Scientific reports*. 6:25524.

Rajagopalan, S., V. Wachtler, and M. Balasubramanian. 2003. Cytokinesis in fission yeast: a story of rings, rafts and walls. *Trends in genetics : TIG*. 19:403-408.

Rayment, I., W.R. Rypniewski, K. Schmidt-Base, R. Smith, D.R. Tomchick, M.M. Benning, D.A. Winkelmann, G. Wesenberg, and H.M. Holden. 1993. Three-dimensional structure of myosin subfragment-1: a molecular motor. *Science (New York, N.Y.)*. 261:50-58.

Reijnst, P., S. Jorde, and J. Wendland. 2010. Candida albicans SH3-domain proteins involved in hyphal growth, cytokinesis, and vacuolar morphology. *Current genetics*. 56:309-319.

Ren, L., A.H. Willet, R.H. Roberts-Galbraith, N.A. McDonald, A. Feoktistova, J.S. Chen, H. Huang, R. Guillen, C. Boone, S.S. Sidhu, J.R. Beckley, and K.L. Gould. 2015. The Cdc15 and Imp2 SH3 domains cooperatively scaffold a network of proteins that redundantly ensure efficient cell division in fission yeast. *Molecular biology of the cell*. 26:256-269.

Rice, R.H., and H. Green. 1978. Relation of protein synthesis and transglutaminase activity to formation of the cross-linked envelope during terminal differentiation of the cultured human epidermal keratinocyte. *The Journal of cell biology*. 76:705-711.

Rincon, S.A., P. Bhatia, C. Bicho, M. Guzman-Vendrell, V. Fraisier, W.E. Borek, L. Alves Fde, F. Dingli, D. Loew, J. Rappsilber, K.E. Sawin, S.G. Martin, and A. Paoletti. 2014. Pom1 regulates the assembly of Cdr2-Mid1 cortical nodes for robust spatial control of cytokinesis. *The Journal of cell biology*. 206:61-77.

Rincon, S.A., B. Santos, and P. Perez. 2006. Fission yeast Rho5p GTPase is a functional paralogue of Rho1p that plays a role in survival of spores and stationary-phase cells. *Eukaryotic cell*. 5:435-446.

Roberts-Galbraith, R.H., J.S. Chen, J. Wang, and K.L. Gould. 2009. The SH3 domains of two PCH family members cooperate in assembly of the Schizosaccharomyces pombe contractile ring. *The Journal of cell biology*. 184:113-127.

Roberts-Galbraith, R.H., M.D. Ohi, B.A. Ballif, J.S. Chen, I. McLeod, W.H. McDonald, S.P. Gygi, J.R. Yates, 3rd, and K.L. Gould. 2010. Dephosphorylation of F-BAR protein Cdc15 modulates its conformation and stimulates its scaffolding activity at the cell division site. *Molecular cell*. 39:86-99.

Rohl, A., J. Rohrberg, and J. Buchner. 2013. The chaperone Hsp90: changing partners for demanding clients. *Trends in biochemical sciences*. 38:253-262.

Rosenfeld, S.S., J. Xing, L.Q. Chen, and H.L. Sweeney. 2003. Myosin IIb is unconventionally conventional. *The Journal of biological chemistry*. 278:27449-27455.

Roy, A., L. Lordier, S. Mazzi, Y. Chang, V. Lapierre, J. Larghero, N. Debili, H. Raslova, and W. Vainchenker. 2016. Differential activity of nonmuscle myosin II isoforms determines their localization at the cleavage furrow of megakaryocytes. *Blood. in press*.

Ruiz-Herrera, J., M. Iranzo, M.V. Elorza, R. Sentandreu, and S. Mormeneo. 1995. Involvement of transglutaminase in the formation of covalent cross-links in the cell wall of Candida albicans. *Archives of microbiology*. 164:186-193.

Sagona, A.P., and H. Stenmark. 2010. Cytokinesis and cancer. *FEBS letters*. 584:2652-2661.

Saha, S., and T.D. Pollard. 2012a. Anillin-related protein Mid1p coordinates the assembly of the cytokinetic contractile ring in fission yeast. *Molecular biology of the cell*. 23:3982-3992.

Saha, S., and T.D. Pollard. 2012b. Characterization of structural and functional domains of the anillin-related protein Mid1p that contribute to cytokinesis in fission yeast. *Molecular biology of the cell*. 23:3993-4007.

Sakata, Y., and N. Aoki. 1980. Cross-linking of alpha 2-plasmin inhibitor to fibrin by fibrin-stabilizing factor. *The Journal of clinical investigation*. 65:290-297.

Sambrook, J., E.F. Fritsch, and T. Maniatis. 1989. Molecular cloning : a laboratory manual. Cold Spring Harbor Laboratory, Cold Spring Harbor, N.Y.

Sanchez-Diaz, A., V. Marchesi, S. Murray, R. Jones, G. Pereira, R. Edmondson, T. Allen, and K. Labib. 2008. Inn1 couples contraction of the actomyosin ring to membrane ingression during cytokinesis in budding yeast. *Nature cell biology*. 10:395-406.

Satchwell, T.J., D.K. Shoemark, R.B. Sessions, and A.M. Toye. 2009. Protein 4.2: a complex linker. *Blood cells, molecules & diseases*. 42:201-210.

Schmidt, G., J. Selzer, M. Lerm, and K. Aktories. 1998. The Rho-deamidating cytotoxic necrotizing factor 1 from Escherichia coli possesses transglutaminase activity. Cysteine 866 and histidine 881 are essential for enzyme activity. *The Journal of biological chemistry*. 273:13669-13674.

Schwartz, M.L., S.V. Pizzo, R.L. Hill, and P.A. McKee. 1973. Human Factor XIII from plasma and platelets. Molecular weights, subunit structures, proteolytic activation, and cross-linking of fibrinogen and fibrin. *The Journal of biological chemistry*. 248:1395-1407.

Sckolnick, M., E.B. Krementsova, D.M. Warshaw, and K.M. Trybus. 2016. Tropomyosin isoforms bias actin track selection by vertebrate myosin Va. *Molecular biology of the cell*. 27:2889-2897.

Shannon, K.B. 2012. IQGAP Family Members in Yeast, Dictyostelium, and Mammalian Cells. *International journal of cell biology*. 2012:894817.

Shi, H., and G. Blobel. 2010. UNC-45/CRO1/She4p (UCS) protein forms elongated dimer and joins two myosin heads near their actin binding region. *Proceedings of the National Academy of Sciences of the United States of America*. 107:21382-21387.

Simanis, V. 2015. Pombe's thirteen - control of fission yeast cell division by the septation initiation network. *Journal of cell science*. 128:1465-1474.

Singh, U.S., M.T. Kunar, Y.L. Kao, and K.M. Baker. 2001. Role of transglutaminase II in retinoic acid-induced activation of RhoA-associated kinase-2. *The EMBO journal*. 20:2413-2423.

Sirotkin, V., J. Berro, K. Macmillan, L. Zhao, and T.D. Pollard. 2010. Quantitative analysis of the mechanism of endocytic actin patch assembly and disassembly in fission yeast. *Molecular biology of the cell*. 21:2894-2904.

Skoumpla, K., A.T. Coulton, W. Lehman, M.A. Geeves, and D.P. Mulvihill. 2007. Acetylation regulates tropomyosin function in the fission yeast Schizosaccharomyces pombe. *Journal of cell science*. 120:1635-1645.

Sladewski, T.E., C.S. Bookwalter, M.S. Hong, and K.M. Trybus. 2013. Single-molecule reconstitution of mRNA transport by a class V myosin. *Nature structural & molecular biology*. 20:952-957.

Sladewski, T.E., M.J. Previs, and M. Lord. 2009. Regulation of fission yeast myosin-II function and contractile ring dynamics by regulatory light-chain and heavy-chain phosphorylation. *Molecular biology of the cell*. 20:3941-3952.

Sohrmann, M., C. Fankhauser, C. Brodbeck, and V. Simanis. 1996. The dmf1/mid1 gene is essential for correct positioning of the division septum in fission yeast. *Genes & development*. 10:2707-2719.

Srikakulam, R., L. Liu, and D.A. Winkelmann. 2008. Unc45b forms a cytosolic complex with Hsp90 and targets the unfolded myosin motor domain. *PloS one*. 3:e2137.

Stachowiak, M.R., C. Laplante, H.F. Chin, B. Guirao, E. Karatekin, T.D. Pollard, and B. O'Shaughnessy. 2014. Mechanism of cytokinetic contractile ring constriction in fission yeast. *Developmental cell*. 29:547-561.

Stark, B.C., M.L. James, L.W. Pollard, V. Sirotkin, and M. Lord. 2013. UCS protein Rng3p is essential for myosin-II motor activity during cytokinesis in fission yeast. *PloS one*. 8:e79593.

Stark, B.C., T.E. Sladewski, L.W. Pollard, and M. Lord. 2010. Tropomyosin and myosin-II cellular levels promote actomyosin ring assembly in fission yeast. *Molecular biology of the cell*. 21:989-1000.

Stegmeier, F., and A. Amon. 2004. Closing mitosis: the functions of the Cdc14 phosphatase and its regulation. *Annual review of genetics*. 38:203-232.

Sun, L., R. Guan, I.J. Lee, Y. Liu, M. Chen, J. Wang, J.Q. Wu, and Z. Chen. 2015. Mechanistic insights into the anchorage of the contractile ring by anillin and Mid1. *Developmental cell*. 33:413-426.

Sun, M., M.B. Rose, S.K. Ananthanarayanan, D.J. Jacobs, and C.M. Yengo. 2008. Characterization of the pre-force-generation state in the actomyosin cross-bridge cycle. *Proceedings of the National Academy of Sciences of the United States of America*. 105:8631-8636.

Sweeney, H.L., and A. Houdusse. 2010. Structural and functional insights into the Myosin motor mechanism. *Annual review of biophysics*. 39:539-557.

Tajadura, V., B. Garcia, I. Garcia, P. Garcia, and Y. Sanchez. 2004. Schizosaccharomyces pombe Rgf3p is a specific Rho1 GEF that regulates cell wall beta-glucan biosynthesis through the GTPase Rho1p. *Journal of cell science*. 117:6163-6174.

Takaine, M., O. Numata, and K. Nakano. 2009. Fission yeast IQGAP arranges actin filaments into the cytokinetic contractile ring. *The EMBO journal*. 28:3117-3131.

Takaine, M., O. Numata, and K. Nakano. 2014. Fission yeast IQGAP maintains F-actin-independent localization of myosin-II in the contractile ring. *Genes to cells : devoted to molecular & cellular mechanisms*. 19:161-176.

Takaine, M., O. Numata, and K. Nakano. 2015. An actin-myosin-II interaction is involved in maintaining the contractile ring in fission yeast. *Journal of cell science*. 128:2903-2918.

Tang, Q., N. Billington, E.B. Krementsova, C.S. Bookwalter, M. Lord, and K.M. Trybus. 2016. A single-headed fission yeast myosin V transports actin in a tropomyosin-dependent manner. *The Journal of cell biology*. 214:167-179.

Taylor, K.A., M. Feig, C.L. Brooks, 3rd, P.M. Fagnant, S. Lowey, and K.M. Trybus. 2014. Role of the essential light chain in the activation of smooth muscle myosin by regulatory light chain phosphorylation. *Journal of structural biology*. 185:375-382.

Taylor, K.C., M. Buvoli, E.N. Korkmaz, A. Buvoli, Y. Zheng, N.T. Heinze, Q. Cui, L.A. Leinwand, and I. Rayment. 2015. Skip residues modulate the structural properties of the myosin rod and guide thick filament assembly. *Proceedings of the National Academy of Sciences of the United States of America*. 112:E3806-3815.

Tebbs, I.R., and T.D. Pollard. 2013. Separate roles of IQGAP Rng2p in forming and constricting the Schizosaccharomyces pombe cytokinetic contractile ring. *Molecular biology of the cell*. 24:1904-1917.

Thacher, S.M., and R.H. Rice. 1985. Keratinocyte-specific transglutaminase of cultured human epidermal cells: relation to cross-linked envelope formation and terminal differentiation. *Cell*. 40:685-695.

Thiyagarajan, S., E.L. Munteanu, R. Arasada, T.D. Pollard, and B. O'Shaughnessy. 2015. The fission yeast cytokinetic contractile ring regulates septum shape and closure. *Journal of cell science*. 128:3672-3681.

Trivedi, D.V., J.M. Muretta, A.M. Swenson, J.P. Davis, D.D. Thomas, and C.M. Yengo. 2015. Direct measurements of the coordination of lever arm swing and the catalytic cycle in myosin V. *Proceedings of the National Academy of Sciences of the United States of America*. 112:14593-14598.

Trybus, K.M. 2000. Biochemical studies of myosin. *Methods (San Diego, Calif.)*. 22:327-335.

Trybus, K.M. 2008. Myosin V from head to tail. *Cellular and molecular life sciences : CMLS*. 65:1378-1389.

Trybus, K.M., T.W. Huiatt, and S. Lowey. 1982. A bent monomeric conformation of myosin from smooth muscle. *Proceedings of the National Academy of Sciences of the United States of America*. 79:6151-6155.

Trybus, K.M., and S. Lowey. 1984. Conformational states of smooth muscle myosin. Effects of light chain phosphorylation and ionic strength. *The Journal of biological chemistry*. 259:8564-8571.

Trybus, K.M., and S. Lowey. 1987. Assembly of smooth muscle myosin minifilaments: effects of phosphorylation and nucleotide binding. *The Journal of cell biology*. 105:3007-3019.

Turbedsky, K., and T.D. Pollard. 2005. Assembly of Acanthamoeba myosin-II minifilaments. Definition of C-terminal residues required to form coiled-coils, dimers, and octamers. *J Mol Biol*. 345:351-361.

Ullal, P., N.A. McDonald, J.S. Chen, L. Lo Presti, R.H. Roberts-Galbraith, K.L. Gould, and S.G. Martin. 2015. The DYRK-family kinase Pom1 phosphorylates the F-BAR protein Cdc15 to prevent division at cell poles. *The Journal of cell biology*. 211:653-668.

Urbancikova, M., and S.E. Hitchcock-DeGregori. 1994. Requirement of amino-terminal modification for striated muscle alpha-tropomyosin function. *The Journal of biological chemistry*. 269:24310-24315.

Vavylonis, D., J.Q. Wu, S. Hao, B. O'Shaughnessy, and T.D. Pollard. 2008. Assembly mechanism of the contractile ring for cytokinesis by fission yeast. *Science (New York, N.Y.)*. 319:97-100.

Veeraraghavan, R., and R.G. Gourdie. 2016. Stochastic optical reconstruction microscopy-based relative localization analysis (STORM-RLA) for quantitative nanoscale assessment of spatial protein organization. *Molecular biology of the cell*. 27:3583-3590.

Venolia, L., W. Ao, S. Kim, C. Kim, and D. Pilgrim. 1999. unc-45 gene of Caenorhabditis elegans encodes a muscle-specific tetratricopeptide repeat-containing protein. *Cell motility and the cytoskeleton*. 42:163-177.

Waffenschmidt, S., T. Kusch, and J.P. Woessner. 1999. A transglutaminase immunologically related to tissue transglutaminase catalyzes cross-linking of cell wall proteins in Chlamydomonas reinhardtii. *Plant physiology*. 121:1003-1015.

Wang, F., M. Kovacs, A. Hu, J. Limouze, E.V. Harvey, and J.R. Sellers. 2003. Kinetic mechanism of non-muscle myosin IIB: functional adaptations for tension generation and maintenance. *The Journal of biological chemistry*. 278:27439-27448.

Wang, N., L. Lo Presti, Y.H. Zhu, M. Kang, Z. Wu, S.G. Martin, and J.Q. Wu. 2014. The novel proteins Rng8 and Rng9 regulate the myosin-V Myo51 during fission yeast cytokinesis. *The Journal of cell biology*. 205:357-375.

Warshaw, D.M., W.H. Guilford, Y. Freyzon, E. Krementsova, K.A. Palmiter, M.J. Tyska, J.E. Baker, and K.M. Trybus. 2000. The light chain binding domain of expressed smooth muscle heavy meromyosin acts as a mechanical lever. *The Journal of biological chemistry*. 275:37167-37172.

Wendt, T., D. Taylor, T. Messier, K.M. Trybus, and K.A. Taylor. 1999. Visualization of head-head interactions in the inhibited state of smooth muscle myosin. *The Journal of cell biology*. 147:1385-1390.

Wendt, T., D. Taylor, K.M. Trybus, and K. Taylor. 2001. Three-dimensional image reconstruction of dephosphorylated smooth muscle heavy meromyosin reveals asymmetry in the interaction between myosin heads and placement of subfragment 2. *Proceedings of the National Academy of Sciences of the United States of America*. 98:4361-4366.

Wesche, S., M. Arnold, and R.P. Jansen. 2003. The UCS domain protein She4p binds to myosin motor domains and is essential for class I and class V myosin function. *Current biology : CB*. 13:715-724.

Willet, A.H., N.A. McDonald, K.A. Bohnert, M.A. Baird, J.R. Allen, M.W. Davidson, and K.L. Gould. 2015a. The F-BAR Cdc15 promotes contractile ring formation through the direct recruitment of the formin Cdc12. *The Journal of cell biology*. 208:391-399.

Willet, A.H., N.A. McDonald, and K.L. Gould. 2015b. Regulation of contractile ring formation and septation in Schizosaccharomyces pombe. *Current opinion in microbiology*. 28:46-52.

Win, T.Z., Y. Gachet, D.P. Mulvihill, K.M. May, and J.S. Hyams. 2001. Two type V myosins with non-overlapping functions in the fission yeast Schizosaccharomyces pombe: Myo52 is concerned with growth polarity and cytokinesis, Myo51 is a component of the cytokinetic actin ring. *Journal of cell science*. 114:69-79.

Wong, K.C., N.I. Naqvi, Y. Iino, M. Yamamoto, and M.K. Balasubramanian. 2000. Fission yeast Rng3p: an UCS-domain protein that mediates myosin II assembly during cytokinesis. *Journal of cell science*. 113 (Pt 13):2421-2432.

Wu, J.Q., J.R. Kuhn, D.R. Kovar, and T.D. Pollard. 2003. Spatial and temporal pathway for assembly and constriction of the contractile ring in fission yeast cytokinesis. *Developmental cell*. 5:723-734.

Wu, J.Q., and T.D. Pollard. 2005. Counting cytokinesis proteins globally and locally in fission yeast. *Science (New York, N.Y.)*. 310:310-314.

Wu, J.Q., V. Sirotkin, D.R. Kovar, M. Lord, C.C. Beltzner, J.R. Kuhn, and T.D. Pollard. 2006. Assembly of the cytokinetic contractile ring from a broad band of nodes in fission yeast. *The Journal of cell biology*. 174:391-402.

Yang, Y., H. Yu, and Q. Cui. 2008. Extensive conformational transitions are required to turn on ATP hydrolysis in myosin. *J Mol Biol*. 381:1407-1420.

Yawata, Y. 1994. Band 4.2 abnormalities in human red cells. *The American journal of the medical sciences*. 307:190-203.

Ye, Y., I.J. Lee, K.W. Runge, and J.Q. Wu. 2012. Roles of putative Rho-GEF Gef2 in division-site positioning and contractile-ring function in fission yeast cytokinesis. *Molecular biology of the cell*. 23:1181-1195.

Yee, V.C., L.C. Pedersen, I. Le Trong, P.D. Bishop, R.E. Stenkamp, and D.C. Teller. 1994. Three-dimensional structure of a transglutaminase: human blood coagulation factor XIII. *Proceedings of the National Academy of Sciences of the United States of America*. 91:7296-7300.

Zemskov, E.A., A. Janiak, J. Hang, A. Waghray, and A.M. Belkin. 2006. The role of tissue transglutaminase in cell-matrix interactions. *Frontiers in bioscience : a journal and virtual library*. 11:1057-1076.

Zhang, D., A. Vjestica, and S. Oliferenko. 2010. The cortical ER network limits the permissive zone for actomyosin ring assembly. *Current biology : CB*. 20:1029-1034.

Zhou, Z., E.L. Munteanu, J. He, T. Ursell, M. Bathe, K.C. Huang, and F. Chang. 2015. The contractile ring coordinates curvature-dependent septum assembly during fission yeast cytokinesis. *Molecular biology of the cell*. 26:78-90.

Zhu, Y.H., Y. Ye, Z. Wu, and J.Q. Wu. 2013. Cooperation between Rho-GEF Gef2 and its binding partner Nod1 in the regulation of fission yeast cytokinesis. *Molecular biology of the cell*. 24:3187-3204.